ACTA UNIVERSITATIS SZEGEDIENSIS

ACTA MINERALOGICA-PETROGRAPHICA

Tomus XLVII

SZEGED, 2006-2007

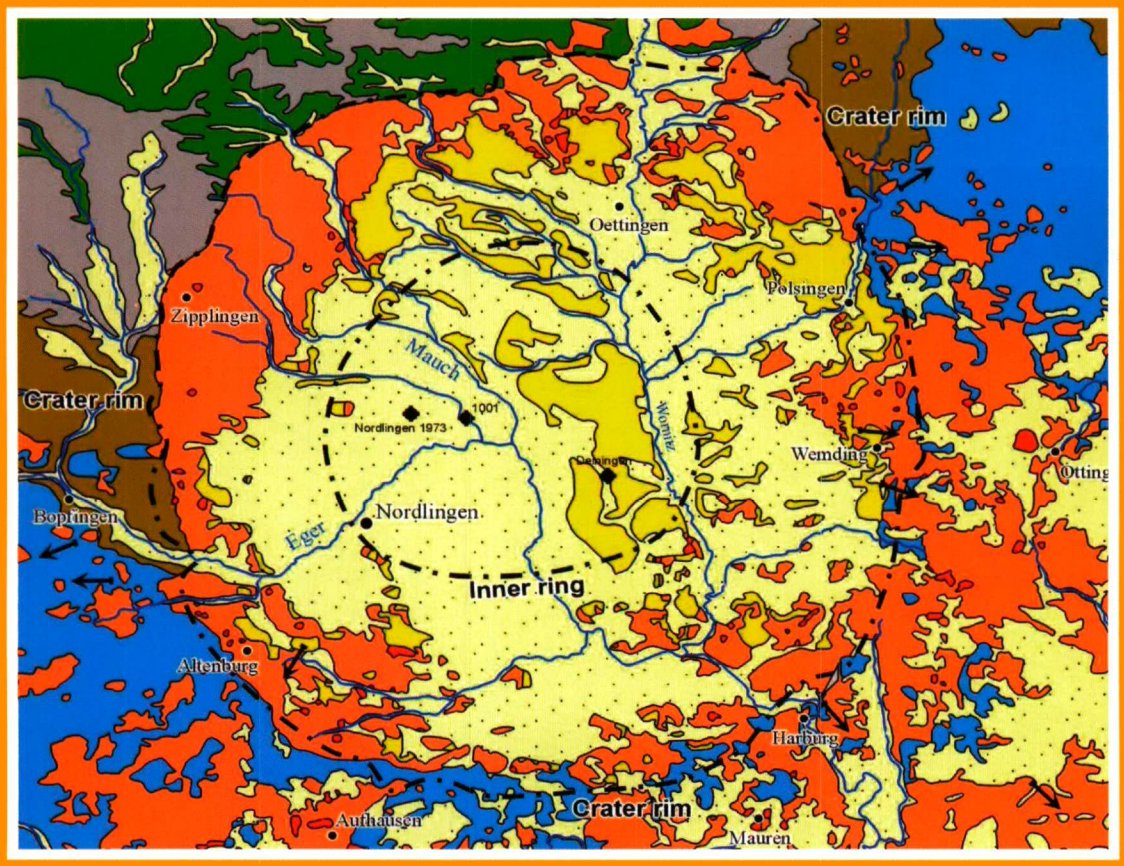

Published by the Department of Mineralogy, Geochemistry and Petrology, University of Szeged

ACTA MINERALOGICA-PETROGRAPHICA
established in 1922
HU ISSN 0365-8066

Abbreviated title:

Acta Mineral. Petrogr., Szeged

The Acta Mineralogica-Petrographica is published by the
Department of Mineralogy, Geochemistry and Petrology, University of Szeged

---

On the cover: Geological map of the Ries Basin, Germany (Gucsik, pp. 17–24) (Cropped from Fig. 1).

Designed by: Elemér Pál-Molnár & György Sipos ©

Acta Mineralogica-Petrographica, Szeged 2006–2007, Vol. 47, pp. 1-16

ACTA Mineralogica Petrographica

STATISTICAL DISTRIBUTIONS OF ORE ELEMENTS IN THE RECSK ORE FIELD, HUNGARY

LAJOS Ó. KOVÁCS[1], GÉZA SZEBÉNYI[2], GÁBOR P. KOVÁCS[1], JÁNOS FÖLDESSY[3]

[1] Hungarian Geological Survey, H-1440 Budapest, P.O. Box: 17, Hungary

[2] Torockói u. 30., H-2030 Érd, Hungary

[3] Department of Geology and Mineral Resources, University of Miskolc, H-3515 Miskolc-Egyetemváros, Hungary

e-mail: okovacs@mgsz.hu, gszebeny@externet.hu, Gabor.Kovacs@mgsz.hu, foldfj@gold.uni-miskolc.hu

ABSTRACT

Statistical frequency distributions of the Ag, Au, Cu, Fe, Mo, Pb, S, Se and Zn contents measured in 51000 rock samples taken from 194 diamond boreholes exploring a large porphyry copper and polymetallic skarn ore deposit-complex were analyzed. The distributions were represented by subsets of their common, and extreme values. The characteristic values of the ore components were displayed, and compared across units within three types of objects: spatial parts, rock-formations, and depth-zones of the deposit-complex. Among the deposit-parts, distributions of Ag, Cu, Pb, S and Au revealed significant differences. Except for a few units and those only in terms of several components, rock-formations exhibited a limited specialty in comparison. Statistically, values of the measured elements showed a notable vertical zoning.

Key words: ore deposit, statistical distribution, percentile, base metal, porphyry copper, polymetallic ore

INTRODUCTION

On the Lahóca Hill, near the village of Recsk, northern Hungary, silver and copper mining started in the 1850-s. During the next one hundred plus years several exploration campaigns were conducted in the area, and in the 1960-s a large, complex, porphyry copper and polymetallic, deep-seated ore deposit (Recsk Deep) was discovered. Detailed explorations resulted in 130 deep (>1,000 m) diamond boreholes, two deep shafts (to 1,200 m depth), tunnels and numerous crosscuts at two levels, and a total of 75,000 m of underground drillholes. After decades Recsk Deep still awaits exploitation and is in the state of long-term suspension. More than 150,000 rock samples have been analyzed for varying sets of ore components. Obviously, during this long exploration history, regulations and techniques of sampling and analysis changed a number of times. The most important analytical methods were, for base metals: atomic absorption spectroscopy, and, in the earlier times, classical wet methods; for gold: fire assay/gravimetric analysis (for Au>0.5 ppm).

In the numerous technical reports and published papers produced during the various exploration, development and assessment periods of the ore field, evaluations and models of statistical distributions of the analyzed metals are rare. Those consistent and based on a number of data comparable with the amount of the available analyses are completely absent. Hence, the aim of this paper is to provide a basic and more or less uniform characterization of the statistical distributions of ore elements, incorporating as many data as possible. As in geology generally, by statistical distributions we mean frequency distributions of values.

Statistical distributions can be treated in many ways, starting from calculation of a central tendency value to elaboration of sophisticated numerical models, not to mention analysis of bivariate and multivariate distributions. Here, statistical distributions serve as a mean to understand the structure and genesis of the ore field better, therefore, instead of thoroughly analyzing the distributions themselves, their effective, robust, unambiguously producible, and comparable representation is searched for, and used.

At this level of description of an ore deposit, no matter how asymmetric or complex a distribution is, the first related question to be answered is: which are the common (usual, typical, normal, "background", etc.), and which are the extreme (exceptional, atypical, deviant, "anomalous", etc.) values of a component. In other words, the representation of a distribution is mainly expected to elucidate this binary property of practically any set of values.

GEOLOGICAL SETTING

The study area lies in eastern Central Europe (Fig. 1), in the Carpathian Basin, a wide lowland with a few hilly patches inside. Geologically, this is the Pannonian Basin system, a Neogene-Quaternary sedimentary basin, surrounded by the arc of the Carpathian Mountains in the north, east, and southeast, bounded by the Eastern Alps in the west, and by the Dinaridic belt in the south. The Cenozoic evolution of the region was largely governed by movements and deformations of two continental plate fragments (Csontos 1995), that were squeezed between the colliding African and European Plates. These plate fragments, now forming the basement of the region, were forced to undergo major displacements, rotations, block-faulting, tilting, and thrusting during the prevailing compressional tectonic regime, whereas at their edges subduction processes took place. The geodynamic events were accompanied by episodic but significant magmatic activity both at the peripheries and in the interiors of the plate fragments, resulting in numerous corresponding volcano-magmatic formations throughout the Cenozoic. In the Paleogene, large andesitic stratovolcanic

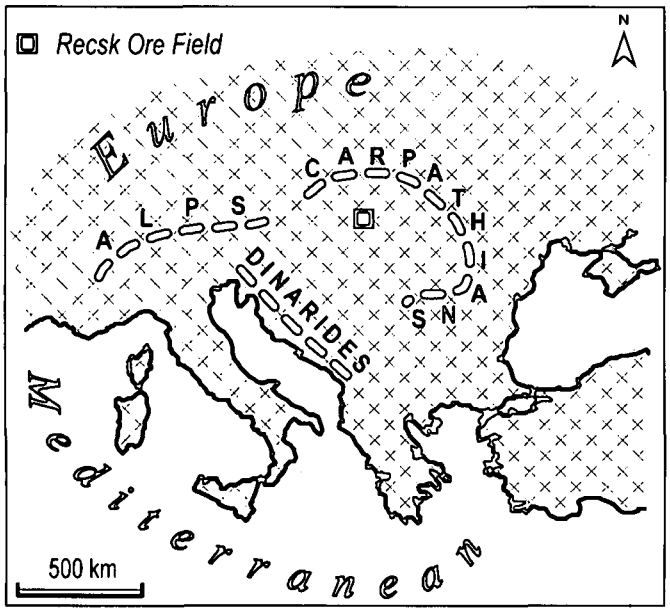

Fig. 1. Location of the Recsk Ore Field.

complexes were formed at several localities in a narrow belt (Csillag et al. 1983) to the north of what is now the Mid-Hungarian fault zone, identified as the boundary of the two plate fragments (Csontos and Nagymarosy 1998). One of these volcanic complexes hosts the Recsk Ore Field, a large mineralized complex, usually divided into Recsk Deep and Lahóca (Fig. 2, and, for certain details, Fig. 3 and Fig. 5).

The pre-volcanic basement of the Recsk area consists of Triassic limestone, quartzite and shales. Due to a post-Triassic uplift, Jurassic and Cretaceous rocks are absent. The Paleogene series starts with Late Eocene shallow-marine limestone and marl, mostly underlying intermediate volcanic rocks. Recent investigations (Less et al. 2005, Földessy et al. 2006) suggest that at least the overwhelming part (if not the whole) of the volcanic complex was formed in the Early Oligocene, as opposed to the traditionally employed Late Eocene age.. The Paleogene volcanic cycle comprises four stages: 1) submarine lavaflows, agglomerates, and peperites (the rocks of this stage do not outcrop on the surface); 2) a stratovolcanic sequence of dacitic character, gradually shifting to volcanites of subaerial environments; 3) a stratovolcanic sequence of biotite-hornblende andesites, their pyroclasts, and reworked andesitic volcanic sediments, with emplaced diorite-porphyry and quartz-diorite intrusions hosting the porphyry copper mineralization; and 4) development of a central explosive caldera in the area linked with the volcanism of stage 3, and formation of pyroxene-andesite dyke-pattern bodies and laccoliths within and around the caldera. Late Oligocene sandstone, clay and marl spread over the area except the central, several sq.km large andesitic horst (Baksa et al. 1988, Gatter et al. 1999, Seres-Hartai et al. 2001).

The deep-seated mineralizations (Recsk Deep) consist of different types of genetically linked ore formations. In the intrusive body, a typical porphyry copper (and subordinate Mo) mineralization with gold developed (Földessy et al. 2004). Along the exo- and endocontacts with the Triassic limestone, a skarn Cu-Zn-Pb-Fe mineralization was formed. In the Triassic limestone metasomatic and vein-type Zn-Pb ores occur. During the alteration of the intrusive body, silicification developed in the central and upper parts. At the top of the intrusion it is associated with an argillic zone containing a quartz-sericite-anhydrite assemblage. The propylitic zone, with albite, chlorite, epidote, anhydrite and calcite, is not continuous, and overlaps with the endoskarn containing diopside, amphibole and phlogopite. The garnet-diopside exoskarn is fringed with a metasomatic zone in which the limestone recrystallized to marble (Csillag 1975).

The porphyry Cu mineralization forms chalcopyrite-pyrite disseminations and stockworks. In the central parts molybdenite occurs in quartz-, and siliceous-anhydrite veins. In the skarn mineralization the basic Cu-bearing mineral is chalcopyrite, accompanied by pyrite, pyrrhotite, magnetite and hematite. Within the skarn polymetallic deposit, sphalerite is essential, associated with pyrite, chalcopyrite, galena and pyrrhotite. In the zones of hydrothermal-metasomatic alterations the polymetallic ore deposits contain sphalerite (dominant), pyrite, galena and chalcopyrite (Csongrádi 1975, Szebényi et al. 1985).

The deep-seated porphyry and skarn Cu deposit (Recsk Deep) has a spatial and, probably, genetic association with the Lahóca epithermal Cu-Au deposits. The Lahóca deposit is located in the NE part in the uppermost zone of the Recsk mineralized complex (Fig. 2). It can be considered as a typical high-sulfidation epithermal system (Földessy 1997, Gatter et al. 1999, Seres-Hartai and Földessy 2000, Seres-Hartai et al. 2001).

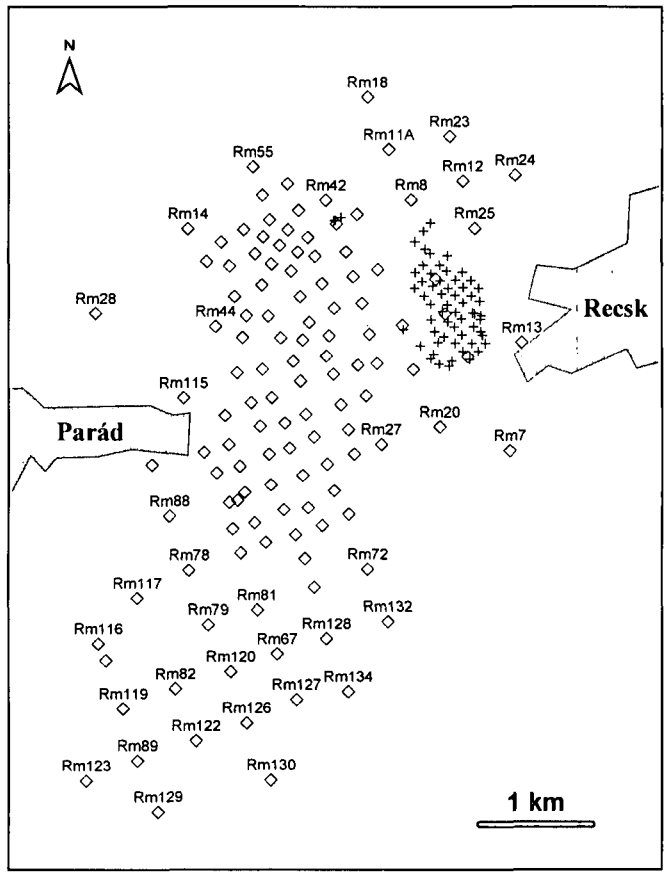

Fig. 3. Map of boreholes used in this study. Diamonds denote deep (1000-1365 m) boreholes, 124 in total, exploring Recsk Deep. For some of them their names are given (e.g. Rm18). Crosses denote shallower (17-400 m) boreholes, 70 in total, exploring Lahóca. Compare with Fig. 5.

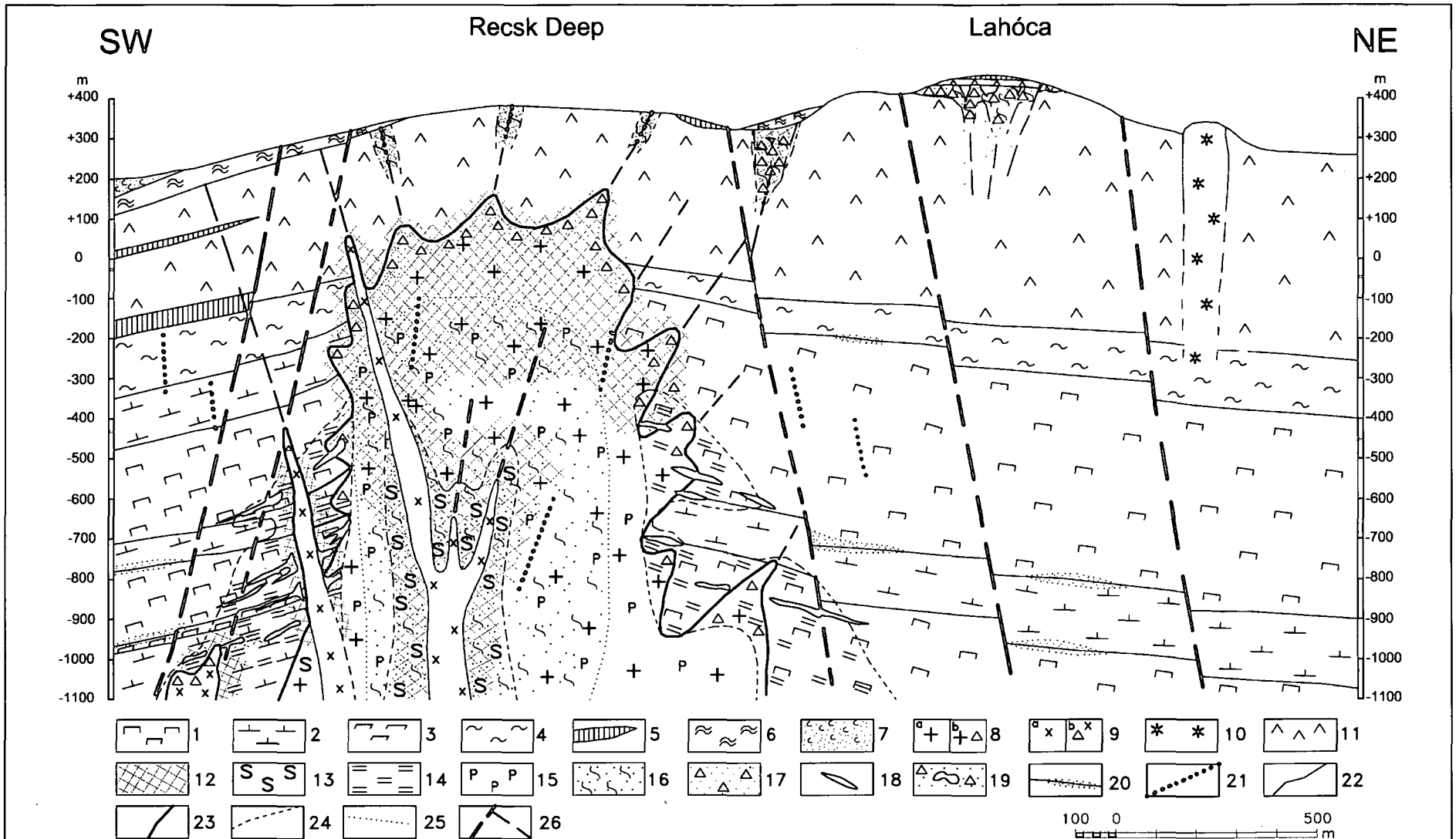

Fig. 2. Schematic geologic section of the Recsk Ore Field (after Zelenka and Szebényi, 2002). 1-limestone (Triassic), 2-quartzite (Triassic), 3-dolomite (Triassic), 4-shale (Triassic), 5-bituminous clay marl, marl, marly limestone, limestone, sandstone, nummulitic limestone (Upper-Eocene), 6-clay marl, sandstone (Oligocene), 7-delivium, alluvium (Quarter), 8a-diorite porphyry (Upper-Eocene–Lower Oligocene), 8b-peripheral breccia of diorite porphyry (Upper Eocene–Lower Oligocene), 9a-quartz-diorite porphyry (Upper-Eocene–Lower Oligocene), 9b-peripheral breccia of quartz-diorite porphyry (Upper-Eocene–Lower Oligocene), 10-post-ore dikes and laccoliths (Upper-Eocene–Lower Oligocene), 11-stratovolcanic andesite and other effusives (Upper-Eocene–Lower Oligocene), 12-quartz-argillic alteration, 13-endoskarn, 14-exoskarn, 15-propylitic alteration, 16-impregnation Cu-Mo or Cu-(Mo) ore (stockwork), 17-brecciated-impregnation Cu-Mo or Cu-(Mo) ore (stockwork), 18-massive-sulphide Cu-Fe or Zn-Fe-Cu-(Pb) ore bodies, 19-impregnation and massive Cu-Au-Ag-As-(Pb-Zn) ore in silicified volcanic breccia, 20-hydrothermal-metasomatic polymetallic (Pb-Zn-Fe) ore, 21-vein-type Pb-Zn-(Fe)-Cu ore, 22-geologic boundaries between main rock types, 23-intrusive boundary, 24-boundaries of alteration zones (fronts), 25-subordinate boundaries of alteration zones, 26-tectonic lines.

Data selection and preparation

It is obvious that for geologic objects of similar complexity descriptions may be provided at a great number of both hierarchical and non-hierarchical levels of homogeneity, from the entire ore field down to rock bodies, ore mineral occurrences, etc. In the given study statistical distributions of elements in three sets of units reflecting three different aspects of the geologic object are described: 1) geologically separable parts of the deposit-complex (hereafter deposit-parts), 2) stratigraphically-petrographically meaningful rock-formations, and 3) geologically-economically interesting depth-zones.

In order to reach a coherent characterization of the distributions, the largest possible but consistent subset of the available data is selected. First of all, this means selection of those boreholes from which methodologically and geometrically comparable samples were taken, and in which levels of knowledge about the geological objects and phenomena are similar. Fig. 3 displays the position of the selected boreholes.

From these boreholes, altogether approx. 70,000 analyzed rock/ore samples are available. These are more or less regularly taken and handled, half-core samples. Among them there are close to 11,000 that have a recorded length of 20 cm, otherwise the majority of samples have a length of 1 meter. Every 5 adjacent samples with a 20 cm length were merged, thus yielding more than 1800 'new' 1 meter long samples. As a result, close to 62,000 samples (still not all having the same lengths, see below) were entered into the work database.

Fig. 4 shows the frequency distribution of sample-length in this database. There are 3 sample-length values (1 m, 5 m, and 10 m) that have very high frequencies (51682, 2140, and 2303, respectively), but a wide range of values occurs. From the long-time experience of exploration geologists it is known that mixing of samples with different geometry may bias the results of a statistical analysis, therefore below only the 1 m samples are used.

Representation of the statistical distributions

In most of the units gained by divisions of the given huge dataset from three different aspects (see above)

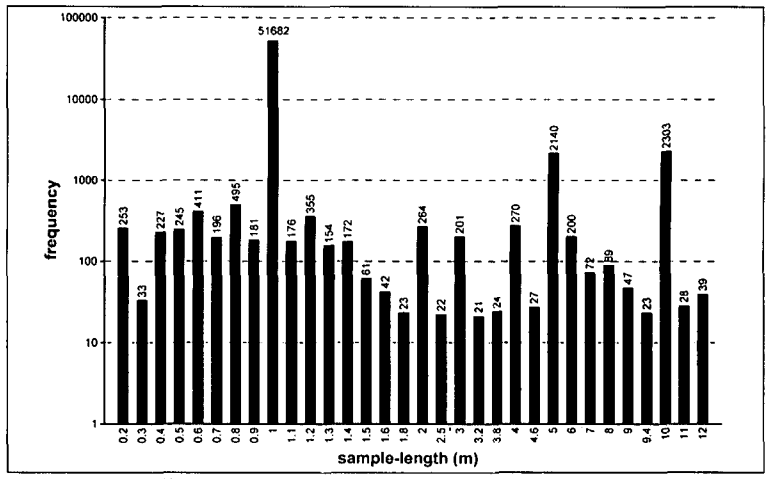

Fig. 4. Frequency distribution of sample-length in the analyzed data set. Only sample-length values with a frequency more than 20 are shown.

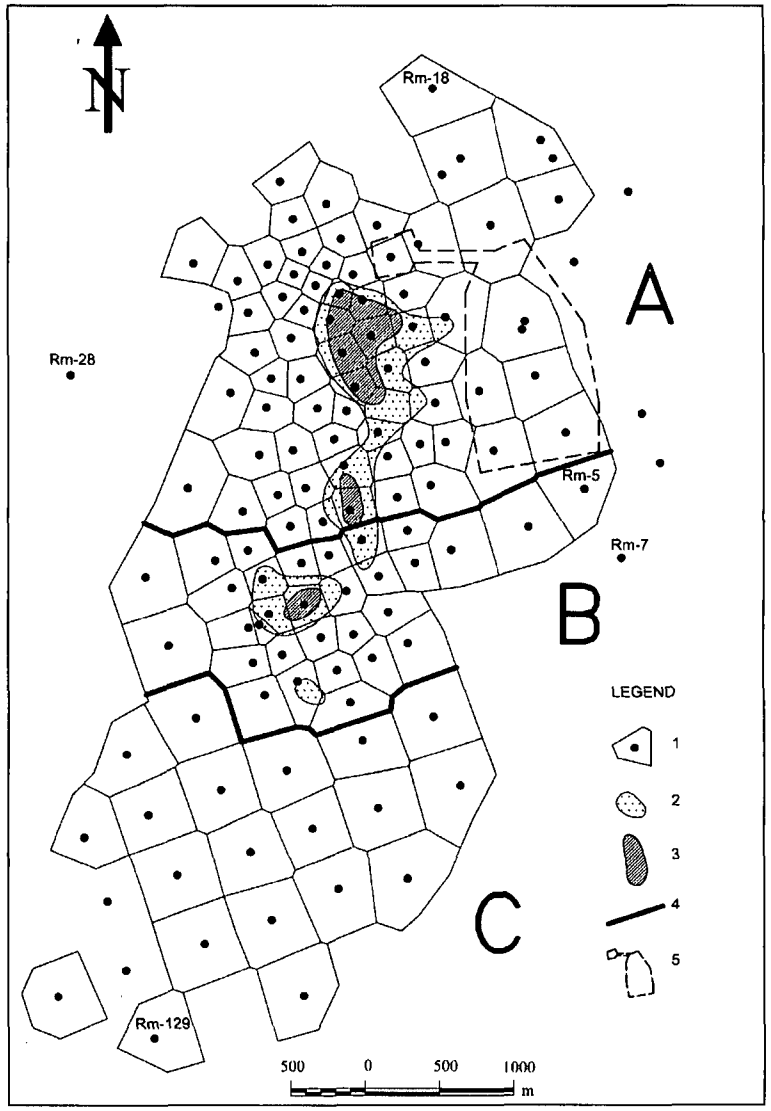

Fig. 5. Map showing the main deposit-parts of the Recsk Ore Field. 1- deep exploration borehole (compare with Figure 3) surrounded by ore reserve estimation polygon, 2-area where the total intersected thickness of porphyry body/bodies exceeds 300 m, 3-area where the total intersected thickness of porphyry body/bodies exceeds 500 m, 4-boundary between the main parts, A, B and C, of Recsk Deep, 5-mining plot of Lahóca. For more explanation see text.

measured values are available for nine chemical elements (Ag, Cu, Mo, Pb, Se, Zn, Fe, S, and Au), which means a great number of distributions are to be analyzed. The distributions are also expected to be compared across the units (within each of the three division schemes). All this requires a simple and efficient representation. From the numerous possible solutions proposed by statistics (e.g. Henley 1981, Marsal 1987, Rock 1988, SPSS 1998a, 1998b) using suitably chosen percentiles seem to be adequate and profitable (for another application of percentiles in geochemistry see Ó.Kovács and Kovács, 2002).

When talking about distribution, in most cases common values are considered those falling somewhere towards the central part of the whole range of values. This is true even when the distribution is asymmetric, multimodal, or unimodal but a result of superimposed processes, etc., which often occurs in a complex ore deposit. Extreme values are those falling towards the (higher) end of the occupied range. Hence, at the given basic level of description, we essentially need a definition of two sub-ranges for each distribution. In an ore exploration context the boundary between these sub-ranges is often called 'anomaly threshold', and there are a lot of methods suggested for its calculation, both parametric and non-parametric. A definition of anomaly should always be target-dependent, and is often conditional and subjective. We keep using the less formalized, intuitive terms 'common' and 'extreme', and separate them at a simple but robust, non-parametric statistics: at the 90th percentile. It should be emphasized that in the given study this definition is not crucial, it could also be the 95th, or the 99th, or probably even the 75th percentile, because we just need to produce sets of comparable representations of frequency distributions, from which plausible sub-ranges of common, and extreme values are immediately seen.

The chosen representation is introduced in Fig. 6 and Fig. 7 (geochemically evaluated in the next section). In Fig. 6, displaying the common values, each thin bar extends from the 10th to the 90th percentile, i.e. the inner 80% of the valid measured values fall into this sub-range. Thick bars portray interquartile ranges (extending from the 25th to the 75th percentiles), i.e. the 'central' 50% of the valid measured values fall into these sub-ranges. Knots on the bars represent the medians (that is the 50th percentiles). In Fig. 7, displaying the extreme values, each thick bar extends from the 90th percentile to the measured maximum, representing the sub-range of the highest values making 10% in number. Horizontal ticks on the bars represent the 95th percentiles, marking the boundary of the upper 5% of the values. N stands for the number of measurements in each particular case. Values above upper detection limits are omitted, luckily there are only a few of them in the whole dataset. Below-detection-limit values are represented by zeros. Sometimes a great proportion of values are such zeros; there, the picture of common values shrinks to that of the median (e.g. Se in Deep-C). Similarly, the range of extreme values may be very limited, e.g. Au in Deep-C. Obviously, these cases are less informative, still they provide a part of the characterization.

Even when a distribution is perceptibly displayed, e.g. any of the Fe distributions in Fig. 6 and Fig. 7, particular values characteristic of the given distribution are usually needed to comprehend it. When the picture is uncertain, e.g. that of Se in Fig. 6, discrete numbers are indispensable. Therefore, for all represented distributions characteristic values are also given. It is obvious, that a distribution comprising a (possibly large) set of values can only be represented with a few numbers at a price of significant simplification, made always from a deliberately, or inherently, chosen aspect. In order to be treatable, the number of characteristic values should also be limited. It has been found that the triplet (see Table 1, evaluated later) of the 25th percentile, the median, and the 75th percentile is very handy, especially when regarded together with the corresponding graphs. Values below detection limits, here too, are replaced by zeros. Hence, if the 25th percentile is zero (S in Deep-B), or the median is also zero (Pb in Deep-C), or the 75th percentile is also zero (Au in Deep-C), we immediately know that at least 25%, or 50%, or 75%, respectively, of the values were below detection limit. In similar cases, further statistics may be greatly influenced by these conditions. Otherwise, median is usually a powerful estimation of the central tendency, while the other two percentiles used mark a range of presumably the most frequent and ordinary, and, hence, characteristic values of the given set.

Table 1. Common values within deposit-parts

	Ag	Cu	Mo	Pb	Se	Zn	Fe	S	Au
	ppm	%	%	%	%	%	%	%	ppm
Deep-A	0	0.03	0.001	0	0	0	2.7	5.9	0
	1.2	0.08	0.005	0	0	0.01	4.0	11.6	0
	2.9	0.23	0.012	0	0	0.13	5.9	19.6	0.1
Deep-B	0	0.01	0	0	0	0	2.4	0	0
	2.1	0.03	0.004	0	0	0.01	3.4	1.3	0
	7.4	0.09	0.008	0	0	0.05	4.8	3.9	0.1
Deep-C	3.3	0.01	0	0	0	0	2.0		0
	10.5	0.03	0.001	0	0	0.02	3.2		0
	21.2	0.08	0.008	0.09	0	0.24	4.2		0
Lahóca	0	0.005							0.016
	0	0.009							0.139
	3.0	0.023							0.460
ALL	0	0.01	0	0	0	0	2.6	5.7	0
	1.0	0.05	0.005	0	0	0.01	3.7	10.7	0.09
	3.1	0.14	0.010	0.01	0	0.11	5.4	19.5	0.30

Each triplet represents the 25th percentile, the median, and the 75th percentile.
ALL stands for the entire deposit.

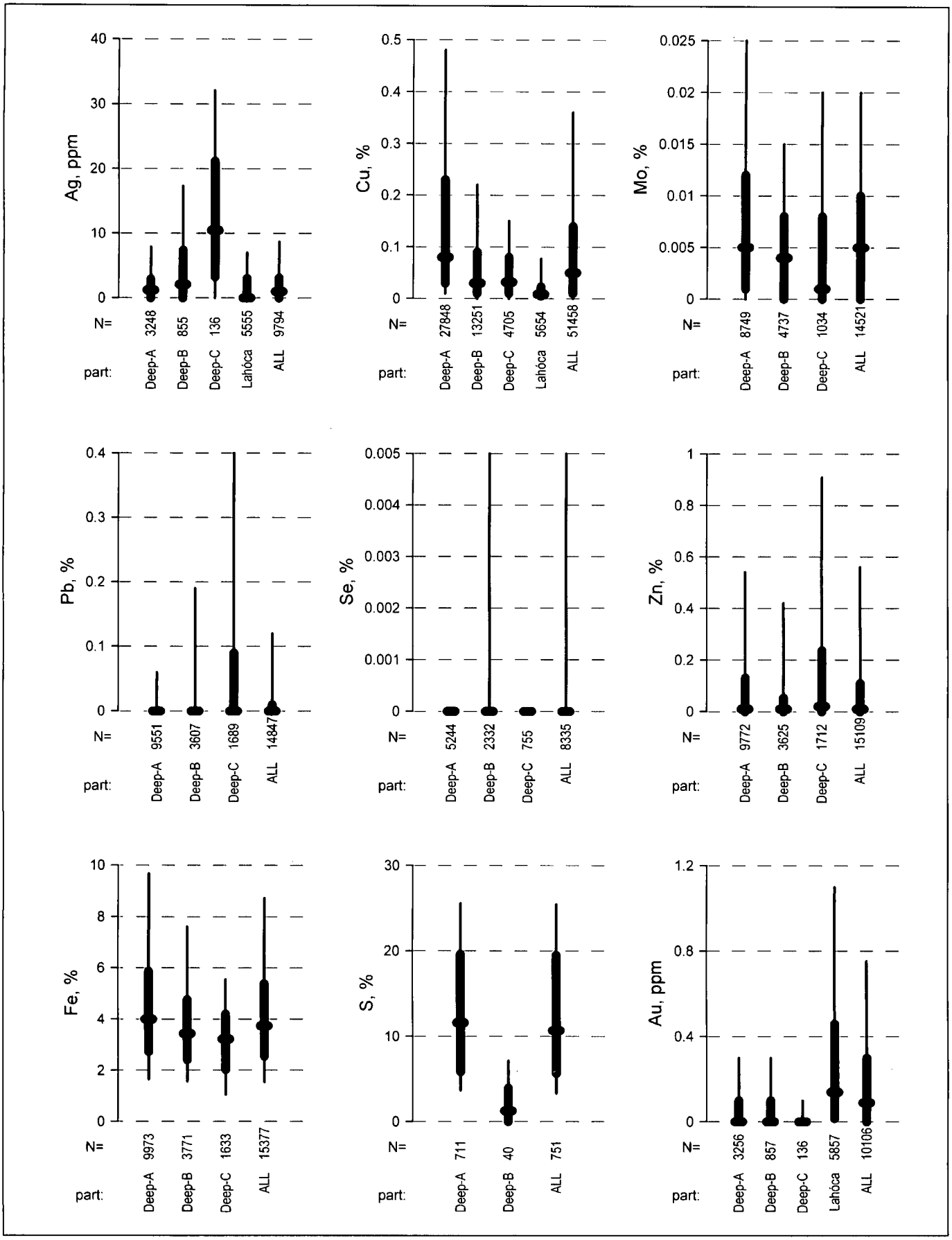

Fig. 6. Common values of ore components within deposit-parts. Thin bars extend from the 10th to the 90th percentiles. Thick bars represent interquartile ranges. Knots on the bars represent the medians. N denotes the number of valid values. ALL stands for the entire deposit.

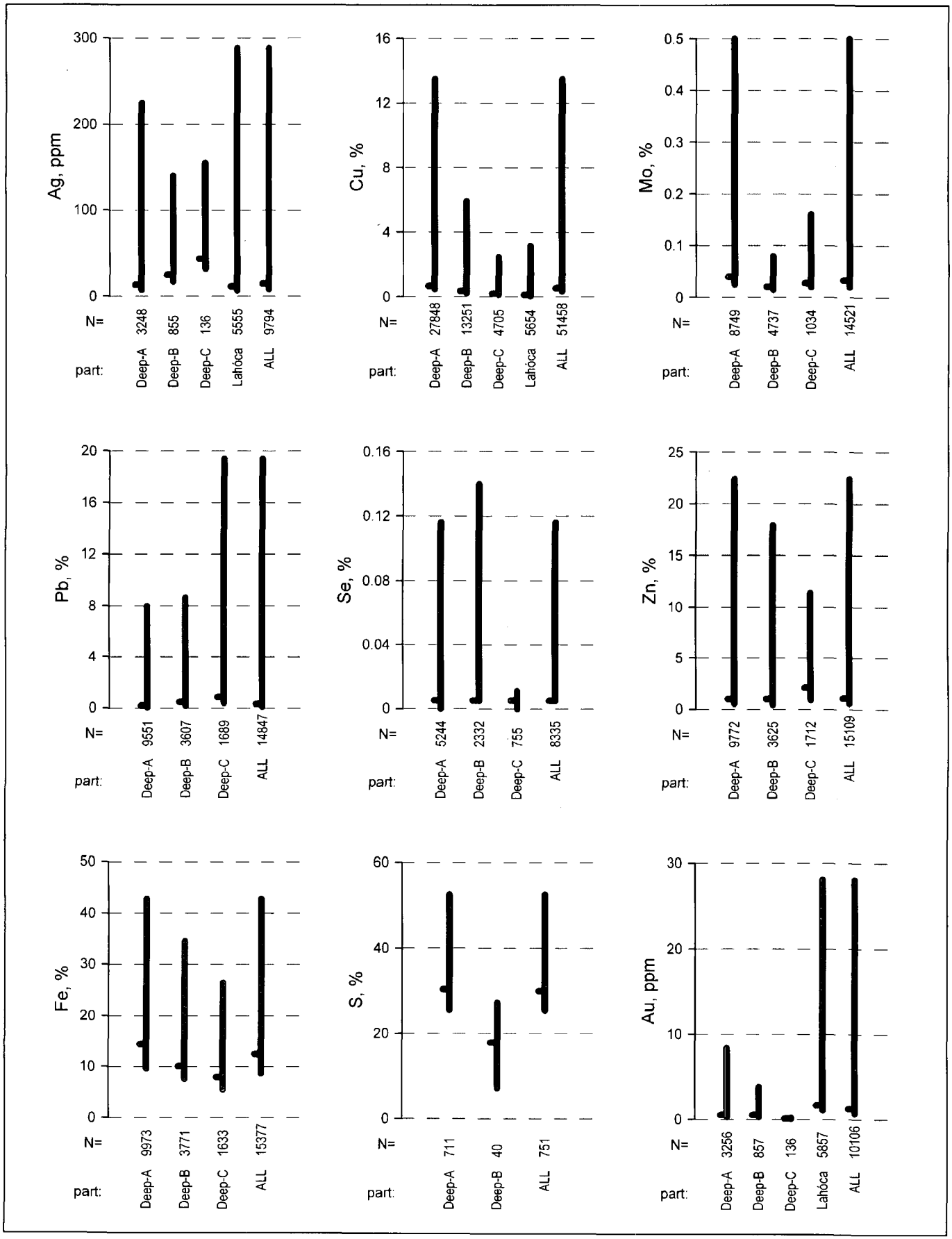

Fig. 7. Extreme values of ore components within deposit-parts. Thick bars extend from the 90th percentiles to the measured maxima. Horizontal ticks on the bars represent the 95th percentiles. N denotes the number of valid values. ALL stands for the entire deposit.

Table 2. Rock-formations examined in this study

Symbol	Age	Description / Traditional name	Thickness
O	Oligocene	claystone, marl	250-430 m
a1	Late Eocene – Early Oligocene	upper member of the stratovolcanic series (with that in Lahóca)	0-100 m
a1q	Late Eocene – Early Oligocene	middle member of the stratovolcanic series	120-250 m
a2	Late Eocene – Early Oligocene	lower member of the stratovolcanic series	50-200 m
a3	Late Eocene – Early Oligocene	intrusive complex, altered, partly with ore mineralization	0-863 m, mean: 400 m
ERC	Late Eocene – Early Oligocene	rock essentially composed of sulphide ore (mainly pyrite)	0-28 m
Sk	Late Eocene – Early Oligocene	skarn	0-162 m
Ap1/Kv1	Mesozoic	'upper shale'/'upper quartzite' group	120-600 m, mean: 180 m
Mk1	Mesozoic	'upper limestone' group	120-557 m, mean: 236 m
Kv2	Mesozoic	'middle quartzite' group	40-260 m, mean: 103 m
Mk2	Mesozoic	'lower limestone' group	100-290 m, mean: 122 m
Ap2/Kv3	Mesozoic	'lower shale'/'lower quartzite' group	0-78 m, mean: 49 m
üa	uncertain	fresh, cutting intrusive rocks (dyke, laccolith)	0-80 m

As pointed out by Földessy et al. (2004), among the Au determinations from Recsk Deep there are seriously biased assay series. Since in these cases the actual concentrations of Au are systematically underestimated, i.e. the nature of the bias is known, the related statistical observations may still be of use, provided this uncertainty is kept in mind.

Distributions within deposit-parts

Along with the history of mining and exploration in the area, mainly thanks to increasing the density of the surface drilling network and to an extensive underground exploration (Szebényi 2000), structural model of the deposit has significantly developed in the sense that it has become more and more detailed and accurate. The applied here subdividing of the complex into deposit-parts (Fig. 5) is based on 1) the total known thickness of intrusive formations (Cseh Németh et al. 1984), 2) spatial distribution of ore mineralizations in Recsk Deep (Cseh Németh 1975), and 3) the map of copper ore reserve estimation from surface boreholes (Cseh Németh et al. 1984, Cseh Németh 1988), and partly explained also in Gagyi Pálffy Sr. et al. (1971) and Baksa et al. (1988).

Deposit-part Deep-A has the largest mass of intrusive rock and connected porphyry copper. Also significant is the amount of skarn copper and zinc ore. In Deep-B the known total thickness of intrusive rocks is smaller, the proportion of skarn ores is higher relative to porphyry copper, and in the composition of skarn ores polymetallic ores are more important than in Deep-A. Deep-A and Deep-B together make the Recsk Deep copper-ore deposit. Deep-C, called also Recsk-South, or the Recsk Deep polymetallic ore deposit, only contains polymetallic ores with subordinate and low-value copper, and has a limited amount of intrusives. Within the Recsk Ore Field, Recsk Deep may be defined as a domain below the depth of 500 m with the joint area of Deep-A, Deep-B and Deep-C. A distinct, near-surface mineralization with enargite, luzonite and Au-pyrite, treated as the fourth part, is Lahóca, developed at the eastern edge of Deep-A. Below, these parts are compared in terms of statistical distributions of ore components.

Regarding the common values (Fig. 6, Table 1), some of the components reveal significant dissimilarities among the deposit-parts. For example, Lahóca is the richest in Au, and the poorest in Cu. Deep-A has significantly higher S values than Deep-B. In Deep-C, bulk of the Ag values are higher than elsewhere, whereas Au is very low. On the other hand, regarding the Mo, the Zn, and the Fe contents, the three parts of Deep are not very different.

The extreme values (Fig. 7) may reflect similar relationships, as in the case of Cu, Pb, S, Au, and especially Fe, the most 'regular' component, in terms of consistency of its plots. For other elements, these values do not repeat the picture of the common values, e.g. for Zn. It should be stressed that extreme values are not necessarily expected to plot similarly to the common values, as they are often extreme just because they do not belong to the same natural population of values. Hence, their plots may be better for displaying their sub-ranges than reflecting the general relative levels of the components.

Distributions within rock-formations

As this ore field extends to a large geologic space with a number of structural and stratigraphic elements, a characterization of distributions within the main rock-formations (Table 2) should not be omitted. Within the research project supporting also the given paper the main geologic formations defined are obviously based on previously described and accepted, by local geologists, models (e.g. Baksa et al. 1980, Földessy 1975, Földessy-Járányi 1975, Komlóssy et al. 2000). Therefore, the symbols figuring here are similar to those used in earlier studies.

Generally speaking, the common values of the analyzed ore components (Fig. 8 and Table 3) reveal a limited specialty for most of the formations. In other words, the statistical distributions are not drastically different from one formation to another. Exceptions, at least in terms of a few components, may be ERC (high Fe and Cu), a1 (high Se and Au, low Zn), and a1q (high Ag, Pb, Se and Au). The Oligocene clayey marls (O) are very poor in Ag, Cu and Au, expectedly.

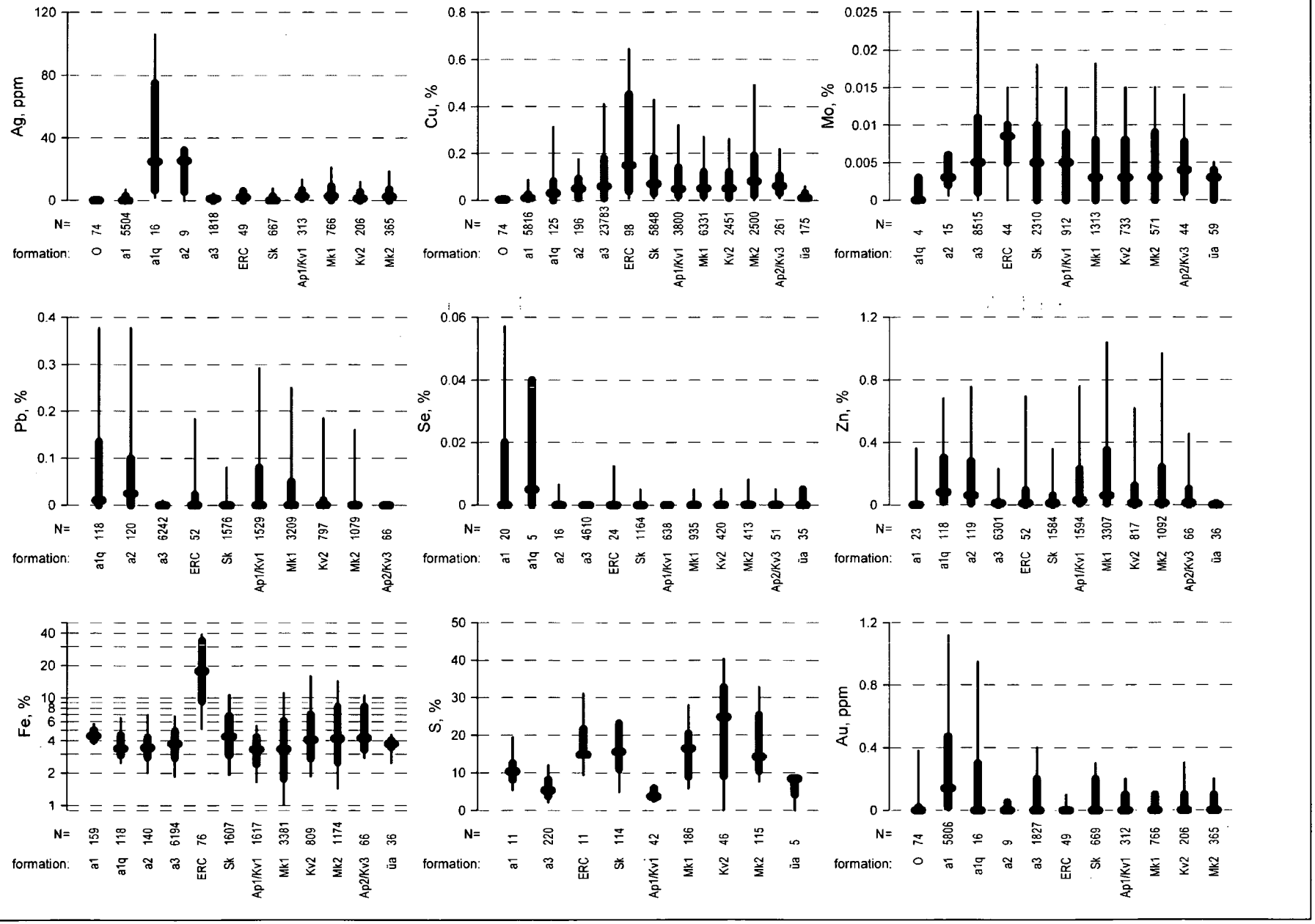

Fig. 8. Common values of ore components within rock-formations. Thin bars extend from the 10th to the 90th percentiles. Thick bars represent interquartile ranges. Knots on the bars represent the medians. N stands for the number of valid values.

Comparing the extreme values (Fig. 9) with the common ones (Fig. 8) demonstrates, in a way, a strength of the given representation of distributions, namely, an ability to reveal possible significant differences in the relative magnitude of values. For example, a1 has the highest extremes in Ag, whereas its common values are low. Or, although Ap1/Kv1 has a few (9, actually) high Se values, the bulk of the analyses yielded a value below detection limit. Similarly, a large part of the Cu values in ERC are high, the highest values in the dataset, however, belong to other formations (Mk2, Mk1 and a1). On the other hand, there are cases when the extreme values suggest the same conclusion, e.g. Zn exhibits similar sets of ranges, regarding both the extreme and the common subsets. Or, in both subsets it is probably S the most variable across the formations (which, otherwise, may partly be due to the low number of analyses).

Distributions within depth-zones

No matter how important tectonic processes have taken place since the Paleogene in the surrounding areas, the structure of the deposit in terms of position of rock bodies has not been changed significantly. Hence, vertical zoning detectable in the main characteristics of statistical distributions is expected to hint on some basic features of the ore-forming process. This expectation may also be justified by the fact that considering only the main ore minerals, the following very rough vertical distribution can be outlined: down to the depth of +100m a.s.l. association of (epithermal) enargite-luzonite-pyrite-Au; between -300m and -900m (porphyry-related, mesothermal) chalcopyrite-molybdenite(sphalerite)-pyrite; between -500m and -1100m (skarn-metasomatic, mesothermal) chalcopyrite-sphalerite-pyrite; and in several depth intervals, importantly close to the surface and at +100m, (mesothermal) galena-sphalerite-gray copper-pyrite. This is a very generalized picture but can be derived from the related studies, e.g. Gagyi Pálffy Sr. et al. (1971) and Gatter et al. (1999). In the present work, vertical intervals with a thickness of 200 m were chosen, and distribution plots produced for each.

Table 3. Common values within rock-formations.

	Ag ppm	Cu %	Mo %	Pb %	Se %	Zn %	Fe %	S %	Au ppm
O	0	0.0024							0
	0	0.0027							0
	0	0.0037							0.021
a1	0	0.005			0	0	4.0	8.2	0.02
	0	0.009			0	0	4.4	10.3	0.14
	3.0	0.026			0.02	0	5.0	12.5	0.47
a1q	6.8	0	0	0	0	0.02	2.9		0
	24.9	0.03	0	0.010	0.005	0.08	3.4		0
	75.2	0.08	0.003	0.135	0.040	0.30	4.5		0.3
a2	5.9	0.01	0.002	0	0	0.01	2.8		0
	25.6	0.05	0.003	0.025	0	0.06	3.4		0
	32.1	0.09	0.006	0.100	0	0.28	4.3		0.05
a3	0	0.01	0.001	0	0	0	2.8	3.8	0
	1.2	0.06	0.005	0	0	0.01	3.8	5.3	0
	2.1	0.18	0.011	0	0	0.02	4.9	8.2	0.2
ERC	0	0.04	0.005	0	0	0	9.4	14.8	0
	2.1	0.15	0.009	0	0	0.010	17.8	14.8	0
	6.0	0.45	0.010	0.023	0	0.095	34.0	21.7	0
Sk	0	0.03	0	0	0	0	3.0	11.1	0
	0	0.07	0.005	0	0	0.01	4.4	15.6	0
	2.8	0.18	0.010	0	0	0.06	6.8	23.2	0.2
Ap1/Kv1	1.1	0.02	0	0	0	0.01	2.4	3.2	0
	2.5	0.05	0.005	0	0	0.03	3.3	3.7	0
	6.5	0.14	0.009	0.08	0	0.23	4.3	5.9	0.1
Mk1	0	0.02	0	0	0	0.01	1.8	8.9	0
	2.7	0.05	0.003	0	0	0.06	3.3	16.5	0
	9.0	0.12	0.008	0.05	0	0.35	6.1	20.4	0.1
Kv2	0	0.01	0	0	0	0	2.7	9.1	0
	1.2	0.05	0.003	0	0	0.01	4.1	24.8	0
	5.4	0.12	0.008	0.01	0	0.12	7.0	32.7	0.1
Mk2	0	0.02	0	0	0	0	2.5	10.5	0
	2.5	0.08	0.003	0	0	0.01	4.2	14.3	0
	7.2	0.19	0.009	0	0	0.24	8.2	25.4	0.1
Ap2/Kv3		0.03	0.001	0	0	0	3.3		
		0.06	0.004	0	0	0.01	4.2		
		0.11	0.008	0	0	0.1	8.3		
üa		0.01	0		0	0	3.5	4.2	
		0.01	0.003		0	0	3.8	8.5	
		0.03	0.004		0.005	0.01	4.0	8.5	

Each triplet represents the 25th percentile, the median, and the 75th percentile.

And indeed, all charts of distributions of the common values (Fig. 10), together with the tabulated data (Table 4), reveal some kind of vertical zoning. Ag, Pb, and Zn show a general decrease towards the depth. Mo exhibits an opposite tendency, and Fe, too, except for the uppermost zone where it also has slightly elevated values. Although with some differences in the relative magnitudes, Cu, S, and Au show a nice wavy change: first decrease, then grow, and, at the end—in the deepest zones—decrease again. The detection limit for Se was obviously too low, it has a few elevated common values however in the uppermost zone.

Just as with the deposit-parts and rock-formations, here too, the extreme values (Fig. 11) do not unequivocally correlate with the common values. Behavior of the two sets of distribution ranges is identical in the case of S, similar, maybe with some disturbances, at Ag, Cu, Mo and Au, notably different at Se, and Fe, and essentially opposite at Pb and Zn. One might pick up zones where the range of extreme

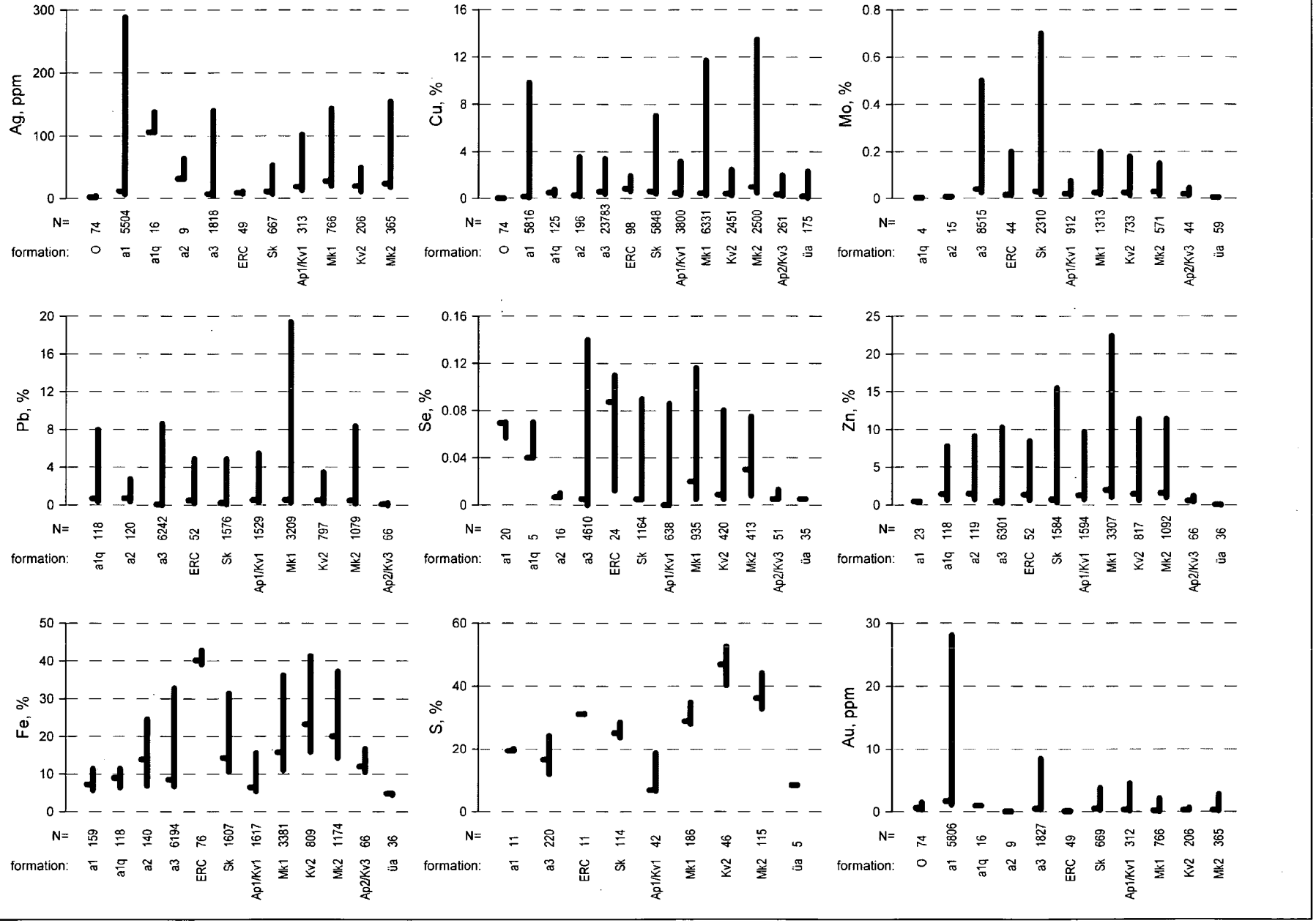

Fig. 9. Extreme values of ore components within rock-formations. Thick bars extend from the 90th percentiles to the measured maxima. Horizontal ticks on the bars represent the 95th percentiles. N stands for the number of valid values.

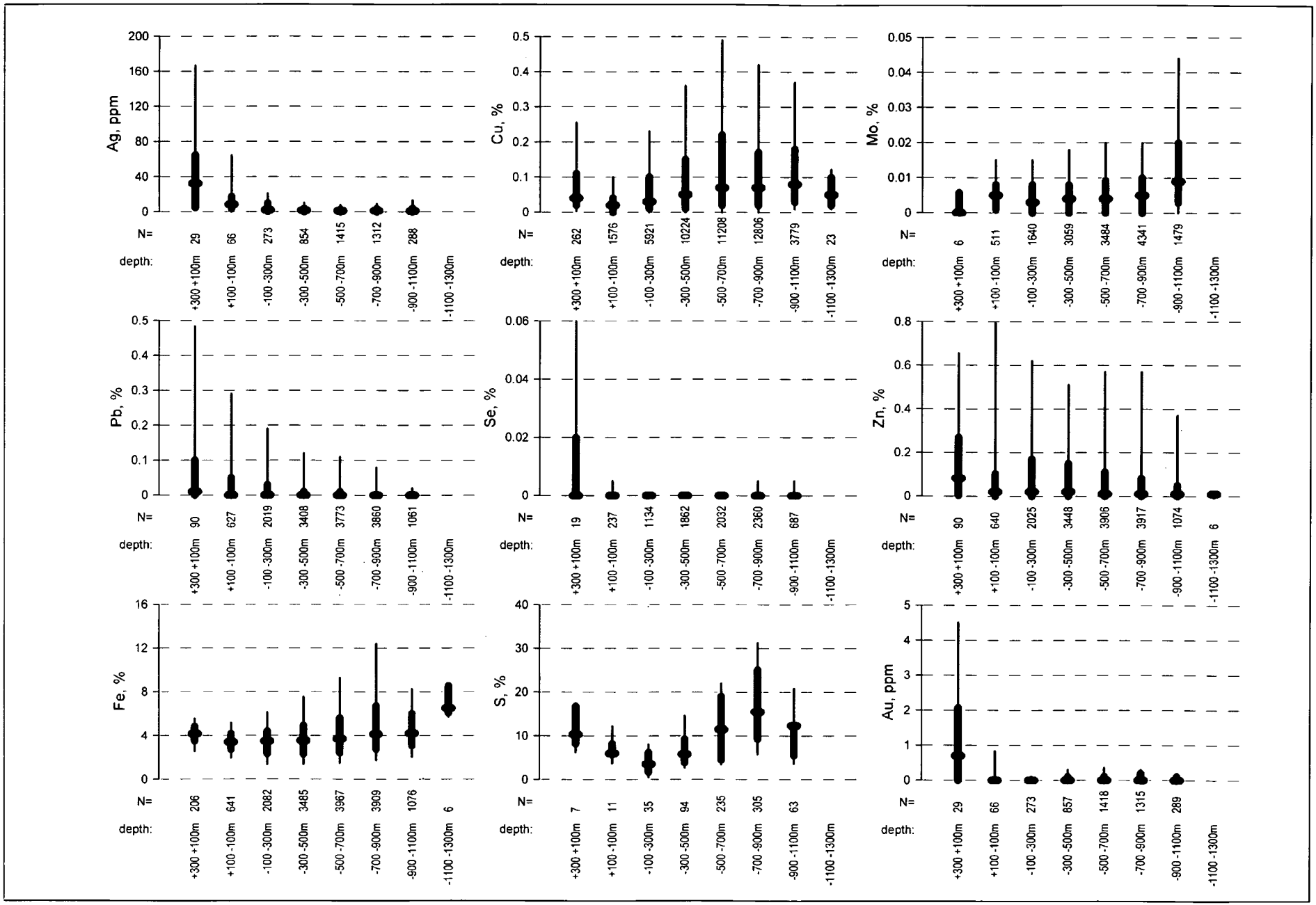

Fig. 10. Common values of ore components within depth-zones. Thin bars extend from the 10th to the 90th percentiles. Thick bars represent interquartile ranges. Knots on the bars represent the medians. N stands for the number of valid values.

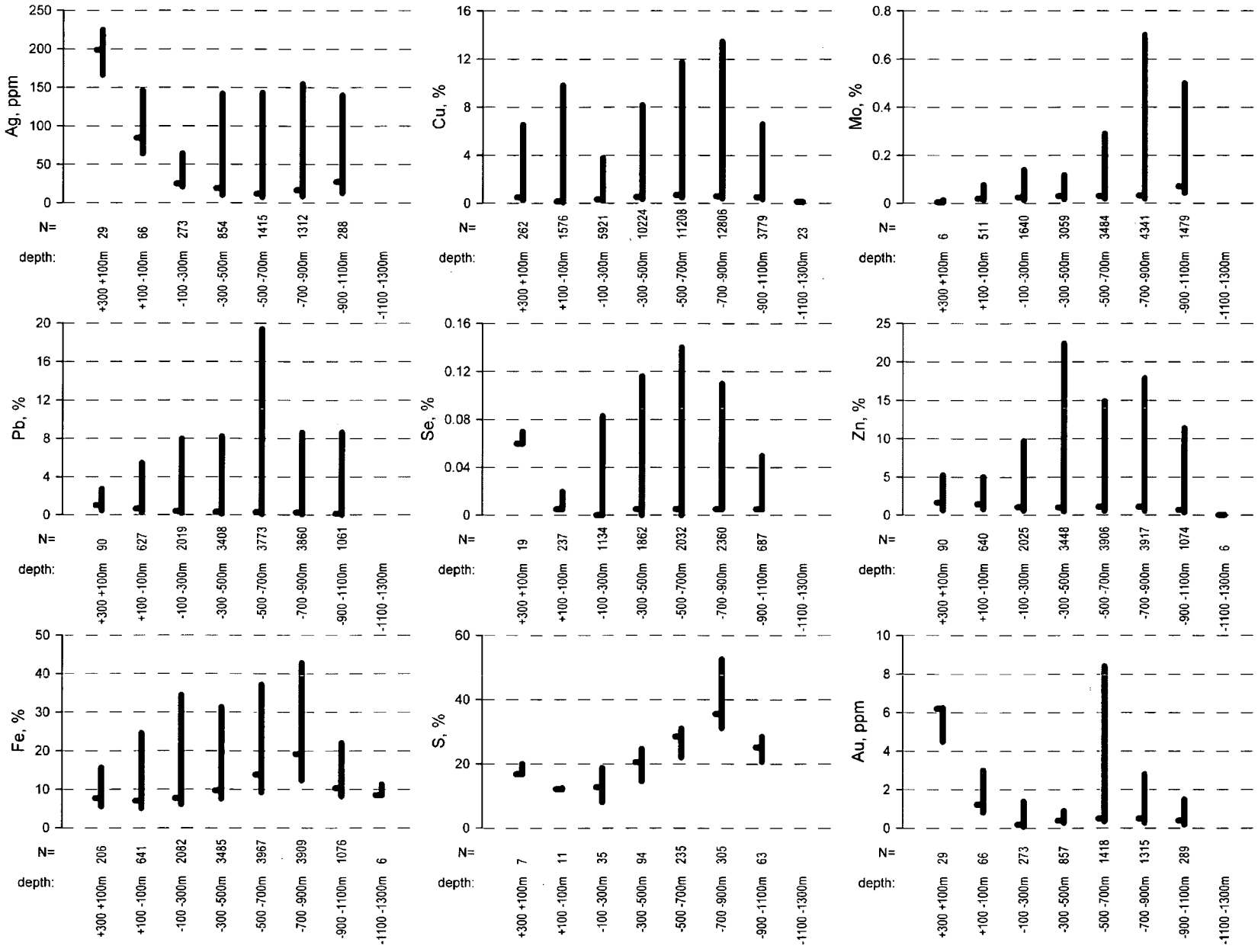

Fig. 11. Extreme values of ore components within depth-zones. Thick bars extend from the 90th percentiles to the measured maxima. Horizontal ticks on the bars represent the 95th percentiles. N stands for the number of valid values.

values in one or two components has a spectacularly high upper limit. Clear examples are Zone "+300 +100m" regarding Ag, and Zone "-500 -700m" with Pb and Au. Taking into consideration the relatively large number of data, the above quantitative features surely have a certain economic relevance.

Discussion

We never feel the number of data is optimal. Because, especially when dealing with mineral deposits, if the amount of numerical data is very low, the conclusions seem to contain too much interpretation; if there are a lot of quantitative data, nothings seems 100% true as we always have contradicting values. Statistics obviously helps, although if we are honest, the way we use statistics is always charged with some subjectivity. Nevertheless, the need for conclusions requires a purposeful evaluation. Below, a few points are discussed, helping to more appropriately treat the observations presented in the given study.

In Fig. 6 distributions are given also for the entire deposit ('ALL'). Although numerically its plots are correct, their mainly descriptive character should be emphasized, be-cause they merge otherwise separable populations. For example, Cu is very different in Deep-A and in Lahóca which is masked in ALL. In addition, significant differences in the size of subsets may cause a 'loss' of one of them when combined, as with S. Nonetheless, if someone is interested in the most common values of ore components in the ore field, these charts together with Table 1 may be used.

Understandably, the set of distributions of the common values within the formations (Fig. 8) and that within the depth-zones (Fig. 10) show visually perceptible elements of correlation. Ag, Se and Au have elevated common values in units located in higher spatial position. Cu is characterized with slightly elevated common values in units representing intermediate depths of the sampled space domain. While there is consi-derable overlapping in the distributions across the units for most components, S tends to reveal somewhat more specialized units in this sense.

Concerning all the given distributions, in principle, when the common values and extreme values represent two distinct populations, a limit between them could easily be defined. This may be a rare case anyway, but at the given basic level of description it is not necessary. However, the goodness of the chosen separation (at the 90th percentile) may indirectly be confirmed considering the fact that the relative behavior of the common and extreme values is realistic: in cases similar, in other cases different, or even reverse, corresponding to the properties and relative importance of the ore-forming processes. In such a complex geologic object this is what may intuitively be expected.

This huge dataset may (and hopefully will) be a basis of more sophisticated statistical analyses. Here, the representation and evaluation of the data are deliberately kept as unfussy as possible, because these basic descriptive statistics, calculated for the given data for the first time, are meant also for comparisons with analogous deposits.

The investigated subdividing schemes may seem formalized or generalized (and the others analyzed in the project but not presented here, too). Indeed, from the point of view of ore mineralizations, for example, the cleverest subdivision would be that one where each type of the occurring ore mineralizations is individually represented. And as was indicated, there are quite a number of different types present, in cases with a distinct structural character (strata-bound, depth-controlled, cutting, etc.). The problem is, in this particular case, that the analyzed rock/ore samples were not (and could not be) regularly classified in a corresponding way during the exploration. And this is true more generally as well: we can only deal with subdivisions for which the pertinent information is registered in, or can be generated from, the database, or at least the technical documentation.

At the end, we have to remember again, that this is statistics, i.e. it may mask many details, be too general from certain points of view, nevertheless, the features it reveals are numerically established observations.

Table 4. Common values within depth-zones

	Ag ppm	Cu %	Mo %	Pb %	Se %	Zn %	Fe %	S %	Au ppm
+300 +100m	4.9	0.02	0	0	0	0.004	3.5	8.2	0
	32.1	0.04	0	0.01	0	0.082	4.2	10.3	0.7
	64.7	0.11	0.006	0.10	0.02	0.270	4.8	16.8	2.1
+100 –100m	3.7	0	0.001	0	0	0	2.8	5.8	0
	8.2	0.02	0.005	0	0	0.02	3.4	6.0	0
	17.3	0.04	0.008	0.05	0	0.10	4.2	8.2	0
–100 –300m	0.3	0.01	0	0	0	0	2.3	1.7	0
	2.0	0.03	0.003	0	0	0.02	3.5	3.6	0
	9.9	0.10	0.008	0.03	0	0.17	4.4	6.2	0
–300 –500m	0	0.01	0	0	0	0	2.3	3.9	0
	1.6	0.05	0.004	0	0	0.02	3.6	5.8	0
	3.6	0.15	0.008	0.01	0	0.15	4.9	9.2	0.1
–500 –700m	0	0.02	0	0	0	0	2.4	4.6	0
	1.1	0.07	0.004	0	0	0.01	3.7	11.5	0
	2.9	0.22	0.009	0.01	0	0.11	5.6	19.0	0.1
–700 –900m	0	0.02	0	0	0	0	2.8	9.4	0
	1.4	0.07	0.005	0	0	0.01	4.1	15.5	0
	4.0	0.17	0.010	0	0	0.08	6.7	25.0	0.2
–900 –1100m	0	0.03	0.003	0	0	0	3.1	5.6	0
	1.2	0.08	0.009	0	0	0.01	4.2	12.4	0
	4.1	0.18	0.020	0	0	0.05	6.0	12.5	0.1
–1100 –1300m		0.02				0.008	6.1		
		0.05				0.010	6.5		
		0.10				0.010	8.5		

Each triplet represents the 25th percentile, the median, and the 75th percentile.

Conclusions

Appropriately selected sets of percentiles, either shown on a purposeful graph, or suitably tabulated, serve as a concise and informative representation of statistical frequency distributions of diverse—in cases very large—amounts of values. Graphs made separately for the common, and for the extreme values are effective even in the case of complex distributions. The relative levels of the common, and those of the extreme values within a particular set of the analyzed units (deposit-parts, rock-formations, or depth-zones) may, or may not correlate. The latter case may obviously occur when the two types of values do not belong to the same natural population.

Comparing the deposit-parts, Ag, Cu, Pb, S and Au expose major differences among them—mainly in terms of the common values. Regarding Mo, Zn, and Fe, the three parts of Recsk Deep are not very different. The richest in Au is Lahóca (with common values between 0.02 and 0.46 ppm, and extremes close to 30 ppm), whilst in Cu it is Deep-A (common values between 0.03-0.23%, extremes over 10%).

For most of the rock-formations, distributions of the common values of the analyzed ore components are not peculiar relative to each other. Exceptions are: sulphide ore ('ERC') with high Fe (9.4-34.0%) and Cu (0.04-0.45%); upper member of the Paleogene stratovolcanic series ('a1') with high Se (up to 0.02%) and Au (0.02-0.47 ppm), and low Zn (virtually nil); and middle member of the stratovolcanic series ('a1q') with high Ag (6.8-75.2 ppm), Pb (up to 0.14%), Se (up to 0.04%) and Au (up to 0.3 ppm). Regarding the extreme values, partly different specialties should be noted. Namely, the highest extremes in Ag (close to 300 ppm) belong to the upper member of the Paleogene stratovolcanic series ('a1'); all the detectable Se values in the Paleogene intrusive complex ('a3') and in the Triassic upper shale group ('Ap1/Kv1') are remarkably high (up to 0.14% and 0.08%, respectively); and the highest Cu values are measured in the Triassic lower limestone ('Mk2', up to about 14%), the Triassic upper limestone ('Mk1', up to 12%) and the upper member of the Paleogene stratovolcanic series ('a1', up to 10%). On the other hand, the common and extreme values of Zn result in similar patterns of ranges.

In spite of the fact that the analyzed set of depth-zones is more or less arbitrary, distributions of the common values expose a notable vertical zoning. Towards the depth, Ag, Pb, and Zn show a general decrease, while Mo and Fe exhibit an opposite tendency. Cu, S, and Au display a nice wavy change: first decrease, then grow, and in the deepest zones decrease again. Based on the extreme values, zones can be named where one or two components have a spectacularly high upper limit: Zone "+300 +100m" with Ag nearing 250 ppm, and Zone "-500 -700m" with Pb of up to 20% and Au exceeding 8 ppm.

At last, a few general remarks follow. Within each of the three analyzed sets of units, S is the most variable component in the sense that it reveals the most conspicuous differences across the units. Fe can be regarded as the most regular component in terms of consistency of its plots, and by the undisturbed two-tailed shape of its presumable frequency distribution curves. Although its elevated values in the dataset are noteworthy, the detection limit for Se was obviously too low to provide a representative picture of its distributions.

Acknowledgements

This work was financed by Projects T 037581 and T 037619 of the Hungarian Research Fund (OTKA).

References

Baksa, Cs. (1988): The genetic frameworks of the Recsk ore genesis. Acta Mineralogica-Petrographica, **26**, 87–97.

Baksa, Cs., Cseh Németh, J., Csillag, J., Földessy, J. and Zelenka, T. (1980): The Recsk Porphyry and Skarn Copper Deposit, Hungary. In Janković, S. and Sillitoe, R.H. (eds.): European Copper Deposits. Society for Geology Applied to Mineral Deposits (SGA) Spec. Pub., **1**, 73–76.

Baksa, Cs., Szebényi, G., Gasztonyi, É., Polgár, I., Kun, B., Szilágyi, G., Cseh Németh, J., Holló, S., Csillag, J. et al. (1988): A recski mélyszinti színesfémérc előfordulás bányabeli részletes fázisú földtani kutatásának össszefoglaló földtani jelentése és készletszámítása. 1/1-4, 2/1-4 kötet (Reserve estimation and final geologic report on the detailed underground exploration of the base metal ore deposit of Recsk Deep, vol. 1/1-4, 2/1-4). Recsk (1986, 1988, 1990). MGSZ OFGA Budapest T.15507. (in Hungarian)

Cseh Németh, J. (1975): A recski mélyszinti színesfémérc előfordulás és annak teleptani, ércföldtani képe (Deep-seated base metal ore occurrence of Recsk: geological pattern of ore accumulation). Földtani Közlöny, **105**, 692–708. (in Hungarian)

Cseh Németh, J. (1988): A recski mélyszinti polimetallikus ércek reménybeli vagyonának újraértékelése és készletszámítása (Reevaluation and reserve estimation of polymetallic ores of Recsk Deep). OÉÁ Technical Report, Budapest. (in Hungarian)

Cseh Németh, J., Baksa, Cs., Földessy, J., Földessy-Járányi, K., Gasztonyi, É., Verő, L., Ráner, G., Taba, S., Balla, Z., Schönviszky, L., Karas, Gy., Szalma, S., Szongoth, G., Viola, B., Zelenka, T., Szilágyi, G. et al. (1984): A recski mélyszinti előfordulás külszíni mélyfúrásos kutatásának összefoglaló földtani jelentése és készletszámítása (Reserve estimation and final geologic report on the surface drilling exploration of the base metal ore deposit of Recsk Deep). OÉÁ–KBFI Technical Report, Budapest. (in Hungarian)

Csillag, J. (1975): A recski terület magmás hatásra átalakult képzödményei (Rocks transformed upon magmatic effect in the Recsk area, Hungary). Földtani Közlöny, **105**, 646–671. (in Hungarian)

Csillag, J., Földessy, J., Zelenka T. and Balázs, E. (1983): The plate tectonic setting of the Eocene volcanic belt in the Carpathian Basin. In: Bisztricsány, E. and Szeidovitz, Gy. (eds.): Proceedings 17th Assembly European Seismological Commission, Budapest, 589–599.

Csongrádi, J. (1975): A recski mélyszinti színesfém-ércesedés jellemzése ércmikroszkópiai vizsgálatok alapján (Characterization of the deep-seated base metal ore mineralization of Recsk on the basis of ore-microscopic analyses). Földtani Közlöny, **105**, 672–691. (in Hungarian)

Csontos, L. (1995): Tertiary tectonic evolution of the Intra-Carpathian area: a review. Acta Vulcanologica, **7/2**, 1–13.

Csontos, L. and Nagymarosy, A. (1998): The Mid-Hungarian line: a zone of repeated tectonic inversions. Tectonophysics, 297, 51–71.

FÖLDESSY, J. (1997): A recski Lahóca aranyérc elõfordulás (The Lahóca gold deposit at Recsk). Földtani Kutatás, **34/2**, 12–15.

FÖLDESSY, J. (1975): A recski rétegvulkáni andezitösszlet (The stratovolcanic andesite formation of Recsk). Földtani Közlöny, **105**, 625–645. (in Hungarian)

FÖLDESSY, J., SERES-HARTAI, É. AND SZEBÉNYI, G. (2004): Distribution of gold mineralization in the Recsk ore complex, NE Hungary. Acta Geologica Hungarica, **47/2-3**, 247–258.

FÖLDESSY, J., LESS, GY., ZELENKA, T. AND SERES-HARTAI, É. (2006): A recski (ÉK-Magyarország) paleogén vulkáni-üledékes összlet fejlődéstörténeti vázlata (Draft of history of the Recsk (NE-Hungary) Paleogene volcano-sedimentry complex). Bányászati, Kohászati és Földtani Konferencia, Sepsiszentgyörgy, 2006, 139–144. (in Hungarian)

FÖLDESSY-JÁRÁNYI, K. (1975): A recski mélyszinti alaphegységi üledékes képződmények (Deep-seated sedimentary rocks of the basement at Recsk). Földtani Közlöny, **105**, 598–611. (in Hungarian)

GAGYI PÁLFFY SR., A., CSEH NÉMETH, J., ZELENKA, T., GAGYI PÁLFFY JR., A., LÁZÁR, B., CSILLAG, J., NAGY, I., SZILÁGYI, G. ET AL. (1971): A recski mélyszinti ércelőfordulás külszíni mélyfúrásos kutatásának összefoglaló földtani jelentése és készletszámítása (Reserve estimation and final geologic report on the surface drilling exploration of the Recsk Deep ore deposit). OÉÁ Technical Report, Budapest.

GATTER, I., MOLNÁR, F., FÖLDESSY, J., ZELENKA, T., KISS, J. AND SZEBÉNYI, G. (1999): High- and Low-Sulphidation Epithermal Mineralization of the Mátra Mountains, Northeast Hungary. In Molnár, F., Lexa, J. and Hedenquist, J.W. (eds.): Epithermal Mineralization of the Western Carpathians. Guidebook Prepared for Society of Economic Geologists Field Conference, 4-13 September, 1999. Society of Economic Geologists Guidebook Series, **31**, 155–179.

HENLEY, S. (1981): Nonparametric Geostatistics. Applied Science Publishers, London, 1–145.

KOMLÓSSY, GY. (ED.), CSILLAG, J., GASZTONYI, É., FÖLDESSY, J., POLGÁR, I., SZEBÉNYI, G., SZENDREY, A. AND SZILÁGYI, G. (2000): Recsk II. (mélyszint): egységesített földtani zárójelentése (Unified final geologic report on Recsk II. (Recsk Deep)). Geo-Kom Kft., Budapest, Recski Ércbányák Rt., Recsk. MGSZ OFGA Budapest T.20093. (in Hungarian)

LESS, GY., BÁLDI-BEKE, M., ZELENKA, T., FÖLDESSY, J., KOLLÁNYI, K. AND KERTÉSZ, B. (2005): A Recski Andezit korának revíziója (Revision of the age of the Recsk Andesite). 8. Magyar Őslénytani Vándorgyűlés, Hátszeg-Őraljaboldogfalva, 2005, 17–18. (in Hungarian)

MARSAL, D. (1987): Statistics for Geoscientists. Pergamon Press, Oxford, 1–175.

Ó.KOVÁCS, L. AND KOVÁCS, P.G. (2002): Statistical review of major element data from the Miocene tuffs in Hungary. Geoinformatics, Japan Soc. Geoinformatics, Nara, **13/3**, 153–166.

ROCK, N.M.S. (1988): Summary statistics in geochemistry: a study of the performance of robust estimates. Mathematical Geology, **20/3**, 243–275.

SERES-HARTAI, É. AND FÖLDESSY, J. (2000): Appearance of gold in some drillholes of the Lahóca epithermal deposit. Acta Mineralogica-Petrographica, 1999, supplementum, 2000, 41.

SERES-HARTAI, É., FÖLDESSY, J. AND KOVÁCS, Á. (2001): Mineralogy and genetic aspects of gold in the Lahóca (Recsk, Hungary): high sulfidation type epithermal deposit. Acta Montanistica Slovaca, **6/1**, 19–26.

SPSS (1998a): SPSS Base 8.0 User's Guide. SPSS, Chicago, 1–701.

SPSS (1998b): SPSS Base 8.0 Applications Guide. SPSS, Chicago, 1–372.

SZEBÉNYI, G., GASZTONYI, É., BAKSA, CS. AND ZELENKA, T. (1985): Полиметаллические руды скарного-метасоматической зоны месторождения Речк (Венгрия) (Polymetallic ores of the skarn-metasomatic zone of the Recsk ore deposit, Hungary). Proceeding Reports of the XIIIth Congress of KBGA 1985, Part II, 123–126. Published by Geological Institute, Krakow, Poland. (in Russian)

SZEBÉNYI, G. (2000): A recski mélyszinti ércelőfordulás bányabeli kutatásának módszertani és földtani-teleptani sajátosságai (Methodological and geologic-metallogenic features of underground exploration of Recsk Deep). Bányászati és Kohászati Lapok, Bányászat, **133/1**, 136–143. (in Hungarian)

ZELENKA, T. AND SZEBÉNYI, G. (2002): A Recsk mélyszinti színesfémérc-lelőhely földtani kutatástörténete (Geologic exploration history of the base metal ore deposit of Recsk Deep). Közlemények a magyarországi ásványi nyersanyagok történetéből, XIII. (Érckutatások Magyarországon a 20. században), Miskolc, 169–198. (in Hungarian)

Received: September 12, 2006; accepted: December 7, 2007

Acta Mineralogica-Petrographica, Szeged 2006–2007, Vol. 47, pp. 17-24

ACTA Mineralogica Petrographica

MICRO-RAMAN SPECTROSCOPY OF REIDITE AS AN IMPACT-INDUCED HIGH PRESSURE POLYMORPH OF ZIRCON: EXPERIMENTAL INVESTIGATION AND ATTEMPT TO APPLICATION

ARNOLD GUCSIK

Max Planck Institute for Chemistry, Department of Geochemistry, Joh.-J.-Becherweg 27. Mainz, D-55128, Germany
e-mail: gucsik@mpch-mainz.mpg.de

ABSTRACT

Thorough understanding of the shock metamorphic signatures of zircon will provide a basis for the application of this mineral as a powerful tool for the study or recognition of old, deeply eroded, and metamorphically overprinted impact structures and formations. This study of the micro-Raman spectroscopic signatures of naturally shocked (Ries Crater, Germany) zircon crystals and experimentally (38, 40, 60, and 80 GPa) shock-metamorphosed single crystals of zircon contributes to the understanding of the formation of shock-induced microdeformations and phase transformation in zircon under very high, dynamic pressures. The purpose of this investigation is to further investigate the capability of the Raman spectroscopy to document shock deformation and to determine whether specific Raman effects in zircon/scheelite-structure (reidite) can be utilized to determine particular shock pressure stages.

Key words: zircon, high-pressure polymorph, reidite, shock metamorphism, Raman spectroscopy

INTRODUCTION

Zircon is a highly refractory and weathering-resistant mineral that has proven useful as a shock level indicator of shock metamorphism in the study of impact structures and formations that are old, deeply eroded, and metamorphically overprinted (e.g., Bohor et al. 1993, Kamo et al. 1996, Krogh et al. 1996, Reimold et al. 2002, Wittmann et al. 2006). Zircon has advantages compared to quartz or other shock-metamorphosed rock-forming minerals that have been widely used as impact indicators, but are far less refractory than zircon. Furthermore, U-Pb dating of zircon can provide constraints on the ages of impact events or deposition of impact formations (e.g., Deutsch and Schärer 1990, Kamo et al. 1996, and references therein). Table 1 shows the main physical and optical properties of zircon, baddaleyite, and reidite.

Shock metamorphic effects in zircon have been described from a number of impact environments, including confirmed impact structures (e.g., Kamo and Krogh 1995, Krogh et al. 1996, Kamo et al. 1996, Gibson et al. 1997, Glass and Liu 2001), the Cretaceous-Tertiary boundary (Bohor et al. 1993, Kamo and Krogh 1995), and the Upper Eocene impact ejecta layer (e.g., Glass and Liu 2001), as well as from tektites (Deloule et al.

Table 1. Basic physical and optical properties of zircon, baddeleyite and reidite.

Chemical Formula (name)	**$ZrSiO_4$** (zircon)	***ZrO_2*** (baddeleyeite)	***$ZrSiO_4$*** (reidite)
Z (formula units per unit cell)	4	4	4
Crystal System	*Tetragonal* Ditetragonal Dipyramidal (H-B Symbol: 4/m 2/m 2/m)	*Monoclinic-* Prismatic (H-B Symbol: 2/m)	*Tetragonal-* Dipyramidal (H-B Symbol: 4/m)
Space Group	$I\,4_1/amd$	$P\,2_1/c$	$I\,4_1/a$
Cell Dimensions (Á)	a=6.604 c=5.979	a=5.1477 b=5.203 c=5.3156	a=4.738 c=10.506
Axial Ratios	a:c=1:0.90536	a:b:c=0.9893:1:1.0216	a:c=1:2.21739
Density (g/cm^3)	4.6-4.7, average=4.65	5.5-6, average=5.75	5.2
Optical Data	Uniaxial (-) ε=1.92-1.96 ω=1.967-2.015 bire=0.047-0-055	Biaxial (-) Refractive index varies from 2.13 to 2.20 bire=0.07	Uniaxial (+) ε=1.655 ω=1.64 bire=0.015
Cleavage	[001] Indistinct	[001] Distinct	None
Fracture	Uneven-Flat surfaces (not cleavage) fractured ina n uneven pattern	Brittle-Conchoidal-Very brittle fracture producing small, conchoidal fragments	Brittle-Irregular-Very brittle fracture producing irregular fragments

Data from: http://euromin.w3sites.net/mineraux, and http://webmineral.com/AtoZ/IndexB.shtml

2001, Glass and Liu 2001). Shock-induced microdeformation in experimentally shock-deformed zircon crystals has also been reported (Deutsch and Schärer 1990, Leroux et al. 1999, Gucsik et al. 2002).

The phase transformation from the zircon crystal structure (ZrSiO4) to a scheelite (CaWO4)-structure phase as reidite was described in shock-metamorphosed zircon by Kusaba et al. (1985) to begin at about 30 GPa and to be complete at around 53 GPa. These observations were confirmed by Leroux et al. (1999) through their TEM investigations of experimentally shocked zircon. More recently, according to Scott et al. (2002), high-pressure X-ray data show that a small amount of residual zircon-structured material remained at 39.1 GPa on ZrSiO4-scheelite material. Glass et al. (2002) found the scheelite-type phase (reidite) in zircon samples from marine sediments from an upper Eocene impact ejecta layer sampled near New Jersey and Barbados. They named this mineral phase 'reidite' after Alan F. Reid, who first produced this high shock-pressure polymorph of zircon (Reid and Ringwood 1969).

This review study has been based on Gucsik et al. (2004) published In Dypvik, H., Burchell, M., Claeys, Ph. (eds.): Cratering in Marine Environments and on Ice, Springer-Verlag, Heidelberg, 281-322, emphasizing manly the micro-Raman spectroscopy and its application to study of high-pressure polymorphs associated to the impact terrestrial cratering record.

Samples and experimental procedures

Two natural zircon crystals of about 1 cm length and 0.5 and 0.7 cm width from Australia (sample A) and from Sri Lanka (sample B), respectively, were experimentally shock deformed at shock pressures between 38 and 80 GPa at room temperature. Shock recovery experiments were performed on such plates using the shock reverberation technique at the Ernst-Mach-Institute, Germany (e.g., Deutsch and Schärer 1990). For this study, polished thin sections, produced from the experimentally shocked plates of zircon crystals (A and B sample sets), were utilized. However, only the specimens from A sample were selected for further CL- and Raman spectroscopic investigations, because the sections are of better quality than those from sample B. Carbon-coated, polished thin sections had been produced from all samples. The samples were first examined under a petrographic microscope. Raman spectra were obtained with a Renishaw RM1000 confocal micro-Raman spectrometer (at University of Vienna, Austria) with a 20 mW, 632 nm He-Ne laser excitation system and a thermo-electrically cooled CCD detector. The power of the laser beam on the sample was approximately 3 mW. Spectra were obtained in the range

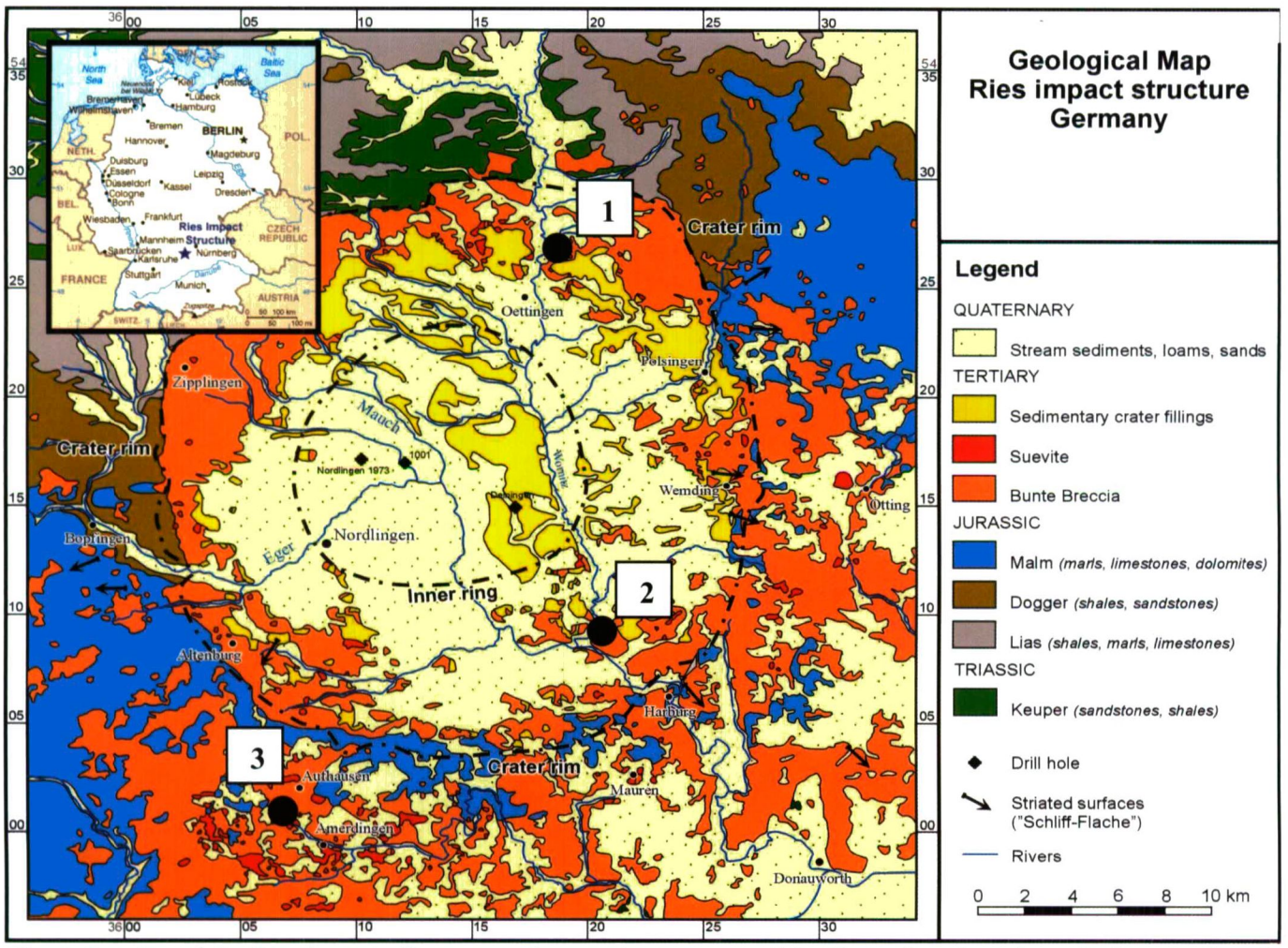

Fig. 1. Locality of the Ries basin in Germany and approximate extent of the Bunte Breccia and suevite breccia. Sample localities are indicated as ● 1=Aumühle, 2=Appertshofen, 3=Seelbronn (from Osinski et al. 2003).

100-1200 cm-1, with approximately thirty seconds total exposure time. The spectral resolution was 4 cm-1. Raman spectra were taken from 3 μm3 sample volume. Further details on the experimental procedure and samples can be found in Gucsik et al. (2004).

Regional geology of the Ries impact crater

The Ries (also called "Nördlinger Ries") is a complex impact structure, located in Southern Germany (centered at: N 48o53', E 10o37'), with a rim-to-rim diameter of about 26 km (e.g., Engelhardt 1990, Deutsch 1998). The well-preserved ejecta blanket (Geologische Karte des Rieses, Bayerisches Geologisches Landesamt, 1: 50 000, 1999) and intra-crater breccia lens offer excellent conditions for studies of terrestrial impact structures (e.g., Engelhardt 1990) (Fig. 1). According to the level of shock metamorphism, the ejecta from the Ries crater divided into two formations: (1) Low shock level (<10 GPa), represented by the Bunte Breccia (sediments from the upper 600 m of the target area), megablocks of sedimentary rocks (Upper Jurassic limestone blocks occurring in the Megablock zone), and megablocks and monomict breccias derived from the crystalline basement (from the surrounding area of the Inner Crater). (2) High shock level (>10 GPa), represented by polymict crystalline breccias (are common in the Megablock Zone), fall-out suevites, crater suevite, and tektites (moldavites) (Engelhardt 1990). A 15 Ma age was determined for the Ries impact by the 40Ar-39Ar method on impact glasses from suevitic impact breccias (Staudacher et al. 1982). The present structure formed as the result of the collapse of the transient impact crater by subsurface readjustment, which caused upward movement of the initial crater bottom and slumping of parts of the primary rim into the crater, producing a compensating ring depression (the so-called Megablock Zone) (Engelhardt 1990). The pre-impact stratigraphy of the target region includes a crystalline basement of pre-Variscan gneisses and amphibolites, and Variscan granite. These crystalline rocks were overlain by sedimentary rocks of Upper Jurassic (limestone), Middle Jurassic (sandstone, marlstone, limestone), Lower Jurassic (sandstone, marlstone, limestone), Upper Triassic (sandstone, siltstone, marlstone, claystone) and Lower Triassic (sandstone) age. The southern part of the target area was covered by ~25 m of unconsolidated Upper Miocene sands, marls and clays (Engelhardt 1990) (Fig. 2).

According to Stöffler (1974) and Engelhardt (1990), the stages of shock metamorphism in minerals from the impact formations of the Ries impact crater can be classified into six stages (known as 0, I, II, III, IV, and V) that are characterized by various elastic and plastic deformation phenomena as well as isotropization of minerals, the formation of high-pressure phases and the occurrence of mineral or bulk rock melting (Table 2).

Basics of Raman spectroscopy

According to Roberts and Beattie (1995), when a monochromatic beam of light illuminates a transparent medium (e.g., gas, liquid or solid), most of the light will traverse the

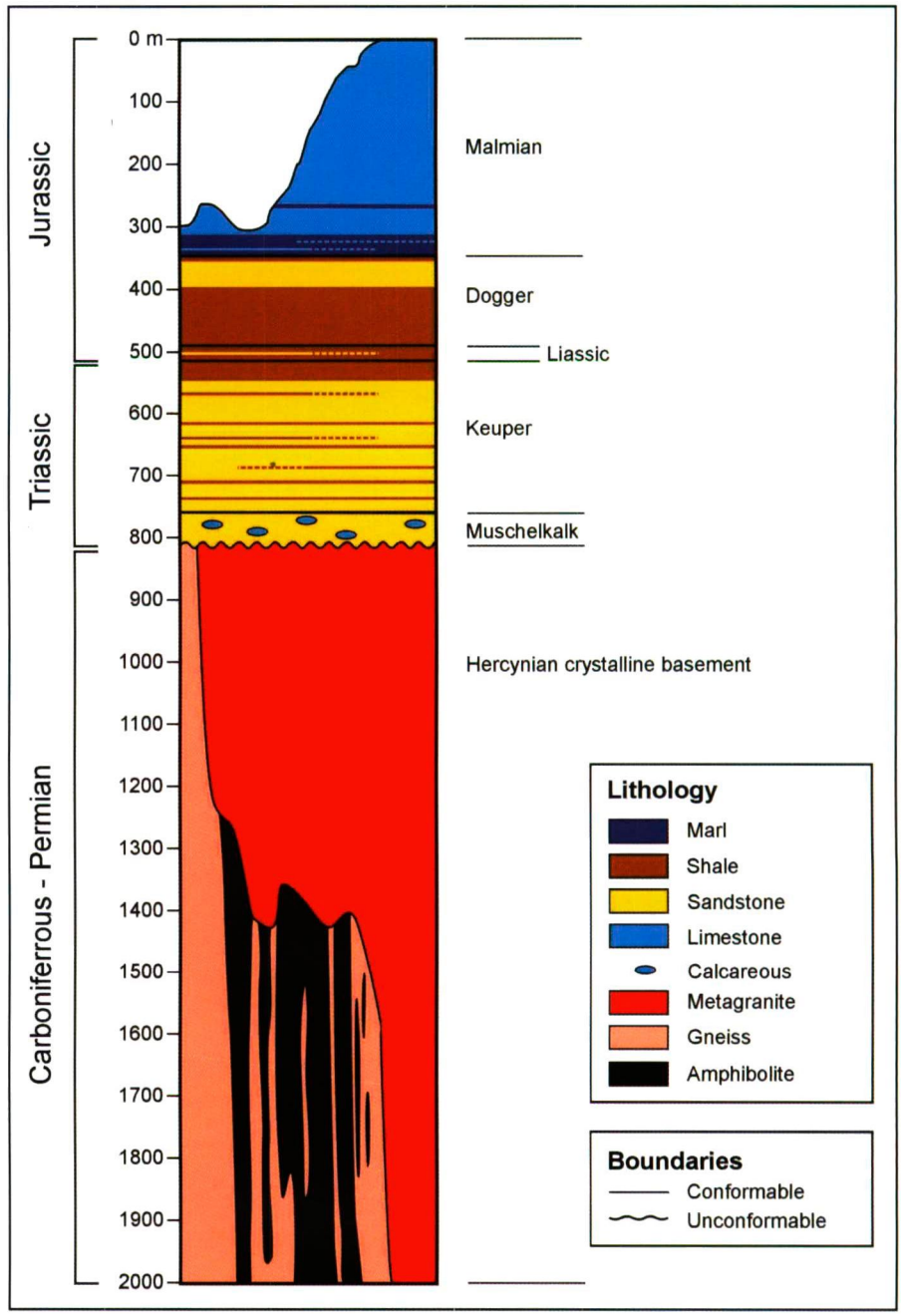

Fig. 2. The idealized stratigraphic sketch of the Ries carter exhibits the pre-and post impact stratigrapy (after Osinski et al. 2003).

sample without undergoing any changes. Approximately 10-3 of the incident intensity is scattered with the same frequency as that of the incident light source (elastic or Rayleigh scattering). Raman scattering ("Raman effect") occurs when, in addition to the Rayleigh scattering, about 10-6 of the incident intensity is scattered at new frequencies above and below the incident frequency. This effect was first documented by the Indian physicist Chandrasekhara Venkata Raman in 1928, who observed color changes in the scattered light of focused sunlight. The shifts in frequency from that of the incident radiation are independent of the exciting radiation and are characteristic of the species that gives rise to the scattering.

Raman transitions to lower frequency (i.e., red shifted bands) are referred to as Stokes lines, whereas transitions to higher frequency (i.e., blue shifted bands) are referred to as anti-Stokes lines. Stokes lines are normally much more intense than anti-Stokes lines, as the population of the ground state is usually very much greater than that of the excited state of the molecule. Not all molecular vibrations are Raman active. A Raman active vibration can be expected if the polarizability in a molecule is changed during the normal vibration (Roberts and Beattie 1995). The frequencies of vibrations depend upon the vibrating masses and the forces between them, including the anharmonic nature of interatomic and inter-and intramolecular interactions. If a phase transition occurs, the Raman selection rules, which ultimately depend on crystal and molecular symmetries, will also change (as well as forces) and new spectral features, characteristics for the new lattice, will appear (e.g., Williams and Knittle 1993, Nasdala et al. 1995). Thus, this method is not only of great help in elucidating crystal structures (e.g., McMillan and Hofmeister 1988), but can also be used as a method of qualitative analysis, e.g., in determining the presence of specific phases of small thin section areas without destroying them.

Table 2. Stages of shock metamorphism in the Ries impact structure, Germany (after Engelhardt, 1990).

Stage	Shock effects	Pressure (GPa)	Post-shock Temp. (°C)
0	Fragmentation; mosaicism; undulatory extinction; deformation bands in quartz; kinkbands in biotite; shatter cones	0-10	0-100
I	Planar elements in quartz; planar deformation lamellae in feldspar, amphibole and pyroxene; stishovite, coesite; kink bands in biotite	10-35	100-300
II	Diaplectic glasses of quartz and feldspar; deformation lamellae in amphibole and pyroxene; kinkbands in biotites	35-45	300-900
III	Selectively fused alakali-rich feldspar; diaplectic quartz glass; thermal decomposition of biotite and amphibole	45-50	900-1300
IV	Complete fusion of rocks (granitic composition); impact melts	60-80	1500-3000
V	Vaporization	>80	>3000

RAMAN SPECTROSCOPY OF EXPERIMENTALLY SHOCK-DEFORMED ZIRCON SAMPLES

The Raman spectra of the unshocked and experimentally shock-deformed zircon samples (38, 40, 60 and 80 GPa) show significant differences (Fig. 3). The Raman spectra of the unshocked samples (parallel) contain seven peaks at 202, 215, 225, 356, 439, 974, 1008 cm-1 (Fig. 3A) indicating the zircon-type structure (Williams and Knittle 1993, Kolesov 2001). Whereas all these peaks are characteristic for the zircon-type structure, the bands at 356 439, 974 and 1007 cm-1 appear most useful to distinguish this phase from the scheelite-type structure as reidite (Fig. 3A). It is important to note that the narrow line widths of the Raman bands of both unshocked samples indicate a highly crystalline structure without major zoning or defects.

The spectra of the 38 GPa samples (parallel) are dominated by a number of peaks at 204, 223, 238, 296, 325, 356, 404, 464, 556, 609, 846, and 883 cm-1. These peaks are characteristic for the reidite (Williams and Knittle 1993). This sample contains an additional peak at around 1000 cm-1 (Fig. 3B), which will be discussed below.

In the 40 GPa samples, typical reidite peaks occur at 204, 238, 296, 327, 356, 404, 464, 558, 610, 847, and 887, (Fig. 3C). In addition, relatively weak peaks appear at 223, 437 and 1005 cm-1 in the spectrum (Fig. 3C).

The Raman spectra of the 60 GPa samples (parallel) show peaks at 204, 238, 297, 327, 353, 406, 464, 558, 610, 847 and 887 cm-1 (Fig. 3D). The peak intensities of these peaks in both samples are approximately equal and all peaks are characteristic for the reidite. It is important to note that these peaks are totally different from the Gucsik et al. (2002), who observed an amorphous state without any vibration modes of Raman spectrum at 60 GPa.

The Raman spectra of the 80 GPa samples exhibit peaks that are typical for reidite at 205, 238, 297, 327, 353, 406 (relatively strong), 464, 558, 610, 847 and 887 cm-1 (Fig. 3E).

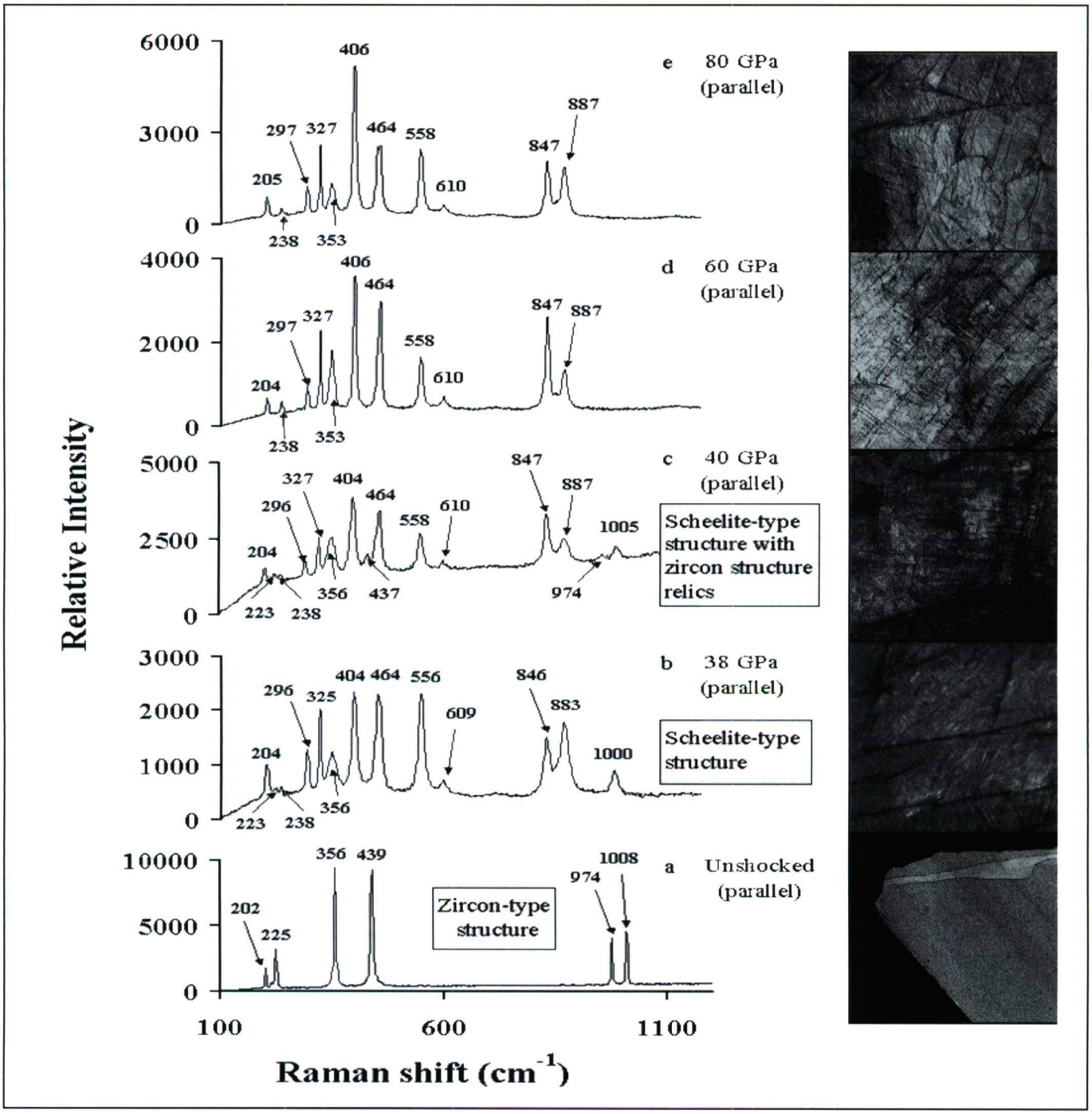

Fig. 3. Raman spectra and CL images of same area of unshocked and experimentally shocked (38, 40, 60, 80 GPa) zircon samples, which were cut parallel to their c-axes. The peaks of the unshocked sample indicate zircon-structure and bands of the shocked samples are characteristic of the high-pressure scheelite-type phase. The 38 and 40 GPa samples, however, exhibit some weak bands that indicate relics of zircon-phase (c). Numbers denote peak positions in [cm^{-1}].

Raman Spectroscopy of naturally shock-deformed zircon samples from the Ries crater

The Raman spectra of the naturally shock-deformed zircon samples from the Ries crater (Stage-II: 35-45 GPa, Stage-III: 45-50 GPa, Stage-IV: >50 GPa) cut parallel and perpendicular to their crystallographic c-axes exhibit differences from each other as it can be seen in Fig. 4. The fluorescence background is considerably higher and Raman bands are wider in all samples than for the experimentally shock-deformed samples, which indicate lower crystallinity with major zoning and defects.

Both Stage-II (35-45 GPa) samples are characterized by five peaks at 224, 356, 439, 974 and 1007 cm-1, indicating zircon-type structure (Williams and Knittle 1993, Kolesov et al. 2001) (Fig. 4A, B). Additionally, a weak peak at 210 cm-1 appears in the Raman spectra of the Stage-II parallel sample (Fig. 4A). The peak intensities of the perpendicular sample are higher than those of the parallel-samples.

The peak at 1007 cm-1 is relatively strong in the perpendicular sample (Fig. 4B).

The Raman spectrum of the Stage-III (45-50 GPa) parallel-sample shows eleven peaks at 202, 224, 327, 356, 404, 439, 465, 558, 845, 974 and 1007 cm-1, which indicates the presence of the scheelite-type phase among predominant zircon-type material (Fig. 4C). In contrast, the Stage-III perpendicular-sample contains only eight peaks at 202, 214, 224, 356, 404, 439, 974 and 1007 cm-1 showing pure zircon-type structure (Fig. 4D). A peak at 1007 cm-1 is relatively strong in the perpendicular-sample (Fig. 4D). In general, the fluorescence background in the parallel-sample is considerably higher than in the perpendicular-sample. In both cases, the peak intensities are similar.

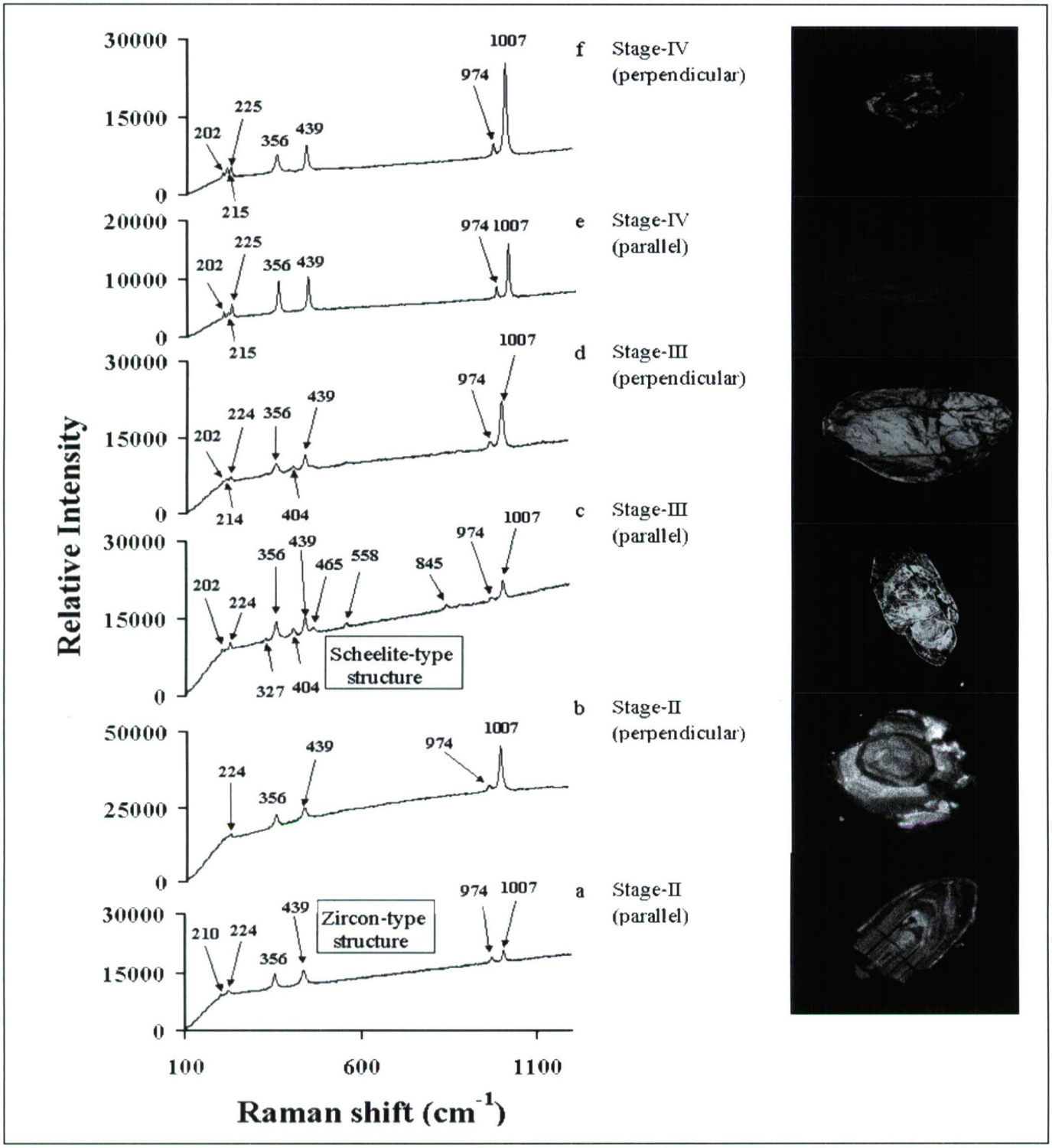

Fig. 4. Raman spectra and CL images of same area of naturally shock deformed zircon specimens from the Ries impact crater (Germany), which were cut parallel and perpendicular to their c-axes including Stage-II, Stage-III and Stage-IV shock stages. The peaks indicate the zircon structure in all shock stages. The bands in the Stage-III parallel-sample indicate also the presence of scheelite-type phase (c). Numbers denote peak positions in [cm^{-1}].

The spectra of the Stage-IV samples (parallel and perpendicular samples) are characterized by seven peaks at 202, 215, 225, 356, 439, 974 and 1007 cm-1, indicating zircon-type phase (Williams and Knittle 1993, Kolesov et al. 2001) (Fig. 4E, F). In both cases, a peak at 1007 cm-1 is relatively strong. The peak intensities of the perpendicular-sample are higher than those of the parallel-sample (Fig. 4F).

Discussion

Raman spectra of natural zircon were described by, e.g., Nasdala et al. (1995) and Kolesov et al. (2001), the spectral signature of the high-pressure scheelite-type phase was reported reported by Williams and Knittle (1993). In general, high-energy modes (at 700-1000 cm-1) might be related to the antisymmetric or symmetric stretching modes of SiO4, whereas low-energy modes (at 100-400 cm-1) might be attributed to the lattice modes. The SiO4 bending modes typically lie in the wave number region of 400-700 cm-1 (Williams and Knittle 1993, Kolesov et al. 2001). The spectra and wave numbers of our Raman modes are in excellent agreement with other studies (Williams and Knittle 1993, Kolesov et al. 2001). Following data presented by Williams and Knittle (1993) and Kolesov et al. (2001), Table 3 and Table 4 give the zircon-and scheelite-type vibrational modes and assignments of the Raman modes observed in this study. The peak positions of scheelite-type modes are very similar to those characteristic of zircon. Even if these features were also observed in the spectra of the high-pressure scheelite-structure phase by Williams and Knittle (1993), there is a high probability that minor amounts of relictic zircon phase material are still present in the 38 and 40 GPa samples. This suggestion is also supported by the TEM investigations of Leroux et al. (1999), who did not observe single-phase scheelite-type material in the 40 GPa (45°-sample), but an epitaxial intergrowth of both phases with a size below the spatial resolution of the micro-Raman spectrometer used in the present study.

Frequency shifts of the 1000 cm-1 band by a few cm-1 might be due to strained zircon caused by shock waves or high-pressure-induced deformation or disorder in zircon. Similar frequency shifts were observed in radiation-damaged zircon (Zhang et al. 2002).

Raman spectra of naturally shock-deformed zircon crystals from the Ries Crater (Stage-II, III and IV) show zircon-type phase. According to Raman spectral measurements and lack of shock-induced planar microdeformations, these samples do not exhibit high-pressure level (the shock pressure that might have been affected the zircon crystals was below 30 GPa). Only the Stage-III (parallel) sample exhibits the presence of traces of scheelite-type vibrational modes, which occur first around 30 GPa (Kusaba et al 1985).

Summary and Conclusions

Raman spectra revealed that the unshocked samples, as well as naturally shock-deformed zircon crystals from the Ries, represent zircon-structure material, whereas the 38 and 40 GPa samples yielded additional peaks with relatively high peak intensities, which are indicative of the presence of the scheelite-type structure of zircon with zircon-structure relics. The 60 and 80 GPa samples display a Raman signature that is characteristic for the existence of only the scheelite-type phase. According to the Raman measurements, the naturally shock-deformed zircons might be related to the low-shock regime (<30 GPa) or recrystallized at the increased post-shock temperature, and do not represent the same shock stages as indicated by whole-rock petrography.

Consequently, the Raman spectroscopy is a potentially useful tool that can be used to characterize the shock stage of zircons from impactites. These results also give new insight into the structural changes that occur in zircons during shock metamorphism, and the pressures associated with these changes.

Table 3. Raman bands and their assignment to vibrational modes of zircon (after Williams and Knittle, 1993; Kolesov et al., 2001).

v_0 (cm^{-1})	Assignment (Raman bands)
1008	v_3: SiO_4 antisymmetric strech
974	v_1: SiO_4 symmetric strech
439	v_2: SiO_4 bend
356	Lattice mode
225	Lattice mode
202	Lattice mode

Table 4. Raman bands and their assignment to vibrational modes of the reidite (scheelite-type structure) (after Williams and Knittle 1993; Kolesov et al. 2001).

v_0 (cm^{-1})	Assignment (Raman bands)
1001	v_3: SiO_4 antisymmetric strech
887	v_3: SiO_4 antisymmetric strech
847	Strain-activated mode
610	v_4: SiO_4 bend
558	v_4: SiO_4 bend
464	v_2: SiO_4 bend
406	Lattice mode
353	Lattice mode
327	Lattice mode
297	Lattice mode
238	Lattice mode
223	Lattice mode
204	Lattice mode

Acknowledgements

As this study was a part of my Ph.D. thesis, I would like to express thank to Profs. Christian Koeberl, Eugen Libowitzky, Uwe Reimold, and Franz Brandstätter supervising my Ph.D. studies at the University of Vienna, Austria. The author is grateful to Dr. Géza Nagy for reviewing this paper.

References

Bohor, B.F., Betterton, W.J., Krogh, T.E. (1993): Impact-shocked zircons: discovery of shock- induced textures reflecting increasing degrees of shock metamorphism. Earth and Planetary Science Letters, **119**, 419–424.

Deloule, E., Chaussidon, M., Glass, B.P., Koeberl, C. (2001): U-Pb isotopic study of relict zircon inclusions recovered from Muong Nong-type tektites. Geochimica et Cosmochimica Acta, **65**, 1833–1838.

DEUTSCH, A. (1998): Examples for terrestrial impact structures. In Marfunin, S.A. (ed.): Mineral Matter in Space, Mantle, Ocean Floor, Biosphere, Environmental Management, and Jewelry, Advanced Mineralogy, Springer-Verlag, Berlin, Heidelberg, 119–129.

DEUTSCH, A., SCHÄRER, U. (1990): Isotope systematics and shock-wave metamorphism: I. U-Pb in zircon, titanite, and monazite, shocked experimentally up to 59 GPa. Geochimica et Cosmochimica Acta, **54**, 3427–3434.

ENGELHARDT, W.v. (1990): Distribution, petrography and shock metamorphism of the ejecta of the Ries crater in Germany - a review. Tectonophysics, **171**, 259–273.

GEOLOGISCHE KARTE DES RIESES, (1999): Bayerisches Geologisches Landesamt, München, 1:50 000

GIBSON, R.L., ARMSTRONG, R.A., REIMOLD, W.U. (1997): The age and thermal evolution of the Vredefort impact structure: A single grain U-Pb zircon study. Geochimica et Cosmochimica Acta, **61**, 1531–1540.

GLASS, B.P., LIU, S. (2001): Discovery of high-pressure $ZrSiO_4$ polymorph in naturally occurring shock-metamorphosed zircons. Geology, **29**, 371–373.

GLASS, B.P., LIU, S., LEAVENS, P.B. (2002): Reidite: An impact-produced high-pressure polymorph of zircon found in marine sediments. American Mineralogist, **87**, 562–565.

GUCSIK, A., KOEBERL, C., BRANDSTÄTTER, F., LIBOWITZKY, E., REIMOLD, W.U. (2004): Cathodoluminescence, electron microscopy, and Raman spectroscopy of experimentally shock metamorphosed zircon crystals and naturally shocked zircon from the Ries impact crater. In Dypvik, H., Burchell, M., Claeys, Ph. (eds.): Cratering in Marine Environments and on Ice, Springer-Verlag, Heidelberg, 281–322.

GUCSIK, A., KOEBERL, C., BRANDSTÄTTER, F., REIMOLD, W.U., LIBOWITZKY, E. (2002): Cathodoluminescence, electron microscopy, and Raman spectroscopy of experimentally shock-metamorphosed zircon. Earth and Planetary Science Letters, **202**, 495–509.

KAMO, S.L., KROUGH, T.E. (1995): Chicxulub crater source for shocked zircon crystals from the Cretaceous-Tertiary boundary layer, Saskatchewan: Evidence from new U-Pb data. Geology, **23**, 281–284.

KAMO, S.L., REIMOLD, W.U., KROGH, T.E., COLLISTON, W.P. (1996): A 2.023 Ga age for the Vredefort impact event and first report of shock metamorphosed zircons in pseudotachylitic breccias and Granophyre. Earth and Planetary Science Letters, **144**, 369–387.

KOLESOV, B.A., GEIGER, C.A., ARMBRUSTER, T. (2001): The dynamic properties of zircon studied by single-crystal X-ray diffaction and Raman spectroscopy. European Journal of Mineralogy, **13**, 939–948.

KROGH, T.E., KAMO, S.L., BOHOR, B.F. (1996): Shock metamorphosed zircons with correlated U-Pb discordance and melt rocks with concordant protolith ages indicate an origin for the Sudbury Structure. In Hart, S., Basu, A. (eds.): American Geophysical Union, Geophysical Monograph **95**, 343–353.

KUSABA, K., SYONO, Y., KIKUCHI, M., FUKUOKA, K. (1985): Shock behaviour of zircon: phase transition to scheelite structure and decomposition. Earth and Planetary Science Letters, 72, 433-439.

LEROUX, H., REIMOLD, W.U., KOEBERL, C., HORNEMANN, U., DOUKHAN, J-C. (1999): Experimental shock deformation in zircon: a transmission electron microscopic study. Earth and Planetary Science Letters, **169**, 291–301.

MCMILLAN, P.F., HOFMEISTER, A.M. (1988): Infrared and Raman spectroscopy. In Hawthorne, F.C. (ed.): Spectroscopic methods in mineralogy and geology, Mineralogical Society of America Reviews, **18**, 99–159.

NASDALA, L., IRMER, G., WOLF, D. (1995): The degree of metamictization in zircon: a Raman spectroscopic study. European Journal of Mineralogy, **7**, 471–478.

OSINSKI, G.R., SPRAY, J.G., GRIEVE, R.A.F. (2003): Impact melting in sedimentary target rocks? Powerpoint Presentation at www.lpi.usra.edu/meetings/impact2003/presentations/osinski8009.ppt

REID, A.F., RINGWOOD, A.E. (1969): Newly observed high pressure transformations in Mn_3O_4, $CaAl_2O_4$, and $ZrSiO_4$. Earth and Planetary Science Letters, **6**, 205–208.

REIMOLD, W.U., LEROUX, H., GIBSON, R.L. (2002): Shocked and thermally metamorphosed zircon from the Vredefort impact structure, South Africa: A transmission electron microscopic study. European Journal of Mineralogy, **14**, 859–868.

ROBERTS, S., BEATTIE, I. (1995): Micro-Raman spectroscopy in the Earth Sciences. In Potts, P.J., Bowles, J.F.W., Reed, S.J.B., Cave, M.R. (eds.): Microprobe techniques in the Earth Sciences. Chapman and Hall, London, 387–408.

SCOTT, H.P., WILLIAMS, Q., KNITTLE, E. (2002): Ultralow compressibility silicate without highly coordinated silicon. Physical Review Letters, **88**, 015506-1-015506-4.

STAUDACHER, T., JESSBERGER, K.E., DOMINIK, B., KRISTEN, T., SCHAEFFER, A.O. (1982): ^{40}Ar-^{39}Ar of rocksand glasses from the Nördlinger Ries crater and the temperature history of impact breccias. Journal of Geophysics, **51**, 1–11.

STÖFFLER, D. (1974): Deformation and transformation of rock-forming minerals by natural and experimental shock processes. Fortschritte der Mineralogie, **49**, 256–298.

WILLIAMS, Q., KNITTLE, E. (1993): High-pressure Raman spectroscopy of $ZrSiO_4$: Observation of the zircon to scheelite transition at 300 K. American Mineralogist, **78**, 245–252.

WITTMANN, A., KENKMANN, T., SCMITT, R.T. STÖFFLER, D. (2006): Shock metamorphosed zircon in terrestrial impact craters. Meteoritics and Planetary Sciences, **40**, 1–16.

Zhang, M., Salje, E.K.H., Ewing, R.C. (2002): Infrared spectra of Si-O overtones, hydrous species, and U ions in metamict zircon: radiation damage and recrystallization. Journal of Physics: Condensed Matter, **14**, 3333–3352.

Received: March 22, 2007; accepted: December 20, 2007

Acta Mineralogica-Petrographica, Szeged 2006–2007, Vol. 47, pp. 25-46

ACTA Mineralogica Petrographica

MINERALOGY OF PLIOCENE TO MIDDLE PLEISTOCENE RED CLAYS IN SE TRANSDANUBIA (HUNGARY). REVIEW OF THE QUANTITATIVE DATA

ISTVÁN VICZIÁN

Geological Institute of Hungary, H-1143 Budapest, Stefánia út 14., Hungary
e-mail: viczian@mafi.hu

ABSTRACT

Red silty clays filling fissures in limestone, karstic depressions and recent caves in the Villány Mts. (SE Transdanubia, Hungary), and Pliocene to Quaternary red clays of the surrounding hilly areas were studied. For comparison also yellow clays and Pannonian basin sediments were investigated. The quantitative mineral composition was determined by X-ray diffraction for the bulk sample and for the <2 μm fraction. For a statistical evaluation in triangular diagrams the data of 181 quantitative analyses of the bulk composition and 129 analyses of the <2 μm fraction were collected. Minerals in the *whole rock* were sorted into 3 groups according to their genetic significance: (1) carbonates, (2) detrital and slightly weathered minerals and (3) products of strong weathering. The 3 groups for clay minerals in the *<2 μm fraction* were: (1) illite and chlorite, (2) smectite and vermiculite and (3) kaolinite and gibbsite. Two main associations of minerals could be distinguished. A *highly weathered association* consisting of the minerals of disordered kaolinite, kaolinite/smectite mixed-layer mineral, smectite and occasionally gibbsite was selected which normally contains Ti-oxides and more hematite than goethite. Quartz contents are low, feldspars are absent. Calcite is high only when secondary cementation or admixture of wall rock fragments occurs. The association represents a weathering crust formed on the karstified surface during a warm and humid climatic period of the Middle Pliocene. The other, more widespread, *less weathered association* contains well crystallised clay minerals, dominantly illite accompanied by smectite, illite/smectite, chlorite or kaolinite, relatively much quartz and feldspars but little calcite. The typical iron mineral is here goethite. This association represents weakly or moderately weathered terrestrial or shallow basin sediments of Pliocene to Middle Pleistocene age. The genetic conclusions obtained agree well with results obtained by the study of Vertebrate fossils.

Key words: red clays, karst, kaolinite, kaolinite/smectite, SE Transdanubia, Tengelic Fm., Pliocene, Quaternary

INTRODUCTION

The range of the Villány Mts. consists mainly of carbonate rocks of Mesozoic age. In the cavities of the karstified limestone, such as fissures, sinkholes and recent caves various fine grained sediments have been accumulated. The most widespread karstic sediments are red clays which are considered to belong to the stratigraphic unit Tengelic Red Clay Formation which is widespread in a large area around the Villány Mts. The formation is part of the young terrestrial sequence of the area. Another type of red clay occurs in basal palaeosol layers underlying the Middle Pleistocene Paks Loess Formation. In the immediate vicinity of the Villány Mts. shallow local basins are filled with lacustrine to terrestrial Upper Pannonian to Quaternary sediments, in which, however, red clays do not occur. These grey and yellow fine grained sediments were studied for comparison with the red clays. The area of study and local names are shown in Fig. 1.

Stratigraphic relations of the terrestrial sediments are described in the classical studies of the Vertebrate fauna by Kretzoi (1956, 1969) and Jánossy (1986) and in the more recent summaries by Kaiser (1999), Kordos (1991, 2001), Koloszár and Marsi (2002), Koloszár (2004) and Császár, Kordos (2004). Schweitzer (1993) collected field observations, geomorphological data such as position of terraces, formation of travertine etc., mineralogical and palaeontological evidence and radioactive age determinations. In conclusion he distinguished and characterised the subsequent periods set up by the former authors called *Ruscinium-Csarnótanum* (4.5-3.0 million years), *Villányium* (3.0-1.8 million years) and *Biharium* (younger than 1.8 million years).

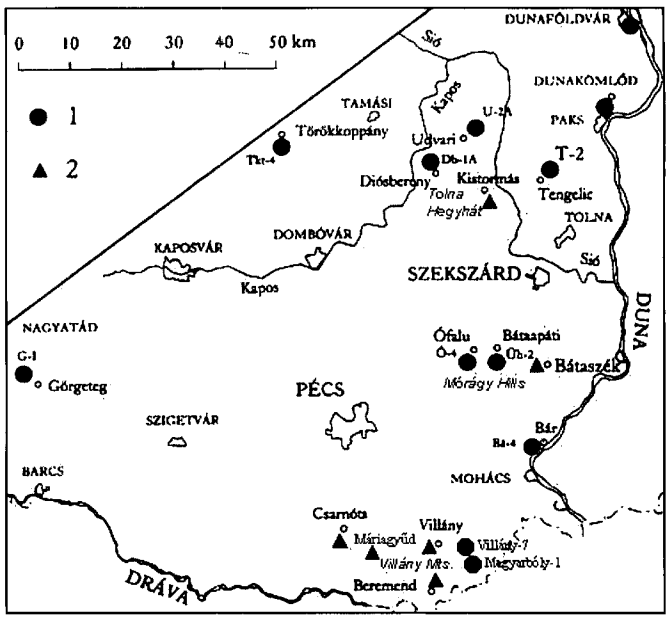

Fig. 1. Map showing SE Transdanubia and localities mentioned in the paper according to Koloszár (2004), modified. Legend: 1: borehole, 2: outcrop.

Mineralogical data related to the Pliocene to Quaternary sediments of the area were collected and evaluated as well as history of the former mineralogical investigations was given

by Viczián (2002a). Karstic sediments of the Villány Mts. were recently investigated in detail by Marsi and Koloszár (2004) and by Dezső et al. (2007). Specimens of special bauxitic composition were investigated by Császár and Farkas (1984). The mineralogy of red clays in the wider surrounding territory was investigated by Földvári and Kovács-Pálffy (2002). They compared three stratigraphic units, (1) loess, (2) palaeosols in the loess, and (3) the Tengelic Red Clay Formation in the Tolna Hegyhát and Mórágy Hills areas. Diagnostic values were set up by which these units can be distinguished.

The core material of some of the boreholes penetrating the Pannonian basin sediments was analysed in the Geological Institute of Hungary and the data are available as unpublished reports. Most published reports contain quantitative data on the mineralogical composition. The aim of the present study is to collect and evaluate these quantitative data and to compare the results with those obtained from geomorphologic and palaeontologic studies.

Methods

Quantitative data related the mineralogy of the samples have been obtained first of all by the X-ray diffraction analysis. In most cases data were corrected by comparison with the results of thermal analysis of Mária Földvári.

The majority of the measurements were carried out in the X-ray laboratory of the Geological Institute of Hungary. The instrumental parameters are the following: Philips PW 1710 type X-ray diffractometer, CuKα radiation, 40 kV, 30 mA, graphite monochromator, goniometer speed: 2 °/min. The X-ray diffraction analysis for the samples considered in the paper by Dezső et al. (2007) was carried out in the laboratory of the Department of Earth and Environmental Sciences, University of Pannonia, Veszprém, by Béla Raucsik. Here the instrumental parameters were very similar: Philips PW 1710 type X-ray diffractometer, CuKα radiation, 40 mA, 50 kV, slits: 1°-1°, proportional counter, graphite monochromator. The X-ray diffraction patterns obtained in Veszprém were evaluated quantitatively in the same way as the patterns obtained in the Geological Institute of Hungary.

Normally in each sample the bulk rock and the <2 μm fraction were investigated. The <2 μm fraction was obtained by sedimentation. The following preparations were used: for bulk samples: random powder preparations and for the <2 μm fraction: oriented samples on a glass plate made by pipette method and dried at laboratory temperature. The oriented specimens were investigated in untreated form and after saturation with ethylene glycol. Only the basal reflections of clay minerals were compared in the <2 μm fraction samples, in order to avoid orientation problems. For the bulk samples the total composition was considered.

The quantitative method used is the standard method of the Geological Institute of Hungary which is based on the works of Náray-Szabó and Péter (1967), Viczián (1967), Rischák and Viczián (1974) and Szemerey-Szemethy (1976). The basic idea of the method is the direct comparison the intensities of selected reflections of minerals. The intensities are multiplied by experimentally determined or estimated factors which enable the direct comparison of the intensities obtained from minerals of different composition and different structural order. Slight differences may occur in the factors applied, depending on the person carrying out the analysis. Considering these circumstances the results obtained cannot be considered as strictly quantitative and have to be considered with some precaution, however, the data obtained are sufficiently uniform to enable comparison of the composition of samples and to reveal basic tendencies in the variation of the composition.

Results

Table 1 contains the source of quantitative data considered in the present review. The data of 180 quantitative analyses of the bulk composition and 129 analyses of the <2 μm fraction were collected. In the table the formations studied are listed according to their relative stratigraphic age.

Results relating the quantitative composition of the various sediment types were summarised in form of triangular diagrams constructed for the bulk composition and for the <2 μm fraction, respectively. In the triangles the 3 vertices represent the percentages of groups of mineral species. The minerals were grouped according to their presumed genetic significance.

In the diagrams relating the composition of the *bulk rock*, these groups are the following:

Carbonate minerals: calcite, aragonite, magnesian calcite, dolomite, siderite. Among these minerals only calcite is abundant, the others are very rare. The calcite contents of the samples are very variable, in most cases however, it does not bear much significance in respect of the provenance of the silicate phase. In the fissure fillings calcite is either secondary precipitation from the karstic water or is the material of limestone blocks that were broken down from the wall of the fissure. It has more significance in the lacustrine basin sediments. In the reduced basin sediments pyrite occurs which was included into this group.

Detrital minerals and products of moderate weathering: The minerals quartz, plagioclase, potassium feldspar, the clay minerals illite and chlorite were considered as detrital phases not affected by weathering. In most cases it can be demonstrated that illite is the well crystallised 2M modification. The clay minerals smectite, mixed-layer illite/smectite and vermiculite however, may be the product of moderate weathering of the former detrital phases under relatively dry climatic conditions. They are here considered together with the unchanged detrital phases, but in diagrams of the <2 μm fraction they will be treated separately.

Products of intense weathering: The phases listed here are considered to be formed during strong weathering under warm and humid circumstances. The most abundant mineral is kaolinite which is typically very disordered and forms mixed-layer structures with smectite. Several oxides and hydroxides are formed during intense weathering, such as the iron minerals goethite, hematite, (lepidocrocite) and amorphous iron hydroxides and the Ti-minerals anatase and rutile. An important member of this group is the bauxite mineral gibbsite.

In the diagrams representing the composition of the *<2 μm fraction* only the relative amounts of the clay minerals and gibbsite were considered. The 3 groups shown on the 3 poles of the triangles are the following:

Table 1. Sources of quantitative mineralogical data on Pliocene to Lower Pleistocene sediments in SE-Transdanubia.

Type of sediment	Locality	Stratigraphic position	Number of analyses Bulk rock	<2 μm	X-ray analyst	References
Grey clay, fissure filling	Magyarbóly-1 borehole	Miocene?	-	2 (<0.06mm)	G. Rischák, revised by I. Viczián	Rischák (1987): unpublished report
Lacustrine and terrestrial sed.	Magyarbóly-1 borehole	Szák Fm., Upper Pannonian, Quaternary	18	11	I. Viczián	Viczián (1988): unpubl. rept., Ta-nács, Viczián (1995)
Lacustrine and terrestrial sed.	Villány-7 borehole	Upper Pannonian, Quaternary	15	-	I. Viczián	Viczián, Földvári (1988): unpubl. rept.
Red bauxitic clays, fissure filling	Beremend	Upper Cretaceous? - Tengelic Fm.?	4	-	L. Farkas	Császár, Farkas (1984)
Red clays, filling of a broad hole	Beremend, locality No. 26	Tengelic Fm., Beremend Member	48	40	P. Kovács-Pálffy	Marsi et al. 2001: unpubl. rept., Marsi, Koloszár (2004)
Yellow silts, fissure filling	Villány, Somssich Hill, locality No. 2	Lower Pliocene	14	-	A. Szemethy, revised by I. Viczián	Szemethy, Földvári (1978): unpublished report
Red clays, terrestrial sed., eluvial-deluvial and residual facies	Bár-5, Tengelic-2 boreholes, Mórágy Hills, Tolna Hegyhát	Tengelic Fm., Tengelic Member	34	32	I. Viczián, P. Kovács-Pálffy	Viczián (1971, 1979): unpubl. rept., Halmai et al. (1982), Földvári, Kovács-Pálffy (2002)
Red clays, palaeosols	Mórágy Hills, Tolna Hegyhát	Basal layers of Paks Loess Fm. (PD, Pv_1-v_5)	27	27	P. Kovács-Pálffy	Földvári, Kovács-Pálffy (2002)
Various karst-related sediments	Villány Mts.	U. Pannonian, Tengelic Fm., basal layers of Paks Loess Fm. (PD)	21	17	B. Raucsik, revised by I. Viczián	Dezső et al. (2007)

Detrital minerals: Illite and mixed-layer illite/smectite, *if* the composition is close to the pure illite.

Products of moderate weathering: As it was discussed in the case of the bulk rock, the minerals smectite and vermiculite are considered here. Mixed-layer illite/smectites belong to this group when their composition varies in wide ranges or is close to pure smectite. Also mixed-layer kaolinite/smectite was listed here, first of all because of methodological reasons, because it cannot be separated safely from pure smectite. However, it is already transition to the intense weathering.

Products of intense weathering: Kaolinite, which is in high amounts, is always very disordered and randomly oriented. The product of the strongest leaching is gibbsite.

In the following the SE-Transdanubian red clay and related formations will be briefly described according to their approximately decreasing geological age. Mineral composition will be characterised using the two triangular compositional diagrams.

Grey clay fissure filling in the Magyarbóly-1 borehole (older than Upper Pannonian)

In the Magyarbóly-1 borehole, a few kilometres away in SE direction of the Villány Mts. Jurassic limestone was cut under the covering Pannonian sediments. There are numerous fissures in the limestone filled with grey or

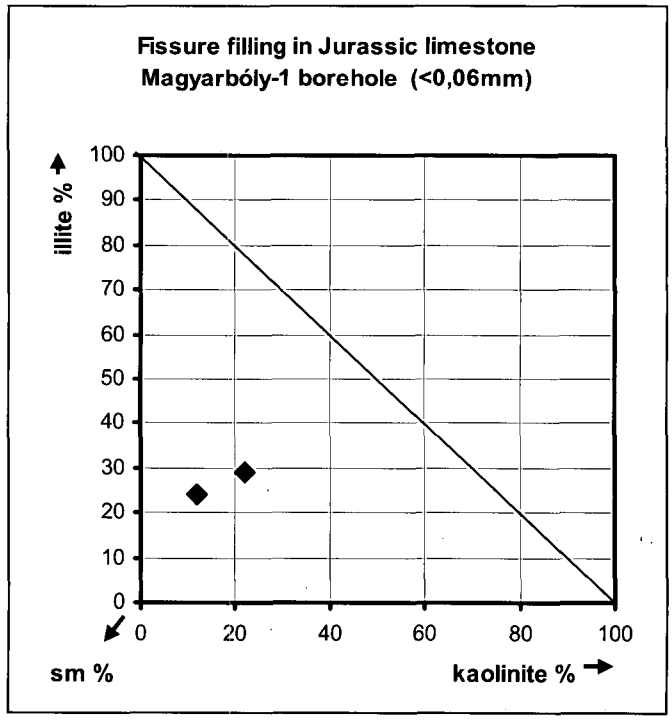

Fig. 2. Clay mineral composition of fissure filling clays in Jurassic limestone, Magyarbóly-1 borehole (<0,06mm).

greenish grey clay. The <0.06 mm fraction of two grey clay samples were analysed (Fig. 2). The clay mineral assemblage is rich in smectite, there is relatively much kaolinite while chlorite is absent. This indicates moderately weathered sedimentary material. The age of the emplacement in the fissure must be older than the oldest covering formation on the top of the limestone, i.e. the Lower Pannonian Szák Fm., and is probably contemporaneous with a tectonic phase which produced the fault system (presumably old Cainozoic, according to Koloszár, 2004). The age of the formation of the corresponding weathering crust on the ancient surface is even more uncertain but may be partly much older than the age of the filling of fissures.

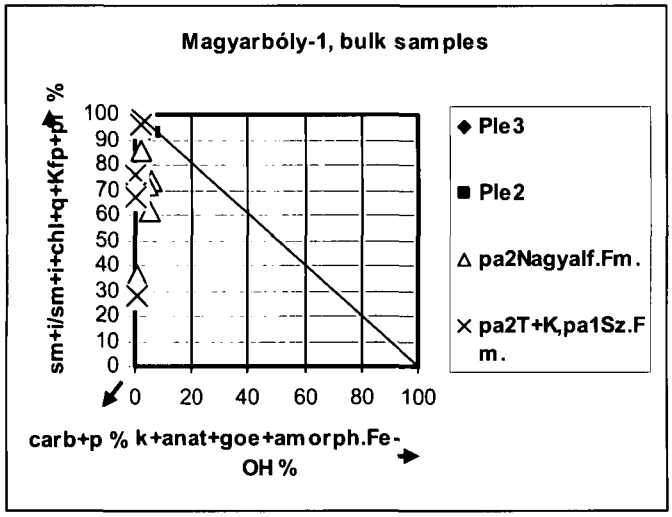

Fig. 3. Mineral composition of bulk samples of fine-grained sediments in Magyarbóly-1 borehole. Legend: Ple2: Middle Pleistocene, Ple3: Upper Pleistocene, pa2Nagyalf.Fm.: Upper Pannonian Nagyalföld Formation, pa2T+K,pa1Sz.Fm.: Upper Pannonian Tihany and Kálla Formations and Lower Pannonian Szák Formation.

Lacustrine and terrestrial sediments in basins adjacent to the Villány Mts. (Pannonian)

There are mineralogical analyses available on the core material from the boreholes Magyarbóly-1 and Villány-7, which are in the immediate vicinity of the eastern end of the Villány Mts. In these boreholes the Lower Pannonian Szák, the Upper Pannonian Kálla, Somló, Tihany and Nagyalföld Formations and Quaternary sediments occur (according to unpublished core descriptions by Jámbor, 1986). In the diagrams representing the whole rocks of the boreholes (Fig. 3 and Fig. 4, respectively) the high variation in the carbonate contents is conspicuous. In the Pannonian there may be high carbonate contents which are not only calcite but also dolomite, sometimes in very high amounts, and magnesian calcite in the Szák Formation. On the other hand, Quaternary sediments in these boreholes are almost carbonate-free. The non-carbonate components are clearly not weathered or moderately weathered. The clay fraction was investigated only in the Magyarbóly-1 borehole. In the diagram (Fig. 5) there is a wide scatter in the low-kaolinite domain, the dominant clay minerals are illite, smectite and mixed-layer illite/smectite. Chlorite and kaolinite are less abundant, they occur in nearly equal amounts, kaolinite however, seems to increase up to almost 20 % with increasing smectite contents. The latter composition corresponds to slightly more weathered material. The variation in the illite to smectite ratio seems to be independent from the stratigraphic position. The scatter is as high in the Pannonian formations as in the Quaternary sediments.

All these features are in accord with the usual composition of the Pannonian and Quaternary basin sediments as found elsewhere in the Pannonian Basin (see e.g. Viczián, 1984, 2002a,b, Tanács and Viczián, 1995) and

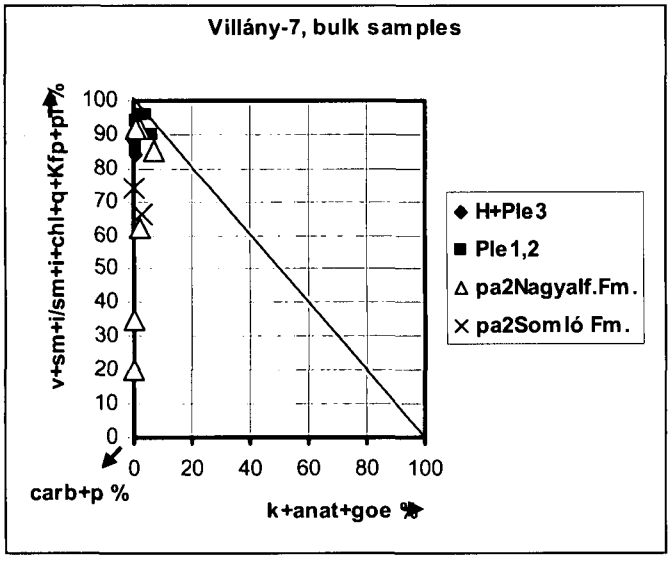

Fig. 4. Mineral composition of bulk samples of fine-grained sediments in Villány-7 borehole. Legend: H+Ple3: Holocene and Upper Pleistocene, Ple1,2: Lower and Middle Pleistocene, pa2Nagyalf.Fm.: Upper Pannonian Nagyalföld Formation, pa2SomlóFm.: Upper Pannonian Somló Formation.

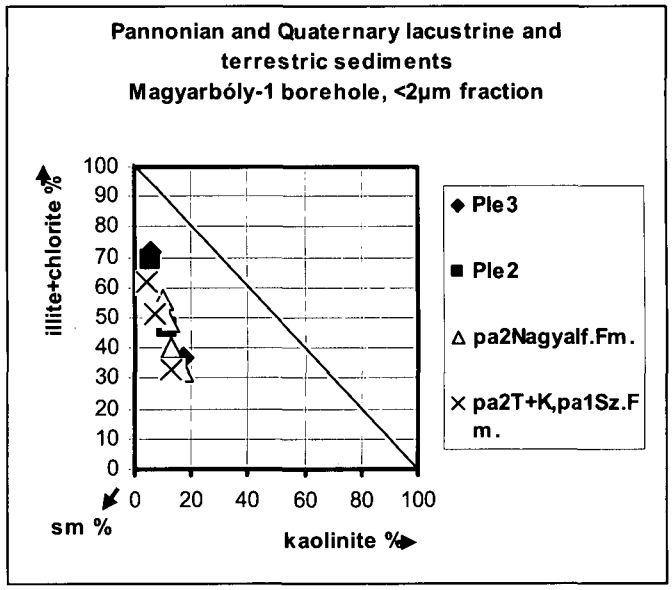

Fig. 5. Clay mineral composition of Pannonian and Quaternary fine-grained sediments, Magyarbóly-1 borehole, <2µm fraction. Legend: see Fig. 3.

are quite different from the composition of the more or less weathered terrestrial sediments preserved in fissures and karstic depressions of the Villány Mts.

Red clays of the Tengelic Formation. Overview of the startigraphic relations and regional distribution

The red clays are widespread in the hilly and mountainous areas of SE Transdanubian area underlying the Pleistocene Paks Loess Formation. Their mineralogy was studied very early by Földvári Vogl by the DTA method (Vadász 1968). Later Szöőr studied these clays by derivatographic thermal and IR methods (Schweitzer, Szöőr 1997, Schweitzer 1993). They recognised that among the red clays two compositional groups can be subdivided: one rich in kaolinite and one rich in illite and smectite.

The kaolinite-rich variety is restricted to the karstic surfaces of the Villány Mts. and it seems to be the older variety (*"Beremend Member"* of the *Tengelic Fm.*, Koloszár 2004). Examples are the localities Siklós, Vokány, Villány, Beremend and Csarnóta which were studied by X-ray diffraction and thermal methods by Bidló (1980, 1983b, 1985). He was the first to recognise the extremely disordered character of the kaolinite in these clays. Red clays occurring at Beremend were investigated recently by Dezső et al. (2007).

The illite-smectite-rich variety is more widespread. It occurs in the hilly areas and is generally younger (*"Tengelic Member"*of the *Tengelic Fm.*, Koloszár 2004). The red clay is the uppermost bed of a 25-60 m thick sequence consisting from the bottom upward of alluvial sand, occasional bentonite derived from basalt tuff, eluvial-deluvial variegated clay and clayey silt and finally the red clay which is of eluvial-deluvial and residual facies. The whole sequence itself deposited with considerable hiatus on the eroded surface of Upper Pannonian sediments. Its age is supposed to be Lower Pleistocene. The thickness of the red clay is varying between a few metres up to nearly 20 m. The red clay beds are overlain by another red clay beds which are the starting members of the Paks Loess Fm. The colour is actually less deep red and has been called "reddish" by Schweitzer and Szöőr (1997).

Red bauxitic clays in the Beremend quarry (Upper Cretaceous?, Beremend Member of Tengelic Fm.)

In the limestone quarry at Beremend red bauxitic clays filling fissures and karstic depressions were described by Császár and Farkas (1984). They published 4 mineralogical analyses, the data of which are shown in the diagram of Fig. 6. The samples differ in carbonate contents. The carbonate-free composition is essentially the same, kaolinite varies between 50-60 %, the bauxite mineral is gibbsite which varies between 2 and 21 %. Typical bauxitic features are the absence of quartz and the presence of anatase, hematite and goethite, but clay minerals like montmorillonite and illite and the very strongly disordered nature of kaolinite are not typical for bauxites. The sample most interesting from the point of view of bauxites is that with 21 % gibbsite and with somewhat better ordering of kaolinite, because of the low gibbsite contents however, even this sample may be called only bauxitic clay according to the classification of Bárdossy (1982, Fig. 66). The authors stressed the difference from the known Lower Cretaceous Harsányhegy Bauxite Fm. because it is surely older than the Nagyharsány Limestone Fm., and because there is no gibbsite in the Harsányhegy Bauxite Fm., where the aluminium minerals are boehmite and diaspore (Dudich, Mindszenty 1984) or diaspore alone (Császár 2002, Table 6 and Table 7, analyses by J. Bognár and M. Földvári).

The age of the bauxitic clay is uncertain. In contrast to the Harsányhegy Bauxite, Császár and Farkas (1984) considered the bauxitic clays of Beremend to represent an "upper" or "second bauxitic horizon". They pointed out that it must be younger than the Lower Cretaceous Nagyharsány Limestone Fm. which is the host rock, but the upper limit is not known because of the lack of covering formation. They tentatively suggested Upper Cretaceous age, either older that the Bisse Marl Fm., or most probably younger than the post-Senonian general uplift and denudation. The same opinion was repeated in the monograph of Császár (2002) and in the field guide by Kordos, Császár (2004). They remarked however that in this case there is not much chance for preservation of a deposit of economic value because the territory remained uncovered until the Miocene. The question of the age of the gibbsite-bearing samples will be discussed later in a separate chapter.

Red clays, filling a broad hole in the Beremend quarry (locality No. 26, Beremend Member of the Tengelic Fm.)

In the Beremend quarry a huge pile of red clay of 24 m height and of diameter of several tens of m was left over by the mining which is the remnant of the filling of a broad karstic depression. The locality listed as No. 26 was subject of detailed study by Marsi and Koloszár (2004). The column was subdivided into 5 horizons and mineralogical analysis was made from samples taken from each half meter. Quantitative X-ray data made by P. Kovács-Pálffy are

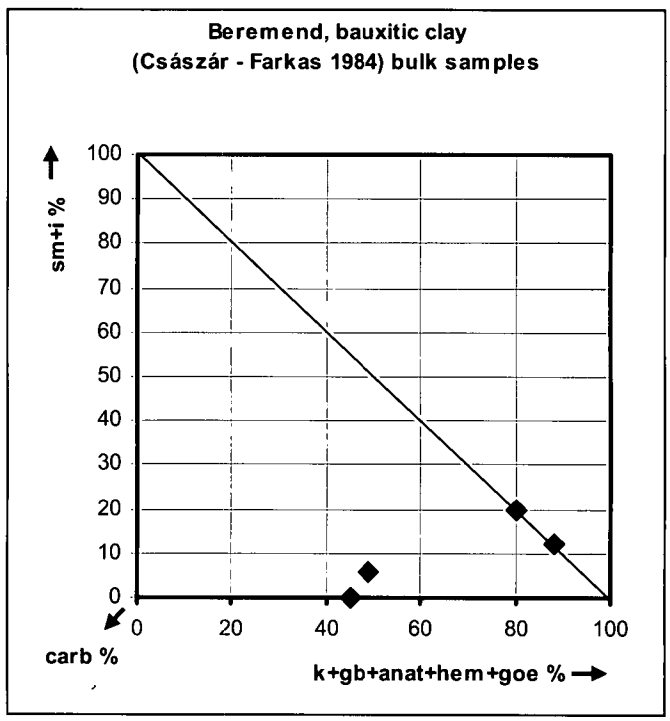

Fig. 6. Mineral composition of bauxitic clays, Beremend quarry, bulk samples (Császár, Farkas 1984).

included into the unpublished report by Marsi et al. (2001). In the diagram of the bulk rock composition (Fig. 7) and of the <2 μm fraction (Fig. 8) the data of each horizon are shown separately. The whole set of data is remarkably uniform: the ranges of scattering of the points in each horizon overlap each other, but the average values for each horizon are nearly the same. Some variation is due only to the carbonate contents in the bulk composition, higher carbonate contents arise from blocks of the host rock which is indifferent from the point of view of genesis of the red clay. This uniformity is in accord with the results of the palaeontological determination which has shown relatively short time interval, about 2 hundred thousand years for the emplacement of the sequence. The age of the deposition of the material in the depression is 3.1 to 3.3 million years according to the Vertebrate fossil studies by Kordos (2001). The locality is the stratotype of the Beremend Member of the Tengelic Formation as proposed by Koloszár (2004).

The mineralogy of the bulk rock (Fig. 7) shows almost carbonate-free, moderately weathered, smectite dominated material. In the composition however, disordered kaolinite is the second abundant clay mineral and also hematite and Ti-oxides are present. Quartz is moderately frequent (10-20 %), illite is low (less than 10 %). In the <2 μm fraction (Fig. 8) the dominance of kaolinite is more striking (60-80 %), smectite is low (<10 %), the second clay mineral is illite+illite/smectite (20-40 %). Kaolinite is very disordered with transitional phases to smectite. No gibbsite was found in this locality (only traces in two samples). The authors consider that the source material of this red clay filling was mainly a locally developed weathering crust on the top of the isolated elevation of the limestone block at Beremend.

Yellow, fissure filling silts at Villány, Somssich Hill, site No. 2 (Lower Pleistocene)

Somssich Hill is an important locality of Vertebrate fossils on the eastern end of the Villány Mts., near the town Villány. At site No. 2 the fissure developed in Upper Jurassic Szársomlyó Limestone and is filled with yellow silty material. The age of the fossils found here is *Templomhegy* stage in Vertebrate stratigraphy, Lower Pleistocene (Jánossy 1986) which corresponds to 0.9 million years. According to the Mollusc studies of Krolopp (2000) the fauna indicates the Lower Pleistocene cooling period.

The composition of the rocks is different from the red clays previously discussed. As it can be seen on the diagram of Fig. 9, the samples contain about 20-40 % carbonate which is exclusively calcite. The silicate phase contains medium quartz (15-30 %), little feldspar. Kaolinite is very low, together with some iron minerals such as goethite and amorphous iron hydroxide, their amount is less than 10 %. The dominant clay mineral is detrital illite, in the diagram the whole compositional range is close to the non-weathered pole of the triangle. The general character of the composition is transitional to that of true loess (Kordos, 1978, unpublished report).

There seems to be some vertical zoning: kaolinite occurs in the lower part of the sequence while in the upper part little chlorite appears instead of kaolinite. In a similar manner, the ecological character of the Vertebrate fossils shifts toward the top of the outcrop what was interpreted by Jánossy (1986) as an episode in the general trend of cooling of the climate in the Early Pleistocene. The shift in the mineralogy is in good agreement with his conclusion.

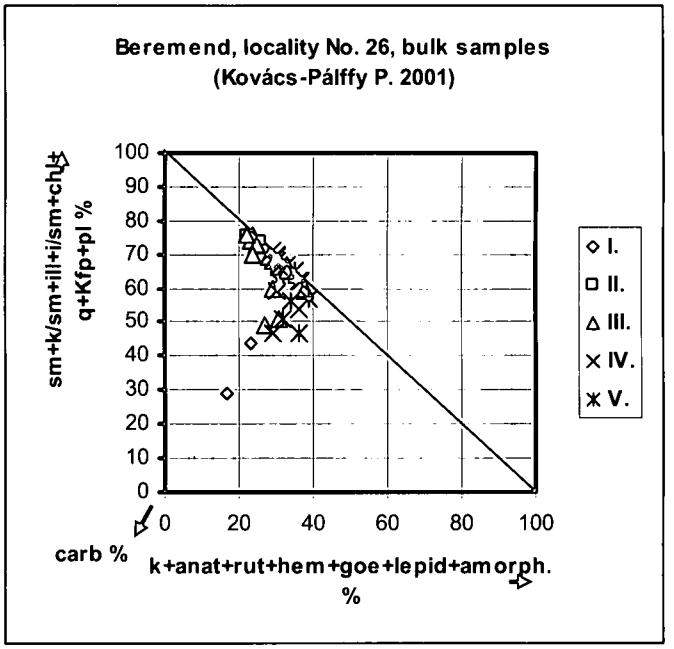

Fig. 7. Mineral composition of red clays, Beremend quarry, locality No. 26, bulk samples (Kovács-Pálffy P. 2001, see Table 1). Legend: I., II., III., IV., V.: horizons from top to bottom.

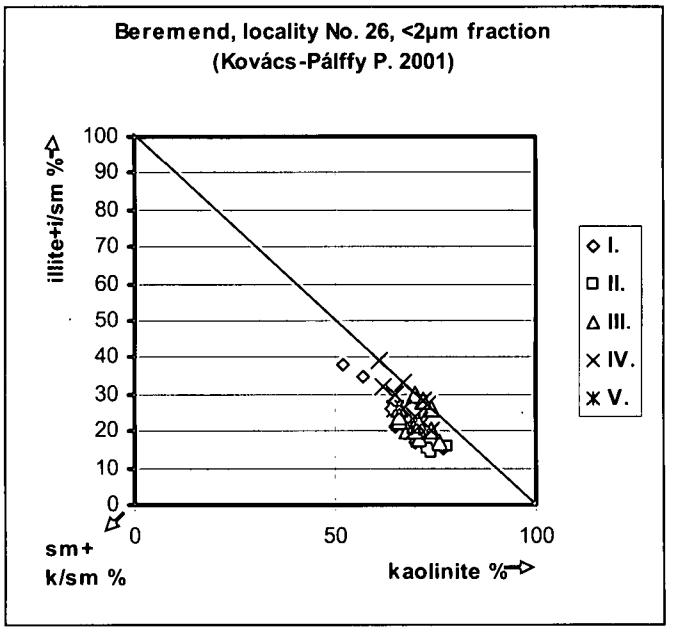

Fig. 8. Clay mineral composition of red clays, Beremend quarry, locality No. 26, <2μm fraction (Kovács-Pálffy P. 2001, see Table 1). Legend: see Fig. 7.

Red or reddish clays of Tengelic Formation in the wider surrounding of Villány Mts. (Tengelic Member of the Tengelic Fm.)

In the hilly areas, at Tétel-halom (SE of Solt) and at Dunaföldvár mixed-layer illite/smectites were identified as the main clay minerals in red clays, accompanied by little

kaolinite at Dunaföldvár (Borsy and Szöőr 1981). It was again Bidló (1983a) who analysed first red clays in this area by X-rays and found dominantly disordered kaolinite in a sample from Dunaújváros (this exceptional composition in the hilly areas indicates probably an occurrence of the *"Beremend Member"*).

The first quantitative X-ray diffraction analyses from the hilly areas were made on a sample of red clay underlying the basalt lava flow at Bár (Viczián 1971). The eruption of the basaltic volcano at Bár (Viczián 1965) occurred before 2.17 Ma, during the period of accumulation of the Tengelic Red Clay Fm. and produced lavas of a potassium rich basaltic rock (Hőnig 1971 in Szederkényi 1980, Balogh et al. 1986). In the borehole Bár-4 loess-containing clay covers and brick red and bright red clay of 12 m thickness underlies the basalt flow. In borehole Bár-5 loess and brick red clay of 14.5 m thickness alternating with loess intercalations covers and 2.6 m brick red clay underlies the basalt flow. In borehole Bár-6 loess with intercalations of red clay overlies basalt. The borehole stopped within the basalt. There are vertical fissures in the central part and vesicles in the upper margin of the basalt flow filled with red clay. The sample studied was taken from the borehole Bár-5, 53.3-53.7 m. This is near to the lower margin of basalt. The composition does not show strong contact effect because it contains much smectite. In addition to smectite it is a typical "detrital" assemblage, much quartz, muscovite, illite, feldspars. There is almost no carbonate, the iron mineral is hematite. The sample can be considered to be an older deposit of the *Tengelic Member* of the *Tengelic Formation*. Its composition fits well into the group of samples of the same unit (Fig. 10).

Later two brownish red clay samples were studied from the Tengelic-2 borehole (Viczián 1979, see Halmai et al. 1982). This borehole gave the name of the *Tengelic Formation* and the sequence found here is now proposed to be the stratotype of the *Tengelic Member* of the formation (Koloszár 2004).

The mineralogy of these "reddish" clays of the has been extensively studied in the last years in connection with the prospecting for disposal of radioactive waste materials. Detailed geological and palaeopedological studies were carried out on occurrences of the Tengelic Fm., such as in the Tolna Hegyhát area by Jámbor (1997), for borehole Udvari-2A: Koloszár (1997), for borehole Diósberény-1A: Marsi (1997) and in the Mórágy Hills area. For the Mórágy Hills see papers by Koloszár and Marsi (1999), Koloszár et al. (2000), Marsi (2000, 2002) and Marsi et al. (2004).

In the present chapter only the relations of the quantitative mineralogical composition of the younger, illite-smectite-rich type are considered. The partly unpublished X-ray diffraction data were collected and made available for our statistical study by M. Földvári. The data comprise samples from the Udvari-2A and Diósberény-1A boreholes from the Tolna Hegyhát area and from the Üveghuta boreholes from the Mórágy Hills area.

In the diagram showing the bulk composition (Fig. 10) data points are concentrated around the non-weathered to moderately weathered pole of the triangle. No significant differences can be recognised between the Mórágy Hills and Tolna Hegyhát areas. Carbonate is usually very low, there is, however, not solely calcite, but a little dolomite, too.

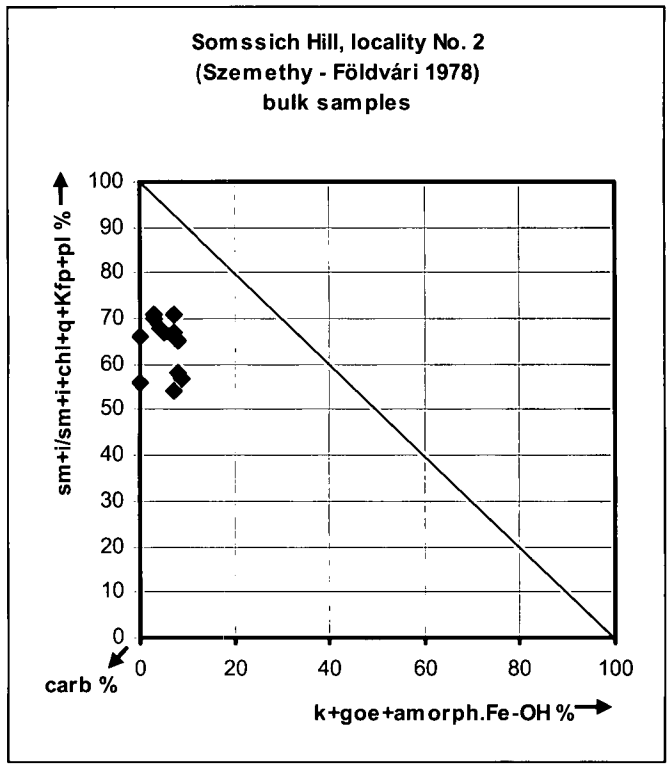

Fig. 9. Mineral composition of yellow clays, Somssich Hill, locality No. 2, bulk samples (Szemethy, Földvári 1978, see Table 1).

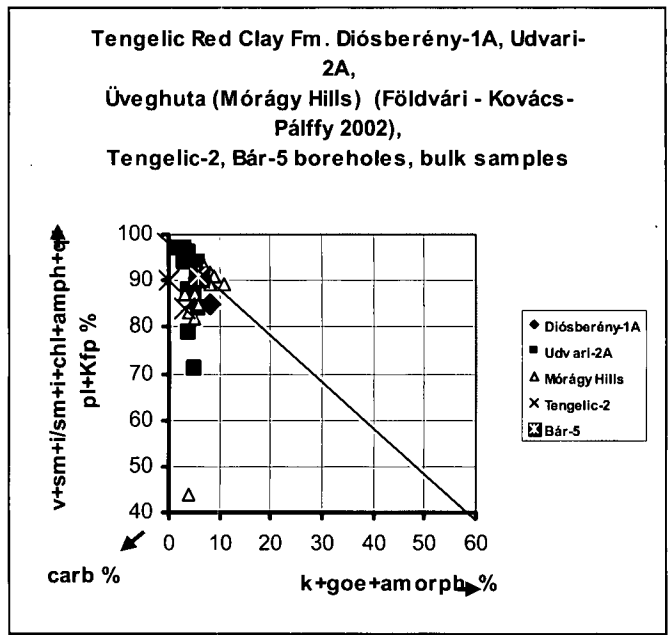

Fig. 10. Mineral composition of Tengelic Red Clay Formation, Diósberény-1A, Udvari-2A, Üveghuta (Mórágy Hills) (Földvári, Kovács-Pálffy 2002), Bár-5, Tengelic-2 boreholes, bulk samples.

Kaolinite is absent or less than 3 %, a few per cents of crystalline or amorphous iron hydroxides are responsible for the red or "reddish" colour of the samples. Among the not weathered silicate minerals quartz is sometimes very abundant ranging from about 35 to 60 %. Marsi (2000)

recognised enrichment of resistant minerals such as quartz in the samples of Tengelic Fm. He thinks that it indicates "long-lasting semi-arid weathering". The feldspars plagioclase and potassium feldspar are well represented in every sample which again indicates absence of strong weathering. Among the clay minerals smectite is the most widespread (15-30 %). Smectite is in some samples replaced by vermiculite. Other clay minerals are in decreasing order illite and chlorite, both are well crystallised.

Comparing these data with the average values for the Tengelic red clays published by Földvári and Kovács-Pálffy (2002) we can find good agreement. In general, they have found that these clays are poor in carbonates (calcite and a little dolomite), plagioclase, illite and chlorite and contain predominantly smectites among the clay minerals. They also stressed the very low kaolinite contents (less than 2 %) and recognised that smectite can be replaced by vermiculite. They have found Mórágy Hills (Üveghuta boreholes) to be somewhat more weathered than the Tolna Hegyhát area. This is more evident in our study from the <2 μm fraction.

Among the clay minerals of the <2 μm fraction (Fig. 11) either illite, or the 14 Å minerals (smectite or vermiculite) are the main clay minerals. Kaolinite is generally low. There is large scatter in the illite to (smectite+vermiculite) ratio. A high variety of mixed-layer structures between vermiculite, smectite, chlorite and illite was identified. Vermiculitic minerals seem to be preferably associated with high illite contents and chlorite, while samples with lower illite contents tend to contain rather smectite and somewhat more kaolinite. This variation can be interpreted by two types of assemblages. There is a very weakly weathered assemblage with dominant illite + chlorite and vermiculite and a moderately weathered assemblage with dominant smectite + illite and kaolinite. As for the regional differences, according to the composition of the <2 μm fraction the red clays of the Mórágy Hills area tend to be somewhat more weathered than those of the Tolna Hegyhát area.

In conclusion, red clay samples in the wide hilly surrounding of the Villány Mts. belonging to the Tengelic Member of the Tengelic Formation reveal little or moderate weathering and oxidation of the terrestrial sedimentary material.

Red palaeosol beds at the base of the Paks Loess Formation in the wider surrounding of Villány Mts.

During the studies connected with the radioactive waste disposal a group of red clays was separated from the Tengelic Fm. and was considered as an independent stratigraphic unit. These are red clays on the basis of the Middle Pleistocene Paks Loess Fm., their stratigraphic position is Lower Pleistocene to lowermost Middle Pleistocene (0.8 to ~1.2 million years). The stratigraphic position is given by the scheme of Koloszár and Marsi (2002). Geology and mineralogy of the palaeosol is treated in the same papers which were cited in the former chapter on the Tengelic Red Clay. In particular, Marsi and Koloszár (2004) identified the red palaeosol layer in the Beremend quarry with the *"Paks Double" soil complex* (PD, 0.8 my). Red palaeosols found in the Diósberény-1A and Udvari-2A boreholes were correlated with the soil beds Pv_1-v_5 and PA (Jámbor, 1997). In the Mórágy Hills area red palaeosols belong to the PD horizon (Koloszár, Marsi 2002).

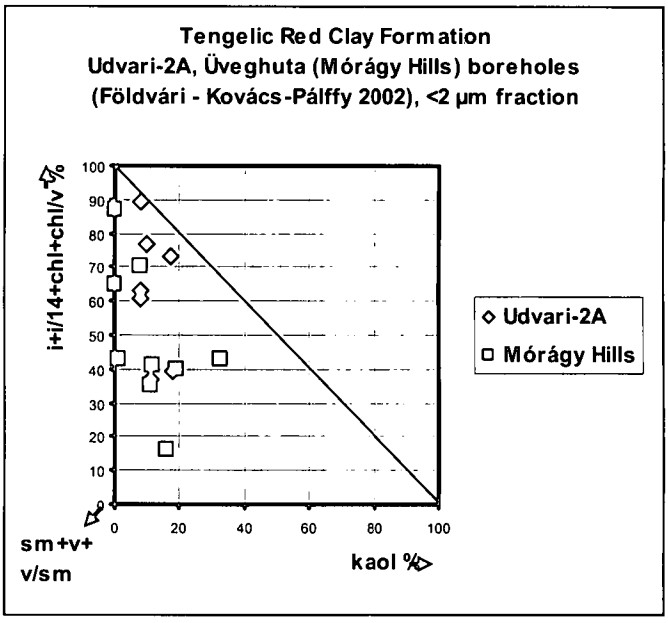

Fig. 11. Clay mineral composition of Tengelic Red Clay Formation, Udvari-2A, Üveghuta (Mórágy Hills) boreholes (Földvári - Kovács-Pálffy 2002), <2 μm fraction.

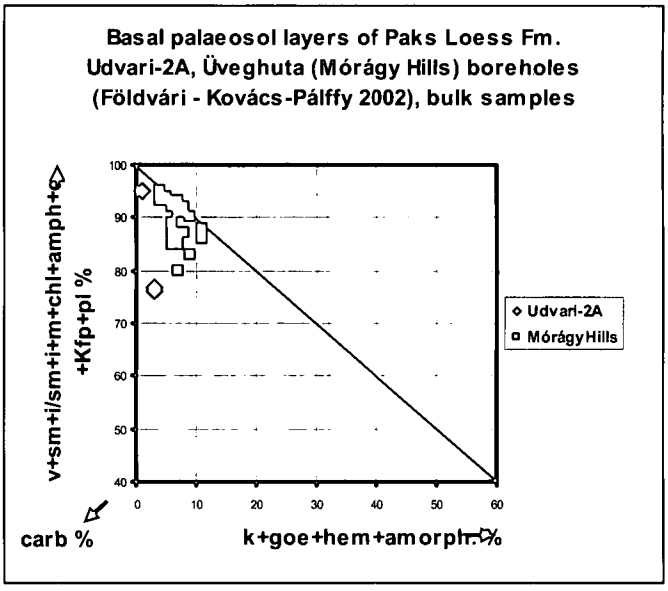

Fig. 12. Mineral composition of Basal Palaeosol layers of Paks Loess Fm., Udvari-2A, Üveghuta (Mórágy Hills) boreholes (Földvári - Kovács-Pálffy 2002), bulk samples.

Similarly to the Tengelic Fm., quantitative mineralogical data were obtained by the courtesy of M. Földvári.

Considering the diagrams for the bulk composition (Fig. 12) and for the <2 μm fraction (Fig. 13) the similarity with the corresponding diagrams of the Tengelic Fm. is conspicuous. General quantitative relations of the minerals in the bulk composition of the Tengelic samples can be applied also for the red palaeosol layers. This fact indicates similar genetic relations for both stratigraphic units. In the <2 μm fraction the differences are more visible. Smectite contents seem to be generally higher and illite and chlorite are lower in the Tengelic clays than in the palaeosol. This observation

agrees with the results of Földvári and Kovács-Pálffy (2002) who demonstrated in more detail that there are significant differences between the Tengelic red clays and the palaeosols in several parameters. They have found higher smectite, total clay mineral, H_2O and (H_2O+OH) contents and lesser illite, chlorite and plagioclase carbonate contents. In general, they have shown higher degree of weathering in the Tengelic Formation than in the palaeosol.

Various karst-related sediments in the Villány Mts. area (Upper Pannonian, Tengelic Fm. and Paks Loess Fm.)

In a comprehensive study completed recently (Dezső et al. 2007) the filling sediments of fissures and caves of various origin were investigated in the central and SE part of the Villány Mts. The sites studied are often closely related to famous localities of fossil Vertebrate fauna. The filling sediments represent various red clays, redeposited loess and in some cases sandy siltstones and products of their disintegration.

The mineralogical composition was determined in the bulk samples (Fig. 14) and in the <2 μm fraction (Fig. 15) by X-ray diffraction. Two types of the mineral associations can be distinguished.

In the *weakly or moderately weathered type* the clay minerals are represented by variable amounts of illite and smectite, less kaolinite or chlorite, fairly much quartz and feldspars. Kaolinite is medium ordered. The iron mineral is dominantly goethite. Weakly or moderately weathered associations can be found

- in Nagyharsány quarry in the debris of the overlying Pannonian siltstone and in redeposited loess,
- in Beremend quarry in the red palaeosol that covers the limestone and underlies the loess and in a few red clay fissure fillings in the limestone and
- at the town Villány in clays deposited in the caves Borpince and Templomhegy-zsomboly (shaft cave).

In the *intensely weathered type* the main clay mineral is strongly disordered kaolinite accompanied by smectite and mixed-layer kaolinite/smectite. There are anatase and rutile and gibbsite appears in lesser or medium amounts. Usually

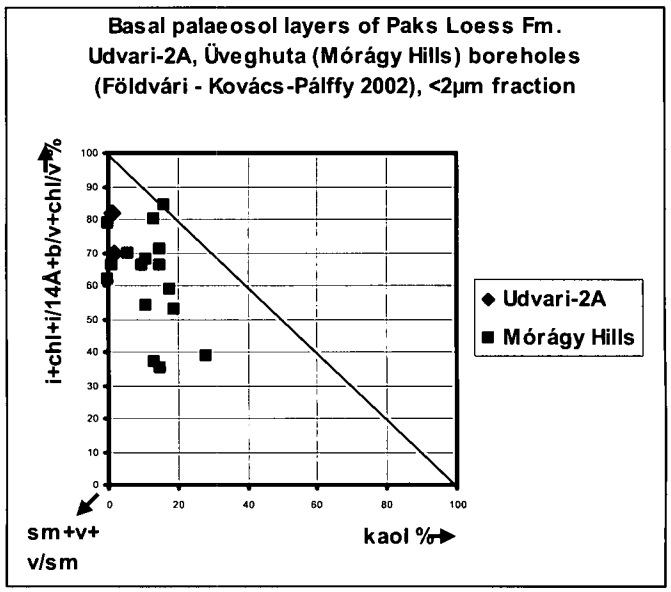

Fig. 13. Clay mineral composition of Basal Palaeosol layers of Paks Loess Fm., Udvari-2A, Üveghuta (Mórágy Hills) boreholes (Földvári - Kovács-Pálffy 2002), <2μm fraction.

quartz is very low or missing. Normally hematite is more abundant than goethite. Such sediments were found

- in several fissure fillings of the Beremend quarry,
- in fine grained clays in the Macskalyuk cave at Máriagyűd.

There are two *transitional* samples between the two types well visible in Fig. 15: the lowermost filling in the Borpince cave at the town Villány, and a concretion from the Nagyharsány quarry.

Considering the age and stratigraphic position, the oldest formations studied in this particular set of samples from the Villány Mts. area are the remnants of the overlying Pannonian sandy siltstone which is normal lacustrine basin sediment. Highly weathered red clays belong to the starting period of terrestrial accumulation of the *Tengelic Red Clay Formation* (*Beremend Member*). For the sample that was taken from the locality No. 26 in the Beremend quarry (see

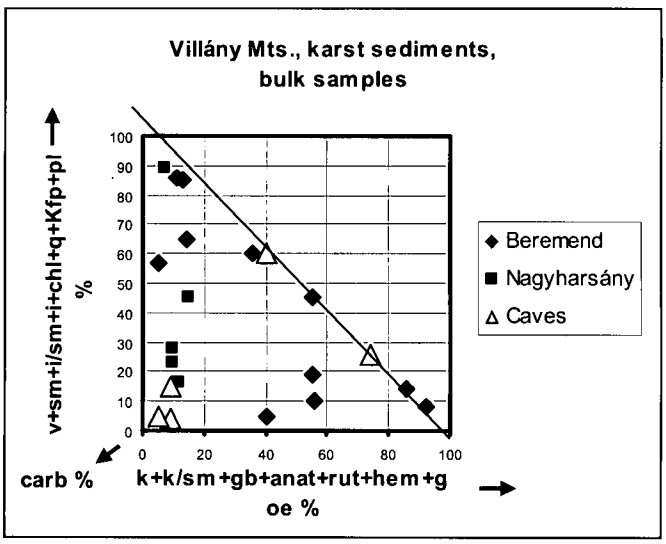

Fig. 14. Mineral composition of karst sediments, Villány Mts., bulk samples.

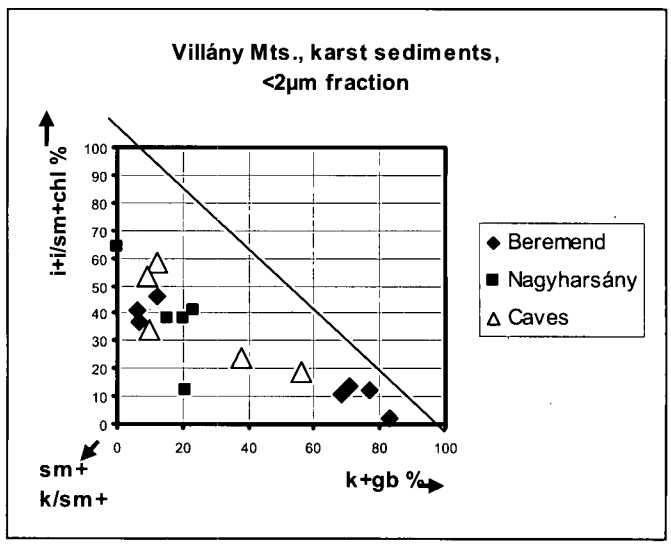

Fig. 15. Clay mineral composition of karst sediments, Villány Mts., <2μm fraction.

the corresponding chapter) this period can be dated to about 3.1 to 3.3 million years in the Pliocene but other red clays may have been deposited earlier or somewhat later. During the further, longer period of the accumulation of *Tengelic Red Clay Fm.* (*Tengelic Member*) as well as during the formation of the red palaeosol and of the loess the weakly or moderately weathered types were formed. Both highly and weakly weathered types may be found among the cave sediments depending on the time of transport and accumulation in the cave.

Discussion

The possible mechanical effect of the transport into the karstic cavities

The granulometry of the karstic sediments of the Villány Mts. was studied by the laser method by J. Dezső (see Dezső et al. 2007). Various environmental factors could be recognised by the statistical evaluation of the grain size distribution curves of fissure fillings and cave sediments, like the effects of aeolian transport, type of the parent rock, the weathering process and ways of underground sediment transport. Most cave sediments and concretions have distribution curves with a single maximum in the clay size domain. Distribution curves with a single maximum in the silt size domain are typical for the debris of the overlying siltstone, for the redeposited loess and for the red palaeosol underlying the loess. Red clay fissure fillings and some cave sediments display bimodal distribution curves with maxima both in the clay and silt domain.

The products of the surface weathering were transported into the karstic cavities by running or slowly infiltrating water. Slow infiltration with intermediate sediment traps may have produced separation of the grain size fractions, and accordingly, further enrichment of the fine-grained weathering products. This may be the case for the cave sediments, especially for the extremely fine-grained clays of the Macskalyuk cave at Mariagyűd. This clay bears only highly weathered mineral assemblage in the bulk composition because coarser, less weathered grains were sorted out during the infiltration (Fig. 14). On the other hand, highly weathered red clays in the karstic cavities of the Beremend limestone quarry are not extremely fine-grained. It was shown by Dezső et al. (2007) that all samples bearing gibbsite and kaolinite and some samples without gibbsite but with high contents of disordered kaolinite have equally bimodal grain size distribution and may be classified as silty clays. The amount of silt-size fraction is in no correlation with the gibbsite or kaolinite contents and the silt/clay ratio is near to 1.

A special way of displacement of the covering sedimentary material is the collapse of the overlying beds. In the Nagyharsány quarry a broad fault is filled with the debris of the overlying Pannonian siltstone. In this case the filling sediment is completely unsorted containing blocks of several 10 cm size embedded in a silt size matrix. The matrix has practically the same mineral composition as the blocks showing that there was no additional chemical alteration in the silt size debris.

All these considerations may concern only the bulk composition. Compositional differences in the <2 μm fraction should not be influenced by the amount of the coarser fraction in the sample and by the way of transport into the underground cavities.

Chemical action of the karst water

Most probably the water which transported the sediments from the surface into the fissures and caves did not modify their chemical composition. The loosely accumulated clay was later saturated by karst water. Under these conditions the possible formation of gibbsite from kaolinite and the possible transformation of other clay minerals into kaolinite are of special interest. Recent measurements have shown that the pH of the karst water below the Beremend quarry is near to neutrality (J. Dezső, pers. comm.). According to experimental data (see Bárdossy 1982, Fig. 157 and Fig. 158) both kaolinite and gibbsite are stable at pH = 7. The decisive factor for the formation of gibbsite from kaolinite is the silica content of the ground water. At concentrations H_4SiO_4 < 2 ppm kaolinite dissolves incongruently and gibbsite remains. When this would be the case, "intense percolation by ground water and a positive Eh made even a kaolinitic primary material yield gibbsite, a situation observed in numerous laterite profiles" (Bárdossy 1982, p. 322). The limiting concentration of silica may be even higher than 2 ppm. According to Lippmann (1981) the metastable equilibrium between kaolinite and gibbsite lies approximately at the activity value $[H_4SiO_4] \approx 8$ ppm.

We have analytical data of the silica concentrations from the water found in a shaft in the Beremend quarry. Here in dominantly Ca-Na hydrocarbonate waters the H_2SiO_3 concentration is 17.80 mg/l, water temperature: 26 °C. The water of the subthermal spring coming from the same limestone contains 2.60 mg/l H_2SiO_3 (20-21 °C) about 5 km away, at Kistapolca (analyses by S. Rapp-Sík, see Fülöp 1966, p. 42 and p. 40). H_2SiO_3 concentrations are in the range of 10-20 mg/l in cool, subthermal waters of similar composition in the Buda Mts. (see Schulhof 1957). We can estimate activity values of $[H_4SiO_4]$ in the range 2 to 20 ppm and this means that water composition is in the metastable stability field of kaolinite but close to the boundary toward gibbsite. Considering the concentration relations of silica gibbsite might have been formed occasionally in the subsurface conditions provided that there were fluctuations in the silica concentration and the water flow was sufficiently strong. On the other hand, montmorillonite (smectite) is surely to be transformed into kaolinite at these concentration values. It is persistent at much higher H_4SiO_4 concentrations than kaolinite (higher than about 0.01-0.1 % H_4SiO_4, Lippmann 1981). Transitional phases like mixed-layer kaolinite/smectite indicate intermediate steps in this transformation. One has to remark that the reaction in the reverse direction is excluded even because of the lack of sufficient silica.

The progress of chemical reactions would be supported by intense movement of water and high permeability. In most cases however, calcitic cement and void-filling druses precipitated from the karst water were observed. We can suppose that cementation prevented further water flow and completion of the progress of the reactions.

Gibbsite formation would require oxidising conditions. The recent descending water in the quarry has positive Eh but the ascending subthermal karst water is in reduced state (J. Dezső, pers. comm.). Therefore gibbsite from kaolinite and kaolinite from smectite have been formed more probably in the well drained and oxidised soil profiles on the surface than in the karstic fissures.

From the point of view of chemical action of the ground water the alteration of a basaltic dyke intruded into the limestone complex of the Beremend quarry may be of interest (Molnár, Szederkényi 1996, Nédli, M. Tóth 2003). The dyke is 1-3 m thick, highly altered. Its age is Upper Cretaceous. The alteration products were identified by XRD as calcite and nontronite. Another two basaltic dykes were described by (Fülöp 1966, the alteration by Viczián). Fülöp considered them to belong to the Lower Cretaceous magmatism but Nédli and M. Tóth (2003) suppose Upper Cretaceous age based on recent measurements and analogies. One dyke occurs in a quarry on the western end of the mountain range at Babarcszőlős. The dyke intruded into Upper Anisian dolomite is 10 to 190 cm thick, and is again highly altered on the rims. The altered rim may be 40-50 cm thick. Its colour is violet and red. The main alteration products are "limonite", calcite and montmorillonite but there is a few kaolinite too. A third dyke occurs in the borehole Turony-1, at 209-213 m. Its colour is grey but the groundmass and most feldspar are altered to nontronite. Nontronite was identified in microscope and by the 060 reflection in the XRD pattern. Additional clay minerals are little illite and mixed-layer illite/nontronite. The dykes never have been exposed to subaerial weathering until the recent mining works they still have highly altered rims. Their alteration must be the effect of the subterranean groundwater flow through the carbonate host rocks. Those being close to the recent surface are highly oxidised. In each case the main alteration product is a smectite mineral (nontronite) which can be accompanied by little illite in the lower levels and by kaolinite close to the recent surface. High amounts of kaolinite and gibbsite do not occur. All that shows that ground water or karst water may cause the transformation of silicatic material into a smectite group mineral.

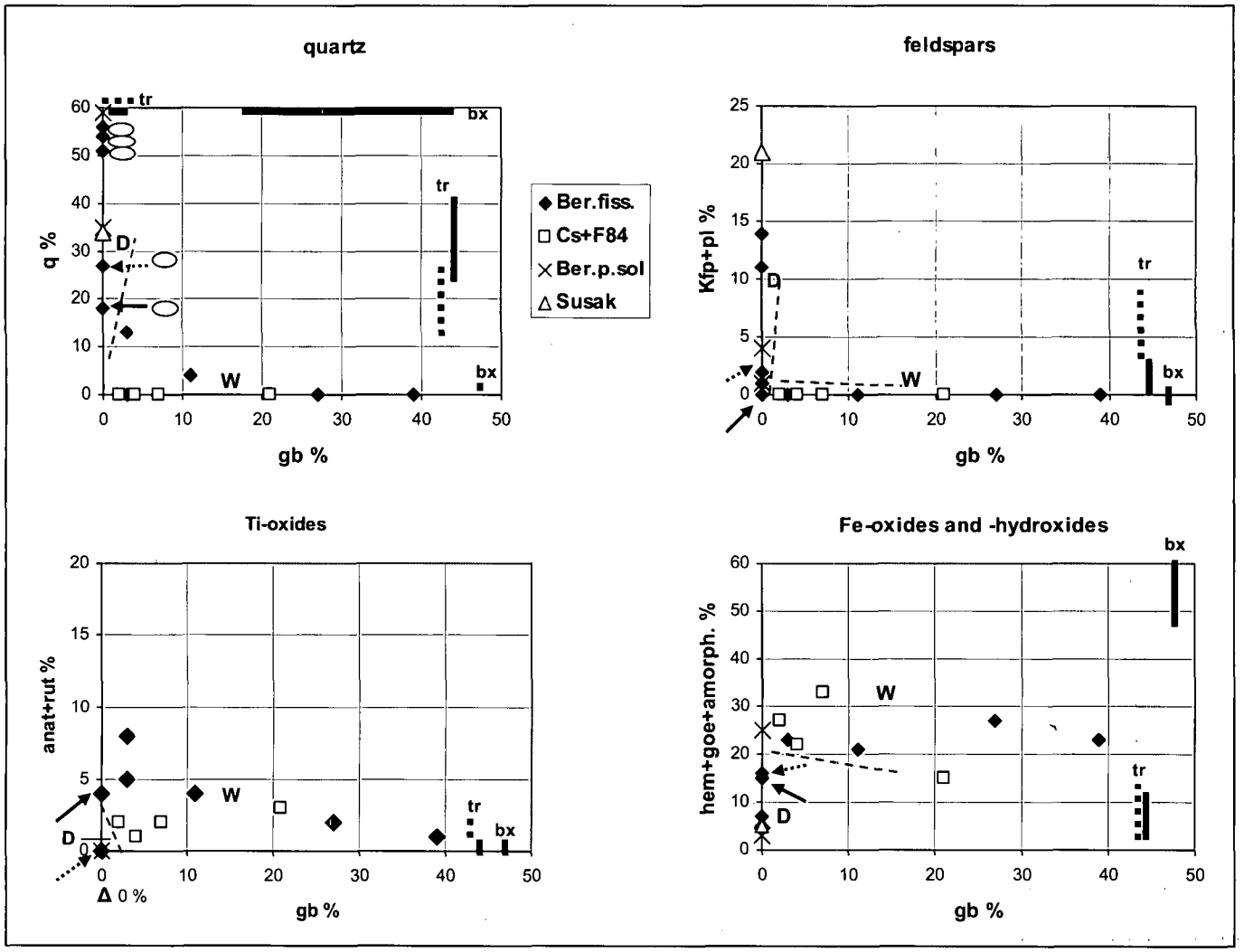

Fig. 16. Variation of minerals in function of the gibbsite contents in the bulk composition of red clays in the Beremend quarry. The percentages are converted to carbonate-free material. Legend: D: "detrital" type, W: "weathered" type. Dotted lines are tentative boundaries of the types. Arrows indicate the point representing locality No. 26. Source of data: *Ber.fiss.*: fissure filling clays (Kovács-Pálffy: average of 40 samples, solid arrow, Dezső et al. 2007: dotted arrow), *Cs+F84*: bauxitic clays (Császár, Farkas 1984), *Ber.p.sol*: palaeosol (Dezső et al. 2007). Ellipses in the quartz diagram indicate fossil bone rests in the sample. Continuous thick lines on the upper and right side of the diagrams indicate ranges of values measured in Aggtelek-Jósvafő area (N Hungary), tr: *terra rossa*, bx: bauxite pebbles in *terra rossa,* dotted thick lines represent *terra rossa* analyses from the Dinaric range (Bárdossy 1982, Tables 48 and 47). Data points for Susak Island: from Bognar et al. (2003).

In conclusion, in most cases, differences in the mineral composition of the fine fraction of the fissure-filling clays should reflect real differences in the intensity of weathering on the ancient surface. In the subsurface conditions weathering processes might have continued until the formation of smectites but only occasionally further, until the formation of kaolinite or gibbsite.

Mineralogical and petrographical aspects of the origin of gibbsite in red clays of the Beremend quarry

From the point of view of prospecting for bauxite deposits the gibbsite-bearing sediments are of special interest. As it was mentioned before, red clays containing gibbsite were found first by Császár and Farkas (1984) in the Beremend quarry. Similar and even higher gibbsite contents were detected also by us from other points in the same quarry. In two now existing caves the lowermost accessible sediments also contain a few per cent gibbsite in the <2 μm fraction (Dezső et al. 2007). The question arises, what is the relation of these gibbsitic or bauxitic clays to other red clays that occur in the quarry. Whether they form two separate compositional groups or are they connected by several transitions. In order to answer these questions diagrams were constructed, in which the variation of the amounts of minerals in function of the gibbsite contents are shown (Fig. 16, Fig. 17 and Fig. to 18). Because the carbonates are supposed to be secondary, not influencing this relationship, the percentages were recalculated into carbonate-free material.

The diagrams of most minerals in the bulk composition (Fig. 16 and Fig. 17) show clearly the difference between the samples without gibbsite and samples containing gibbsite even in low amounts (from 1 % on in the carbonate-free material). The gibbsitic composition can be called here for the simplicity as intensely "weathered" and the gibbsite-free type as "detrital" because it is probably not or only slightly weathered. The gibbsite-containing samples contain no or very little quartz, no feldspar and chlorite. On the other hand, the group with zero gibbsite always contains quartz, usually high quantities, up to almost 60 %, and systematically a few per cent of feldspar and chlorite. As for illite, there is a tendency that illite contents are higher in the no-gibbsite group and lower or zero in the gibbsitic type. In addition, the

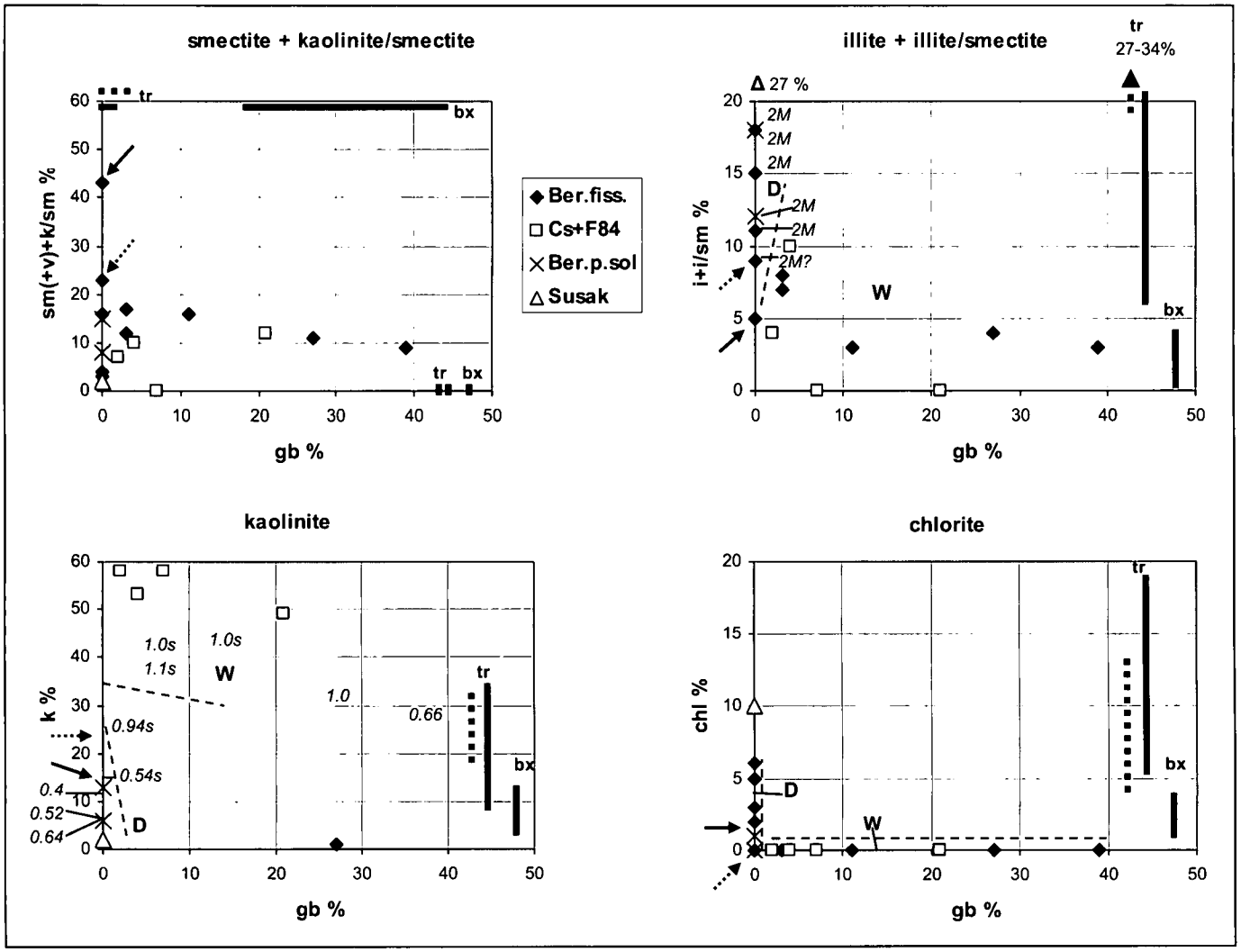

Fig. 17. Variation of clay minerals in function of the gibbsite contents in the bulk composition of red clays in the Beremend quarry. The percentages are converted to carbonate-free material. Legend: In the illite diagram: *2M*: illite-2M can be identified. In the kaolinite diagram: *numbers* refer to width of the 001 basal reflection in 2Θ° units, *s*: k/sm>5 %. For other signs and abbreviations see Fig. 16.

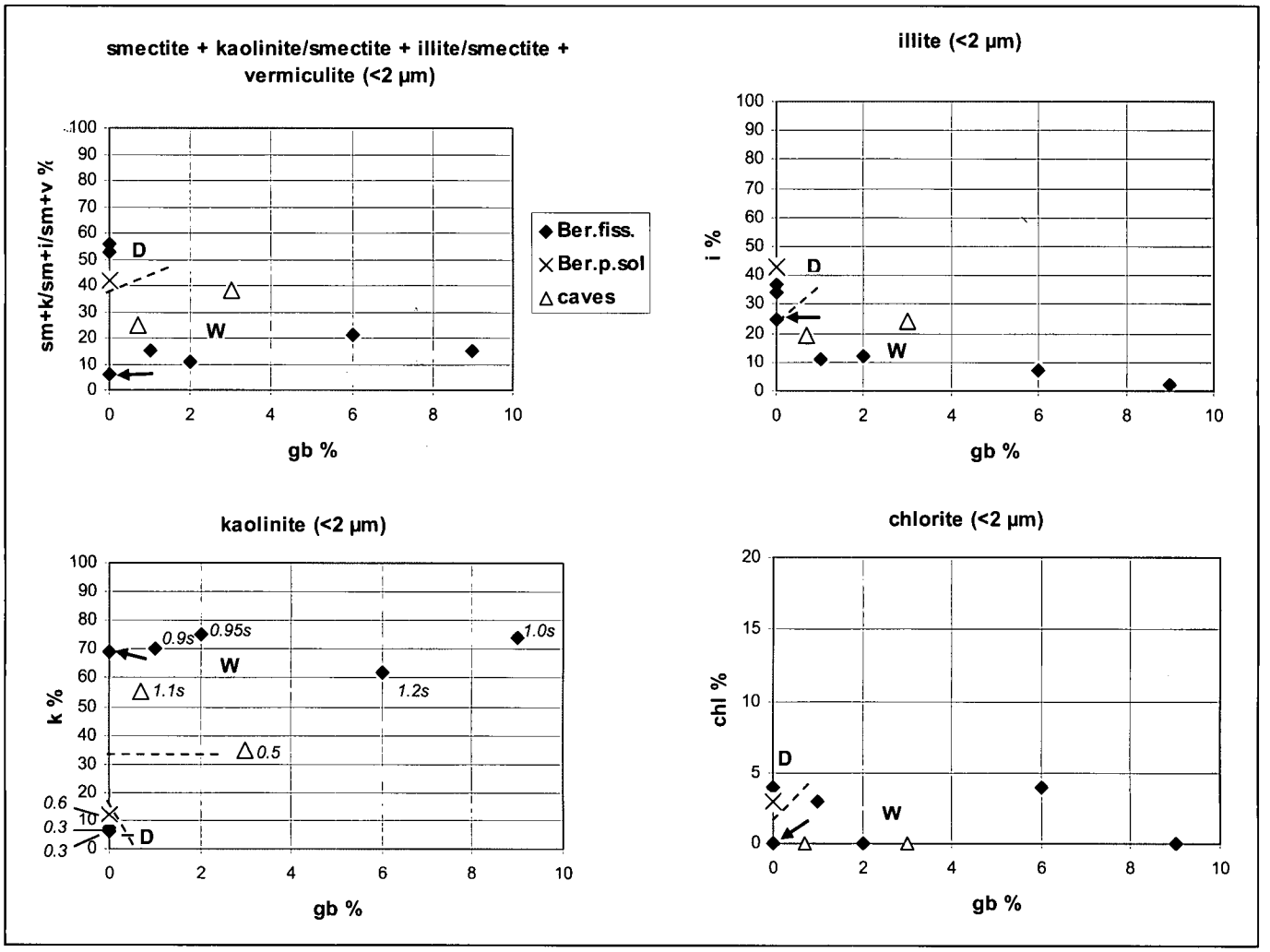

Fig. 18. Variation of clay minerals in function of the gibbsite contents in the <2μm fraction of red clays in the Beremend quarry and in cave sediments of Villány Mts. The percentages are converted to carbonate-free material. For signs and abbreviations see Figs 16 and 17.

well-crystallised 2M modification could be identified exclusively in the no-gibbsite group. The boundary is, however, much less sharp than in the previous cases.

In the gibbsite-free, "detrital" group kaolinite contents are by 10-20 % lower than in the gibbsite-containing group. On the contrary, the most striking feature of the "weathered" group is the high kaolinite content. Kaolinite is about 50-60 % when gibbsite percentages are low. It decreases again to about 25 % when gibbsite contents grow higher than about 25 % (in the bulk composition). It shows probably that kaolinite has been converted to gibbsite during the progress of weathering or alteration. There are clear differences in the degree of order between the kaolinites of the two groups as measured by the width of the first basal reflection at half height in 2Θ° units. In the "detrital" type these values are in the range 0.4-0.6°, kaolinites have sharp basal reflections, they are well or medium ordered. The "weathered" type kaolinites are highly disordered. The width values are between 0.9 and 1.1° when gibbsite is less than about 30 %. Again, in the sample with the maximum gibbsite content the ordering increases, accordingly the width of the basal reflection decreases to 0.66° 2Θ. Similar observation was already made by Császár and Farkas (1984). This shows probably that bauxitisation runs parallel with ordering of the kaolinite structure. The same rule holds when the kaolinite/smectite mixed-layers are considered, the highest amounts are in the low gibbsite range of the "weathered" group (indicated by "*s*" in Fig. 17).

The repartition of the iron oxides and hydroxides (hematite+goethite) is similar to that of kaolinite. In samples where there is no gibbsite, iron minerals are generally low (less than 10 %) and in the gibbsite-containing samples there are high iron mineral contents (20-30 %). There seems to be a compositional gap between the two groups however, the scattering of the data is rather high. As a rule, the gibbsitic samples contain more hematite while the gibbsite-free, less weathered samples more goethite. The gibbsitic clays always contain Ti-oxide minerals, anatase or rutile, or both, while members of the "detrital" group never.

Contrary to the minerals discussed so far, contents of smectites and mixed-layer kaolinite/smectites do not display clear differences between the two groups. Their amounts scatter between 0 and 20 % irrespective of the gibbsite contents throughout the whole range of increasing bauxitisation. This is an indication that the weathering affected a dominantly smectitic material which has gradually transformed into kaolinite, but the process did not went to completion.

The clay minerals in the <2 μm fraction (Fig. 18) display the same regularities as the clay minerals in the bulk composition but the variation of the gibbsite contents is much lower than in the bulk composition. The highest gibbsite percentage is lower than 10 %. The "detrital" and "weathered" types in the smectite-like minerals are more clearly separated here than in the bulk composition. In addition to the Beremend samples two cave sediments are shown here for comparison. The clay sediment from the Macskalyuk cave at Máriagyűd (gibbsite = 1 %) fits more into the "weathered" group than that from the Borpince cave at the town Villány (gibbsite = 3 %), which is somewhat transitional to the "detrital" type.

Although most minerals show two compositional groups, in the case of almost every mineral there are transitional samples between the two groups. This is true also for gibbsite which gradually grows from 0 % to 1 % and so on, higher and higher. It is interesting to mention that the samples taken of the widest karstic depression, locality No. 26 occupy in most cases transitional position between the two groups. The corresponding points are specially noted by arrows in the diagrams. For most minerals, this sample belongs more to the "detrital" group, but its kaolinite is disordered, there is much kaolinite/smectite, and the width of the 001 reflection is 0.9° 2Θ, like in the "weathered" group. In the diagrams the values for the bulk composition from the data set of Dezső et al. (2007) differ from the average values of the quantitative data determined by Péter Kovács-Pálffy (like in Fig. 7). The reason is that the method of the determination was somewhat different and the two data sets cannot be directly compared. Smectites seem to be overestimated at the expense of other clay minerals, kaolinite and illite as compared to the data of Dezső et al. (2007). All other minerals give similar values, transitional between the two compositional groups. Unfortunately, the <2 μm fraction of this sample was not analysed by us. In the diagrams for the <2 μm fraction we have only the average values of the data of Kovács-Pálffy for the locality No. 26 (Fig. 18, signed by arrows). Like for the bulk samples, they occupy transitional position between the two groups, but closer to the "weathered" group. The difference between the bulk composition and the clay fraction indicates the dependence of the mineralogy from the grain size. In the bulk composition there is a considerable proportion of silt size material which is less weathered than the fine fraction. As it was mentioned in the Chapter of the Results, there is practically no gibbsite in the locality No. 26 therefore there is no need to argue for the derivation of a portion of the sedimentary material from the bauxites of Harsány-hegy, as it was done by Marsi and Koloszár (2004) and Koloszár (2004).

The two palaeosol samples are specially noted. It can be seen in the diagrams for the bulk samples (Fig. 16 and Fig. 17) that they are typically in the "detrital" group and fit well into its compositional range with three other red clay samples which were taken from fissures. Also in the <2 μm fraction (Fig. 18) the palaeosol sample is similar to the red clays "detrital" group.

All these considerations show that among the red clays in the Beremend quarry we have to deal with the products of different intensity of weathering:

(1) *Strong weathering* dissolved most silicate minerals and produced much disordered kaolinite, various but mostly low amounts of gibbsite, much hematite, goethite and Ti-oxides. The low gibbsite contents, the disordered nature of kaolinite and the existence of little smectite and of transitional mixed-layer phases show that the most intense phase of weathering approximated but did not reach the true lateritisation or bauxitisation.

One could suppose true bauxitisation only in the case of the occasional high (20-40 %) gibbsite contents. This is restricted to 3 samples coming from 2 occurrences close to each other (or more probably from the same single fissure) in the SE corner of the 100 m working level of the Beremend quarry. In this case derivation from a locally preserved old bauxite or bauxitic clay cannot be completely excluded. The idea of an older generation of fissure filling could be supported by the morphology of this particular fissure. Unlike the others, this fissure is very thin (about 10 cm thick), closed, it does not show the dissolution features of the wall rock limestone. On the other hand, as it was mentioned before, the known pre-Pannonian fissure system in the Magyarbóly-1 borehole is not filled with red or weathered clay material which would be something similar to bauxite. Therefore it seems to be more probable that these samples indicate material coming from the same Pliocene soil sequence as the others, but from its most intensely weathered part.

(2) The other type of weathering, producing the *"detrital"* assemblage was weak, quartz and most silicates remained unchanged. Even in this assemblage there are small amounts of kaolinite, but this is relatively well crystallised and may be detrital. Only iron hydroxides and probably smectite were formed.

The existence of samples with transitional composition, the similar macroscopic appearance and colour in both groups indicate that there were two stages of different weathering intensity following each other rather than two completely different events of mineral formation. The similar secondary calcitic cementation from the karst water with several calcite-filled voids in both groups shows that most red clays were in a loose, soft state during the Pliocene karstification. This and the incomplete lateritisation make less probable that the time of the formation of the gibbsitic composition was as early as Late Cretaceous.

Another argument in favour of the relatively young formation of gibbsite is its thermodynamic nature. Gibbsite is the more metastable, i.e. the least stable phase among the aluminium oxi-hydroxide minerals gibbsite, boehmite and diaspore. Gibbsite relatively easily transforms into boehmite and then boehmite further into diaspore (Lippmann 1981). This statement is supported by the geological evidence collected by Bárdossy (1982). The overwhelming majority of pure gibbsitic bauxites were formed during the Quaternary and the Miocene-Pliocene period (Table 16). Upper Cretaceous to Eocene bauxites, like in the Transdanubian Central range contain rarely gibbsite alone, normally boehmite in addition to gibbsite. Older bauxites, like the Harsányhegy and Pădurea Craiului occurrences have boehmitic-diasporic character and do not contain gibbsite. Gibbsite cannot survive redeposition. According to the observations of the textural elements of bauxites gibbsite "soon worn in the course of transport, ... is fairly rare as an independent clastic mineral" (p. 238).

All this makes improbable that redeposition of gibbsitic bauxite took place from previously existing Upper Cretaceous – Palaeogene bauxites into the fissures during the Pliocene.

Summary of the quantitative results for SE Transdanubia

The existence of two compositional groups of the red clays which were found in the Beremend quarry considering the quantities of minerals in relation to the gibbsite contents can be extended to the whole SE Transdanubian area studied. In order to compare the quantitative mineral compositions found in the localities discussed above the average values were determined and put on similar triangular diagrams as for the particular occurrences. The bulk composition is shown in Fig. 19 and the composition of the <2 μm fraction in Fig. 20. Karst sediments of Villány Mts. studied by Dezső et al. (2007) and other occurrences are shown separately in the diagrams.

Considering the *bulk composition* (Fig. 19), the points obtained by averaging do not express the variation in the carbonate contents which may be high in some groups such as in the Pannonian basin sediments and in the highly weathered red clays and bauxitic clays of Beremend quarry. There is however much less variation in the relation of weakly to highly weathered minerals what is favourable in the genetic evaluation.

Most red fissure filling clays of the Beremend quarry and the red clay sediment of a cave (Macskalyuk cave) belong to the highly weathered type. The average composition of the bauxitic clays formerly studied by Császár and Farkas (1984) is close to these red clays.

Almost all other formations are concentrated in the detrital, slightly or moderately weathered, carbonate-poor corner of the diagram. The less weathered ones are the Pannonian basin sediments, the pre-Pannonian fissure filling in the Magyarbóly-1 borehole, the red clays of the Tengelic Fm. and the Quaternary palaeosol in the Mórágy and Tolna Hegyhát areas. The Lower Pleistocene fissure filling silts of Somssich Hill belong to the same type only the carbonate contents are higher. The palaeosol found at

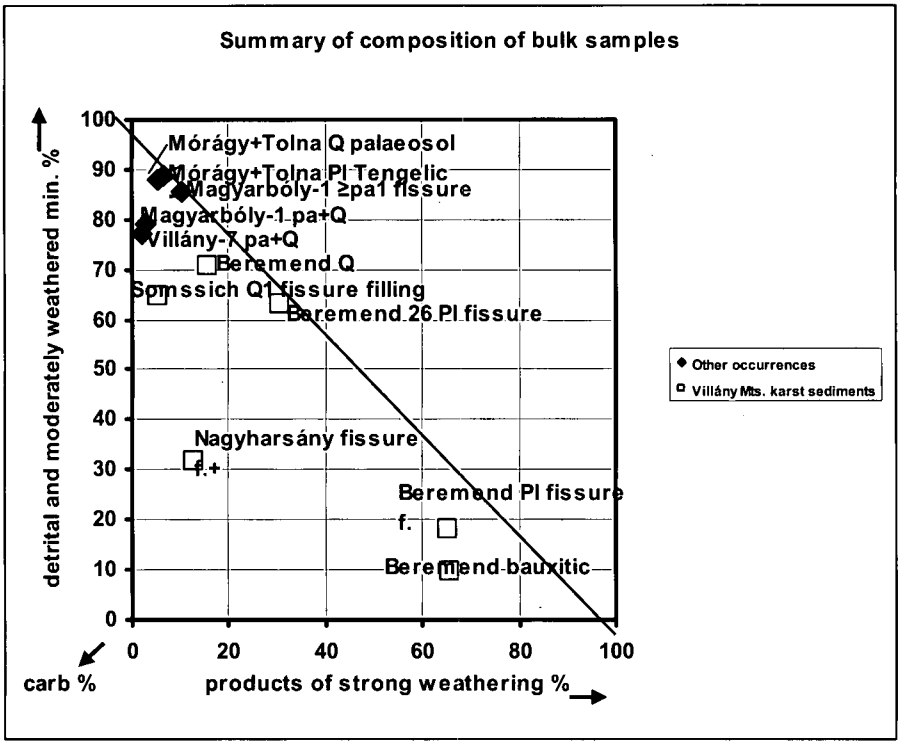

Fig. 19. Summary of mineral composition of bulk samples. Legend: ≥pa1: Lower Pannonian or older, pa: Pannonian, Pl: Pliocene, Q1: Lower Quaternary, Q: Quaternary.

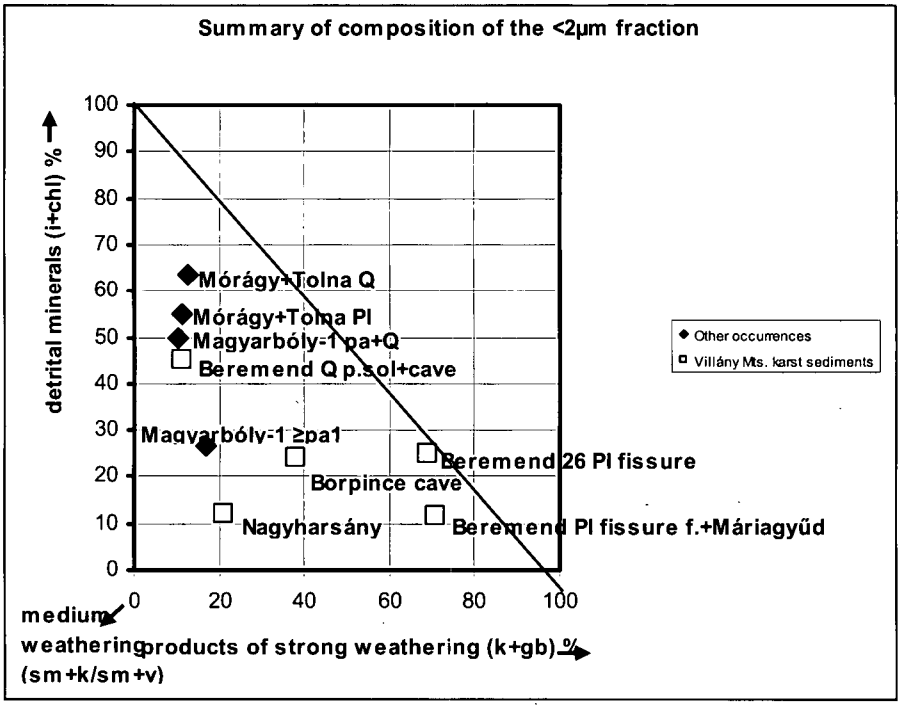

Fig. 20. Summary of clay mineral composition of the <2μm fraction. Legend: see Fig. 16.

Beremend is close to the other palaeosols, however, contains clearly more kaolinite.

The remnants of the former Pannonian covering sandy siltstone found in the fissure filling of the Nagyharsány quarry clearly differ from the Pannonian basin sediments in their higher kaolinite contents which can be due to a higher proportion of local source material. As it was discussed above, the red clays of the locality No. 26 of Beremend quarry studied by Marsi and Koloszár (2004) occupy

transitional position when the bulk composition is considered, however, they move much closer to the highly weathered red clays in the diagram of the <2 μm fraction.

In the diagram summarising the *composition of the <2 μm fraction* (Fig. 20) the localities follow the same arrangement as in the case of the bulk composition. Red clay fissure fillings of the Beremend quarry, including those of the locality No. 26 and the red clay found in the Máriagyűd cave are close to the kaolinite+gibbsite pole of the diagram.

The data points of other localities are in the low-kaolinite range, below about 20 % kaolinite contents. According to the growing smectite contents they are arranged in the following sequence: Quaternary palaeosols of Mórágy Hills and Tolna Hegyhát area seem to be the least weathered, they are followed by the Tengelic Fm. of the Mórágy Hills and Tolna Hegyhát area, the Pannonian basin sediments of Magyarbóly-1 borehole in the surrounding of Villány Mts. The scatter of each data set of these localities is equally high along the same line in the low-kaolinite region, what is not expressed by the average values. Quaternary palaeosol samples of the Beremend quarry, cave sediments of the Borpince cave and those found as collapsed debris in a fissure of the Nagyharsány quarry are shown here by a single point. Their composition is close to each other, it fits well into this series showing the genetic relationship. Unlike the bulk composition, the average kaolinite content in the <2 μm fraction of Beremend palaeosol is not higher than in the analogous occurrences but the higher smectite content indicates somewhat higher degree of weathering than in other Quaternary palaeosols of the surrounding area. The most smectite contents among the low-kaolinite localities are found in the pre-Pannonian fissure fillings of the Magyarbóly-1 borehole indicating either medium strong weathering or admixture of volcanic material. The clay material of two carbonate-cemented concretions is shown here separately because their composition is transitional to the highly weathered type.

The parent material of red clays. The question of the insoluble residue of limestones

In the *mountainous facies*, distinguished as the *Beremend Member* of the Tengelic Formation red clays are deposited immediately on karstified limestone. Therefore the question arises whether they are derived from the insoluble residue the limestone, a question which is frequently discussed in other areas covered by *terra rossa* (see e.g. Bárdossy 1982 and Durn et al. 2006). Concerning the clay mineralogy of the insoluble residue of the carbonate rocks of Villány Mts. we have quantitative data on the composition of formations occurring in the eastern part of the mountain range, namely the Ladinian *Templomhegy Dolomite Member* of the *Csukma Formation* and the Lower Cretaceous *Nagyharsány Limestone*.

In the <2 μm fraction of 2 samples of *Templomhegy Dolomite* taken from the Templom-hegy, lower quarry (see Rálisch-Felgenhauer 1987) the clay mineral is only illite with some mixed-layer illite/smectite of less than about 15 % smectite proportion (unpulished XRD analyses by I. Viczián). This is similar to the composition of the underlying Middle Triassic formations studied in detail in the borehole Nagykozár-2, about 15 km north of the Villány Mts. Here the Anisian *Lapis Limestone Fm.* and *Zuhánya Limestone Fm.* which are analogous with the German Muschelkalk, contain dominantly illite-1Md with some illite/smectite and smectite (Viczián 2000). Such association practically consisting of illite alone does not occur among the red clays. Therefore the insoluble residue of Triassic carbonates in its unaltered form cannot form the red clays. Perhaps they could contribute to the illite content of the red clays to a minor extent.

Concerning the Lower Cretaceous *Nagyharsány Limestone*, we have only one old XRD analysis from the Beremend quarry itself. In the insoluble residue of the limestone there is much illite, medium montmorillonite, little chlorite and goethite and very little kaolinite and quartz (Fülöp 1966, p. 42). In samples taken from the Harsány-hegy quarry 80-90 % of the clay minerals in the insoluble residue is illite + illite/smectite but there is a permanent other component, 10-20 % kaolinite (Császár 2002, Table 6, XRD analyses by G. Rischák). This is again a composition which differs considerably from that of the extremely kaolinite-rich red clays. There is however another mineralogical analysis of *Nagyharsány Limestone* published by Fülöp (1966, p. 29) where the composition is similar to the red clays: At Kistapolca, between the Beremend and Nagyharsány quarry localities medium "metahalloysite" (=disordered kaolinite), montmorillonite, illite and little chlorite and quartz were found in the insoluble residue. It is remarkable that the sample was taken from the immediate vicinity of a subthermal (20-21 °C) karst spring.

In conclusion the insoluble residue of the carbonate rocks of the Villány Mts. cannot be the parent material of the red clays, at least not in its unaltered form. Koloszár (2004) thinks that the main parent material of red clays of the *Beremend Member* was the weathered residue of the Upper Pannonian sedimentary cover of the mountain range which was transported by areal erosion over a pediment surface between the isolated block of the Beremend occurrence and the main body of the mountain range. On the other hand, Dezső et al. (2007) deny the existence of the pediment because in the clastic components on the surface of the Beremend block only local material can be found. According to this opinion, the source material was the weathered soil cover on the top of this local elevation in which the aeolian contribution may have played important role. It is difficult to explain the absence of quartz in the intensely weathered type of red clays. Crystalline quartz is resistant mineral which does not dissolve even during lateritisation (Fekete 1988). One has to suppose that there was little or no quartz in the sedimentary material which underwent weathering. In this respect we can think on very fine-grained sediments, intermediate (andesite) tuffs or vitric tuffs of acid composition. The admixture of basalt tuff is less probable because the eruption of the Bár volcano was by nearly 1 million years later. Unfortunately, micromineralogy was not studied so far.

In the *hilly areas* of SE Transdanubia the question of the parent material is relatively easy to be solved because the red clays in the *Tengelic Member* of the Tengelic Formation are the uppermost members of a generally detrital siliciclastic sedimentary sequence. The immediate parent materials of the red clays are most probably the underlying clay, silty clay and sand beds and locally basalt tuff occurring in the same

Tengelic Member and Upper Pannonian sediments of the surrounding territories. In the particular case of the isolated elevation of the Mórágy Hills the parent material is the granitic rubble underlain by the weathered granite.

As for the *basal palaeosol beds* of the Paks Loess Formation, the red clays occurring here are underlain by a shorter interruption by the red clays of the Tengelic Fm. The parent materials of these red clays are the underlying Tengelic red clays, there may be however already an aeolian contribution (Koloszár 2004). The remarkable similarity of the composition of the two red clay group as was found by us can be explained by the redeposition from the older one into the younger one. On the other hand, the less weathered nature of the *basal palaeosols* of the Paks Loess may be explained by a stronger aeolian contribution as it was found by Földvári and Kovács-Pálffy (2002).

Age and palaeo-environmental relations

It is advantageous that many fissures filled with clays in the Villány Mts. contain Vertebrate fossils. Their study enables us to determine the age and the environmental conditions prevailing during the accumulation of the sediment. The age of the Vertebrate fauna is nearly identical or may be somewhat younger than the age of the soil which the animals were living on. The difference in the age cannot be too large because with the changing environmental conditions the composition of the soil is evolving as well. Unfortunately, mineralogical investigations started much later than palaeontological studies and therefore they were not carried out on the same material except very few cases (e.g. locality No. 26 at Beremend). When determining the age of our samples, in most cases we can rely on analogous occurrences only.

Results of this study are summarised in Fig. 21. We can arrange the age and environmental information concerning the localities studied in this paper in the Vertebrate stratigraphic scheme constructed by Jánossy (1986). For the Pannonian formations occurring in boreholes of the broader surrounding the data of Jámbor were used (1997 and unpublished reports). In the stratigraphic scheme of Fig. 21 the occurrences and formations studied are shown. In each case the name of the locality, the rock, the age, the name of the formation and finally the typical clay mineral association in the <2 μm fraction is given. When considering the palaeo-

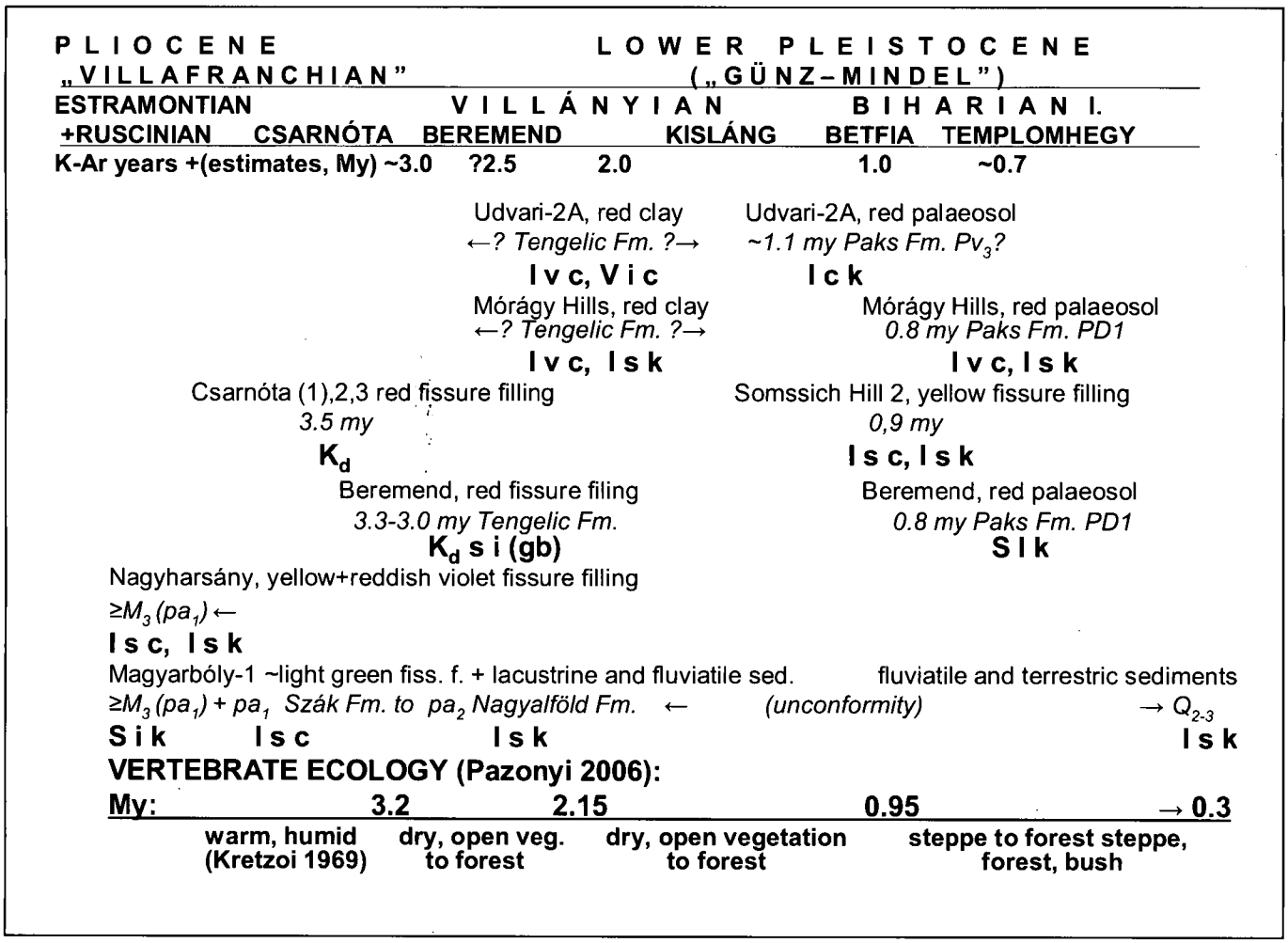

Fig. 21. Typical clay mineral associations of the formations studied. Locality, stratigraphic position, age in million years and ecological condition derived from Vertebrate palaeontology are given. Legend: s: smectite + kaolinite/smectite + illite/smectite, v: vermiculite + vermiculite/smectite, i: illite, k: kaolinite, k_d: disordered kaolinite, c: chlorite, gb: gibbsite. Capital letters: the most frequent clay mineral, small letters: other typical clay minerals; my: million years, $\geq M_3(pa_1)$: Upper Miocene (Lower Pannoniapppn) or older.

environmental relations in the given time period we relied on the comprehensive characterisation of the stratigraphic units made by Schweitzer (1993) and on the systematic summary of the environmental significance of the faunas made recently by Pazonyi (2006).

According to the diagram, the *highly weathered association* with dominant disordered kaolinite and occasionally gibbsite is restricted to the oldest terrestrial sediments, the accumulation of which started about 3.5 million years ago (*Csarnótan* stage of Vertebrate stratigraphy). As it was shown in the previous chapters, the intensity of weathering did not reach the level of true *lateritisation* of the tropical regions however it may have proceeded under warm and humid climate which lasted for a few hundred thousand years in the Middle Pliocene. This association is most common in the Villány Mts. however former mineralogical analyses have shown that the repartition of the highly weathered association is not restricted to the area of the Villány Mts. It may occur far away in the hilly areas of SE Transdanubia and even east of the Danube.

According to the palaeontological study of the site Csarnóta No. 2, it reflects a time interval when gradual transition started "from forest animal community to a grassland – steppe faunal assemblage" (Jánossy 1986, p. 22). Faunas indicating forest and also aquatic (swamp) environment were reported from the Beremend quarry in the review of Pazonyi (2006), which are somewhat younger than those of the Csarnóta locality, corresponding to the beginning of the *Villányian* stage of Vertebrate stratigraphy. Closed forest developed when the climate was warm and humid. Schweitzer (1993) characterised the climate as subtropical to tropical and emphasized the immigration of SE Asian faunal elements. Koloszár (2004) supposes monsoon climate. A good approximation of the climatic parameters is given by the observations made in various climatic zones of California. Here is precipitation in the winter season and the mean annual temperatures are between 15-21 °C. The distribution of clay minerals and gibbsite in residual soils depends on the amount of rainfall. When the mean annual precipitation is more than about 500 mm, the most frequent clay minerals are kaolinite and halloysite. When annual precipitation is higher than 1000-1500 mm gibbsite begins to form while montmorillonite and somewhat later illite disappear. Vermiculite can coexist with kaolinite and gibbsite (Barshad 1966, cited by Singer 1980). This combination of climatic parameters seems to be the most probable during the formation of the "weathered" type mineral assemblage in the Villány Mts. however, there were no high mountains and the rain season was not necessarily in winter.

Stefanovits and Fekete considered that Hungarian red clays are "genetically diverse" but at least part of them is "similar to the tropical and sub-tropical ferrolite soils regarding to their formation and mineral characteristics" (Fekete et al. 2005). This is in accordance with our conclusions regarding the "weathered" red clays in the Villány Mts. We can conclude that the soil types from which these clays are derived belong to the group of *ferrallitic soils* according to the classification of Fekete (1988). Within this group highly kaolinitic red clays with little illite and smectite and much iron-oxi-hydroxide but without gibbsite correspond to *ferruginous soils.* Such soils are formed in savannah environment with much rain but dry winters. Red clays bearing little gibbsite may have been either *weathered ferrallitic soils* which are common on the top of elevated, well drained plateaus of savannahs or *weakly ferrallitic soils* which occur around the border between the rain forests and the summer rain zone of the savannahs. Today such soil types occur around the central areas of Amazonas and Kongo Basins, Eastern India, Indo-China and in Indonesia (called *alferrites* and *reddish brown savannah soils* by Keveiné Bárány 1998).

The highest stage of lateritisation however, the *leached ferrallitic soils* with dominant gibbsite and kaolinite contents were not achieved. They would need permanently wet rain forest and mean annual precipitation higher than 1250-1750 mm. According to Bárdossy (1982) for the intense *lateritisation* somewhat warmer and more humid climate would be needed, when the mean annual temperature is 20-26 °C and the mean annual precipitation is 2000-6000 mm. For bauxitisation is necessary to have the same conditions but also a dry period during the year.

The *weakly weathered assemblage* is present in the Villány Mts. itself however it is more common in the surrounding hilly areas. In almost all cases, *in red clays belonging to the Tengelic Fm. and to the basal layers of the Paks Loess Fm. and in yellow Lower Pleistocene clays* the dominant clay mineral is illite and the associations are similar in composition. In each case tentatively two types can be distinguished according to the second frequent minerals: one characterised by more smectite and kaolinite and a little less weathered one with more chlorite and vermiculite. It may indicate slight variations in climate, probably more and less humidity. According to the conclusions of Pazonyi (2006) the warm and humid climate ended about 3.0 million years ago. From this date on, she subdivided the time span into three main periods, the limiting dates of which are 2.15, 0.95 and 0.3 million years, respectively. In each stage the dominant vegetation was dry, open savannah or later steppe which became more humid and forested toward the end of each period. The temperature was moderately warm, in the last stage cooler. (We did not study the really cold stages of the Pleistocene.) From the mineralogy follows moderate, slightly variable intensity of weathering. It is in good agreement with the conclusions drawn from the palaeontological studies.

An important process of this type of alteration is called *rubefication* because it produces red or reddish oxidised iron compounds (Kubiena 1956, cited by Fekete et al. 2005). In the Transdanubian area the iron compound is preferentially goethite and much less frequently hematite.

It should be remarked that the presence of Pliocene faunas is not restricted to a special type of mineral paragenesis in the enclosing red clay. From a simply granulometric point of view fossil bone rests belong to the coarse grain fraction, therefore their occurrence is shown in the diagram for quartz variation in the Beremend quarry (Fig. 16). Here they can be found most frequently but not exclusively in the samples which contain dominantly "detrital" minerals but also in the transitional assemblage of locality No. 26. Former studies indicate that the rich Vertebrate fauna at Csarnóta is found in enclosing red clays

which consist of highly weathered mineral assemblage (Jánossy 1986, Bidló 1980). It looks like that there is no direct connection between the mere presence of fossil rests and the mineral composition of the enclosing clay in a given occurrence. On the other hand, of course, the specific nature of the fossils and mineralogy are in correlation, as it has been discussed before.

Neither the highly weathered nor the weakly weathered terrestrial composition is reflected in the *basin sediments* which are generally older but partly contemporaneous with the formation of the red clays. According to the core material of Magyarbóly-1 borehole the clay mineral association in the fine fraction is the normal terrigeneous, detrital composition of basin sediments like elsewhere in the Pannonian Basin. The composition of the Upper Pannonian Nagyalföld Fm. which may be contemporaneous with the older Pliocene terrestrial red clays highly differs from their composition but does not differ from the overlying Quaternary basin sediments which in turn are partly contemporaneous with the younger terrestrial red clays. Basin sediments in both cases contain typically much illite and as second frequent minerals smectite and kaolinite. Nagyalföld Fm. is in average somewhat more weathered than Quaternary. The iron mineral is here pyrite, in accord with the reduced state of the sediments.

Analogous occurrences in the Carpathian Basin, Dinaric range and on the Adriatic Carbonate Platform (Istria)

The mineralogy of Pliocene to Pleistocene red clays occurring in mountainous and hilly areas of Hungary was reviewed by Viczián (2002a). Generally similar relations were reported in other more recent publications on various red clay formations of Hungary, from the Aggtelek-Esztramos area (Fekete 2002, Fekete et al. 2005) and from the Northern Bükk Mts. (Vincze et al. 2005). In both areas an older, kaolinite-rich and a younger, less weathered association could be distinguished. The closest correlation can be found with the Mt. Esztramos occurrence and with the Poltár Formation in Southern Slovakia.

On *Mt. Esztramos* red clays occur in a very similar facies as in the Villány Mts. They fill karstic fissures and caves in the limestone. There are numerous fossil Vertebrate finds which make an age determination possible. The mineralogy and the stratigraphic classification of the localities were carried out by Viczián (2002a, see Fig. 4). There are red clays with dominantly strongly disordered kaolinite in accordance with the former results of Bidló. Additional phases are mixed-layer kaolinite/smectite and disordered illite. Calcite and hematite contents are relatively high, quartz is low. The age of the oldest red clay deposits is Middle Pliocene, *Estramontian* in the Vertebrate stratigraphy, which is the same as for the Csarnóta site in the Villány Mts. and only slightly older than the oldest Beremend localities. There are red clays of similar composition with younger faunas of Pliocene to Middle Pleistocene age. There are also red clays with composition corresponding to the less weathered material in the Villány Mts.

No free Al-hydroxides were reported from Mt. Osztramos. Gibbsite was found rarely together with hematite and goethite in rounded bauxite pebbles as allochtonous material in red clays of the *Aggtelek Mts.* (Bárdossy 1982, Table 48).

The "weathered" group of the Villány Mts. red clays can be compared to the bauxite pebbles which were prepared by Bárdossy from the red clays in the Aggtelek – Jósvafő area (N Hungary). He supposed that they were redeposited from older bauxite deposits. From the Beremend samples only the 3 samples having more than 20 % gibbsite contents are comparable with these pebbles. Other samples differ not only in their low gibbsite contents but also in their much higher kaolinite, smectite and mixed-layered kaolinite/smectite contents, in the typical disordered nature of kaolinite and in the occasional appearance of quartz.

The other rock type of similar composition and age is the *Poltár Formation in the Lučenec Basin* in Southern Slovakia (Kraus 1989). This is a fine-grained sedimentary formation overlying sedimentary kaolin deposits. Its age is Pontian, i.e. Pliocene. Kaolinite in this basal sedimentary kaolin is relatively well ordered. On the other hand the main clay mineral of the Poltár Formation is typically disordered kaolinite which is accompanied by smectite of non-volcanic origin and occasionally by small amounts of free Al-oxi-hydroxides, gibbsite and diaspore. Diaspore is more abundant. Diaspore was considered first by Kraus to be product of further weathering of kaolinite. Later he accepted diagenetic genesis of diaspore in the surrounding of coalified plant rests. In any case, there are small amounts of free Al-hydroxides. Very disordered kaolinite is supposed to be the product of intense weathering of metamorphic and granitoid rocks in the broader surrounding. With the exception of the formation of diaspore and the absence of iron minerals, the clay mineralogy, its genesis and the age of the Poltár Formation are very similar to the strongly weathered type of red clays in the Villány Mts. (Viczián 2006).

All these examples show that there was a period during the Pliocene in the Carpathian Basin when conditions were favourable for the formation of intensely weathered soils. All these formations contain typically highly disordered kaolinite and occasionally also free aluminium oxi-hydroxides.

The less weathered assemblage can be compared to red clays which were classified by the former authors as *terra rossa.* In the compositional diagrams of Fig. 16 and Fig. 17 the ranges of composition of various occurrences of *terra rossa* in N Hungary and in the Dinaric range are shown for comparison (data of Bárdossy 1982, Table 47 and Table 48). The "detrital" assemblage formed on the limestone surfaces of the Villány Mts. fits fairly well with the composition of *terra rossa* of these areas. There are only less important differences, e.g. there are more smectite and quartz and less chlorite contents in the Villány Mts. than in the two other areas. This may indicate differences in the parent material and intensity of weathering. Some *terra rossas*, e.g. those occurring on the Istrian peninsula may even lack chlorite and contain dominantly disordered kaolinite (Durn et al. 2006). Even low gibbsite contents are compatible with the notion of *terra rossa.* Bárdossy (1982, p. 336) states that "one of its principal features is that it contains a few percent of gibbsite and nordstrandite as a rule".

Good correlation was found between the red clay deposits on the island of Susak, the westernmost member of the Dalmatian archipelago and the Hungarian occurrences by Bognar et al. (2003). Like in the Villány Mts. in Hungary, two types could be distinguished based on the thermal and

geochemical analysis of Gy. Szöőr. There are typical *red* clays filling the karstic cavities of the underlying limestone. They contain kaolinite and diagenetic spherules indicating warm and humid climate similar to the Hungarian *Csarnótan* (4.0 to 3.0 million years BP according to these authors). The immediately overlying *reddish* clays on the basis of the Susak loess complex (labelled as SAV) were correlated with the Hungarian PD soil complex on the basis of the Paks Loess Fm. The *reddish* clays were considered to be *terra rossa.* They were found to contain predominantly montmorillonite and illite and various horizons of $CaCO_3$ accumulation. Quantitative data of a red clay sample were published in the monograph (Fig. 28) and are included into the diagrams on Fig. 16 and Fig. 17 of the present paper. The composition fits well into the field of other *terra rossas* except kaolinite which is lower and the detrital minerals muscovite (illite) and chlorite which are higher than in other Dinaric *terra rossas.* The composition of the analysed sample shows only weakly weathered material and indicates grassy steppe ecotype according to the authors. They were correlated with the Hungarian *Villányian* stage (3.0 to 1.7 million years according to these authors). In the correlation no distinction was made between the Hungarian "reddish" soils belonging to the Tengelic Fm. and to the basal palaeosol of the Paks Loess Fm.

Conclusions

On the basis of quantitative XRD analyses made on 181 samples correlation was found between the mineralogical composition and environmental relations of Pliocene and Quaternary terrestrial red clays in SE Transdanubia.

1. Little is known about the weathering crust on the top of the Mesozoic sequence of Villány Mts. in the time period *between the post-Senonian uplift and erosion and the Pannonian transgression.* The existence of pre-Pannonian fissure system filled by moderately altered smectite-rich grey clay material under the Upper Pannonian cover can be proved in the borehole Magyarbóly-1. Its age is uncertain, perhaps *Old Cainozoic (?).*

2. The *Upper Pannonian cover* has been mostly eroded during the Early Pliocene. A few blocks were preserved in collapsed breccias accumulated in a wide fissure in Nagyharsány quarry. Pannonian sediments occur in the surrounding shallow basins adjacent to the Villány Mts. The basin sediments are composed of fine siltstones containing normal detrital polymineralic assemblage. Similar compositions are found in other areas of the Pannonian Basin. Remained blocks of the covering sandy siltstones and their debris are of similar composition but contain clearly more relatively well-crystallised kaolinite.

3. The terrestrial red clay formation of Middle Pliocene to Lower Pleistocene age is called *Tengelic Red Clay Formation.* Red clays filling fissures and recently existing caves in limestone of the Villány Mts. can be divided into two types.

4. The older type corresponding to the *Beremend Member of the Tengelic Fm.* and to the *Csarnótan* biostratigraphic stage is red kaolinitic clay. It contains typically disordered kaolinite, mixed-layer smectite/kaolinite, smectite and little gibbsite. It was formed in the local subaerial weathering crust in warm, humid, subtropical or monsoon climate. Products of similar weathering, mineralogy and age can be found on Mt. Esztramos, N. Hungary and in the Poltár Fm., S. Slovakia.

5. Gibbsite in low amounts has been formed most probably during the *Csarnótan* period together with kaolinite in the weathering crust on the surface. In exceptional cases the preservation of high-gibbsitic clays in an older generation of fissures cannot be completely excluded. Transformation in the ground waters may have produced smectites but did not go so far to produce kaolinite or gibbsite.

6. The younger member of the *Tengelic Fm.* called *Tengelic Member* contains red (or "reddish") clay beds. It is found in the Villány Mts. and in wide hilly areas of SE Transdanubia. It contains relatively fresh material in which the weathering products are predominantly smectite and goethite formed under generally warm and dry climate in environmental conditions of savannah and steppe or forest steppe.

7. Yellow fissure filling clays in the Villány Mts. (e.g. at Somssich Hill, site No. 2) correspond to the cooling period of *Lower Pleistocene* period. They are even less altered and less oxidised than the relatively fresh material of the reddish clays of the *Tengelic Member.*

8. The *basal red clay layers of the Middle Pleistocene Paks Loess Fm.* contain remarkably similar material as the former red clays belonging to the *Tengelic Member.* Like in the *Tengelic Member*, they contain relatively much quartz and other detrital minerals. In both formations typical clay minerals are well crystallised detrital illite and mixed layer illite/smectite. Less frequent clay minerals are smectite+kaolinite or vermiculite+chlorite, depending probably on slight climatic fluctuations during this period. The somewhat lesser degree of weathering in the palaeosols as compared to the Tengelic red clays indicates the cooling of the temperature. It is expressed in minor but clearly defined differences in the quantity of minerals.

9. On the top of the limestone surface of the Villány Mts. red clays in both stratigraphic units can be regarded as *terra rossa* in the same sense as similar red clay deposits in N Hungary and in the Dinaric range. The red clays cannot be derived from the insoluble residue of the underlying limestone.

Acknowledgements

József Dezső (University of Pécs) helped in numerous ways in the field work, in collection and granulometric analysis of samples and in the observation of the speleological and geomorphological conditions. Part of the samples was separated and analysed by XRD by Béla Raucsik (University of Pannonia, Veszprém). Thank are due to Mária Földvári and Péter Kovács-Pálffy (Geological Institute of Hungary, Budapest) for submission of their unpublished analytical results and for valuable discussions.

References

Balogh, K., Árva-Sós, E., Pécskay, Z., Ravasz-Baranyai, L. (1986): K/Ar dating of post-Sarmatian alkali basaltic rocks in Hungary. Acta Mineralogica-Petrographica, **28**, 75–93.

Bárdossy, Gy. (1982): Karst bauxites. Bauxite deposits on carbonate rocks. Akadémiai Kiadó, Budapest.

Bidló, G. (1980): Mineralogical investigation of degraded kaolinites from Dunántúl (Transdanubian) area. Acta Mineralogica-

Petrographica, **24**, Supplementum, 111–114. (Proc. 10th Kaolin Symp., Budapest, 1979).

BIDLÓ, G. (1983a): The effect of the mineralogy on near-surface mass movements. Földtani Kutatás (Geological Survey), **26/4**, 47–49. (In Hungarian)

BIDLÓ, G. (1983b): Mineralogische Untersuchung der tonhaltigen Sedimente im Villányer-Gebirge. Anuarul Institutului de Geologie şi Geofizica, **62**, 201-216. (Travaux du XII-ème Congrès de l'AGCB, Bucarest, 1981, Minéralogie – Géochimie et Gisements – Sédimentologie).

BIDLÓ, G. (1985): Mineralogical investigation of Middle Pliocene and Pliocene-Pleistocene transitional clays. 5th Meeting of the European Clay Groups, Prague, 1983, 111–115.

BOGNAR, A., SCHWEITZER, F., SZŐŐR, GY. (2003): Susak. Environmental reconstruction of a loess island in the Adriatic. Geographical Research Institute of Hungarian Academy of Sciences, Budapest.

CSÁSZÁR, G. (2002): Urgon formations in Hungary. Geologica Hungarica, Ser. Geologica, **25**, 1–209.

CSÁSZÁR, G., KORDOS, L. (2004): Beremend, quarry. 7th Hungarian Regional Meeting on Palaeontology, 2004, Beremend. Program, Abstracts, Field Guide, 51–57. (In Hungarian)

CSÁSZÁR, G., FARKAS, L. (1984): Indications of a new bauxite horizon in the Villány Mountains. MÁFI Évi Jelentés (Annual Report of the Hungarian Geological Institute), 1982, 237–243. (In Hungarian)

DEZSŐ, J., RAUCSIK, B., VICZIÁN, I. (2007): Granulometric and mineralogical analysis of karstic fissure filling sediments in Villány Mts., S Hungary. Acta GGM Debrecina, Ser. Geology, Geomorphology, Physical Geography, **2**, (in prep.) (In Hungarian)

DUDICH, E., MINDSZENTY, A. (1984): Contributions to the comparative geochemistry, mineralogy and petrology of bauxites in the Villány Mts, SE-Transdanubia, Hungary and in the Pădurea Craiului – Bihor Mts area, W-Transylvania, Rumania. Földtani Közlöny (Bulletin of the Hungarian Geological Society), **114/1**, 1–18. (In Hungarian)

DURN, G., OTTNER, F., MINDSZENTY, A., TIŠLJAR, J., MILEUSNIĆ, M. 2006: Clay mineralogy of bauxites and palaeosols in Istria formed during regional subaerial exposures of the Adriatic Carbonate Platform. *In* Vlahović, I., Tibljaš, D., Durn, G. (ed.): 3rd Mid-European Clay Conference – MECC 06, Opatija, 2006, Field Trip Guidebook, 3–30.

FEKETE, J. (1988): Tropical soils. Akadémiai Kiadó, Budapest. (In Hungarian)

FEKETE, J. (2002): Physical and chemical features of red clays in Northern Hungary. Acta Geologica Hungarica, **45/3**, 231–246.

FEKETE, J., SZENDREI, G., CSIBI, M. (2005): Pedological characteristics and mineral composition of red clays in Hungary. Acta Mineralogica-Petrographica, **47**, 37–45.

FÖLDVÁRI, M., KOVÁCS-PÁLFFY, P. (2002): Mineralogical study of the Tengelic Formation and the loess complex of the Tolna Hegyhát and Mórágy Hills areas (Hungary). Acta Geologica Hungarica, **45/3**, 247–263.

FÜLÖP, J. (1966): Les formations crétacées de la Montagne de Villány. – Geologica Hungarica, Ser. Geologica, **15**, 1–131.

HALMAI, J., JÁMBOR, Á., RAVASZ-BARANYAI, L., VETŐ, I. (1982): Geological results of borehole Tengelic-2. MÁFI Évkönyv (Annals of the Hungarian Geological Institute), **65**, 1–113.

JÁNOSSY, D. (1986): Pleistocene vertebrate faunas of Hungary. Akadémiai Kiadó, Budapest.

JÁMBOR, Á. (1997): Some problems of the late Cenozoic stratigraphy and history of middle Transdanubia. MÁFI Évi Jelentés (Annual Report of Geological Institute of Hungary), 1996, II, 191–198.

KAISER, M. (1999): Report on the study of the stratigraphic position of the Tengelic Formation. Unpublished report, Geological Institute of Hungary, Budapest. (In Hungarian)

KEVEINÉ BÁRÁNY, I. (1998): Soil geography. Nemzeti Tankönyvkiadó, Budapest. (In Hungarian)

KOLOSZÁR, L. (1997): Geological evaluation of the Udvari-2A borehole. MÁFI Évi Jelentés (Annual Report of Hungarian Geological Institute), 1996, II, 149-153.

KOLOSZÁR, L. (2004): Developments of the Tengelic Formation in South-eastern Transdanubia. Földtani Közlöny (Bulletin of the Hungarian Geological Society), **134/3**, 345-369. (In Hungarian)

KOLOSZÁR, L., MARSI, I. (1999): The Quaternary sequences of the hilly country nearby Üveghuta (eastern part of the Mórágy Hills). Földtani Közlöny (Bulletin of the Hungarian Geological Society), **129/4**, 521-540. (In Hungarian)

KOLOSZÁR, L., MARSI, I. (ed.) (2001): Conservation and geological documentation of Pliocene and Pleistocene beds in the Beremend quarry. Unpublished report, Archives of the Hungarian Geological Survey, Budapest. (In Hungarian)

KOLOSZÁR, L., MARSI, I. (2002): Lithostratigraphic correlation of post-Pannonian deposits in the Mórágy Hill area. Földtani Közlöny (Bulletin of the Hungarian Geological Society), **132**, Special issue 133–149. (In Hungarian)

KOLOSZÁR, L., MARSI, I., CHIKÁN, G. (2000): Cainozoic sedimentary cover of the eastern part of Mórágy Hills. MÁFI Évi Jelentés (Annual Report of Geological Institute of Hungary), 1999, 117–135.

KORDOS, L. (1991): Upper Pliocene paleovertebrate localities, Beremend, Villány Mts). Geological Key Sections of Hungary 91/139. Magyar Állami Földtani Intézet (Geological Institute of Hungary). (In Hungarian)

KORDOS, L. (2001): *In* Koloszár L., Marsi I. (ed.) 2001.

KRAUS, I. (1989): Kaolíny a kaolinitové íly Západných Karpát (Kaolins and kaolinite clays of the West Carpathians). Západné Karpaty, Séria Mineralógia, Petrografia, Geochémia, Metalogenéza, **13**, Geologický Ústav Dionýza Štúra, Bratislava. (in Slovakian)

KRETZOI, M. (1956): Die altpleistozänen Wirbeltierfaunen des Villányer Gebirges. Geologica Hungarica, Ser. Palaeontologica, **27**, 1–264.

KRETZOI, M. (1969): Sketch of the Late Cenozoic (Pliocene and Quaternary) terrestrial stratigraphy of Hungary. Földrajzi Közlemények (Geographical Review), **93/3**, 179–204. (In Hungarian)

KROLOPP, E. (2000): Lower Pleistocene mollusc fauna from the Villány Mts. (Southern Hungary). Malakológiai Tájékoztató (Malacological Newsletter), **18**, 51–58. (In Hungarian)

LIPPMANN, F. (1981): Stability diagrams involving clay minerals. Eight Conference on Clay Mineralogy and Petrology, Teplice, 1979. Geologica, Universitas Carolina, Prague, 153–171.

MARSI, I. (1997): Geological evaluation of the Diósberény-1A borehole. MÁFI Évi Jelentés (Annual Report of Hungarian Geological Institute), 1996, II, 159–165.

MARSI, I. (2000): Geology of overlying beds of granites in the eastern part of the Mórágy Hills. MÁFI Évi Jelentés (Annual Report of Geological Institute of Hungary), 1999, 149–162.

MARSI, I. (2002): Development and characterization of postPannonian deposits in the area of the Mórágy Hill and Hegyhát. Földtani Közlöny (Bulletin of the Hungarian Geological Society), **132**, Special issue 71–82. (In Hungarian)

MARSI, I., KOLOSZÁR, L. (2004): Pliocece and Quaternary sediments of the Szőlő Hill in Beremend, SE Transdanubia. Földtani Közlöny (Bulletin of the Hungarian Geological Society), **134/1**, 75-95. (In Hungarian)

MARSI, I., DON, GY., FÖLDVÁRI, M., KOLOSZÁR, L., KOVÁCS-PÁLFFY, P., KROLOPP, E., LANTOS, M., NAGY-BODOR, E., ZILAHI-SEBESS, L. (2004): Quaternary sediments of the north-eastern Mórágy Block. MÁFI Évi Jelentés (Annual Report of Geological Institute of Hungary), 2003, 343–369.

MOLNÁR, S., SZEDERKÉNYI, T. (1996): Subvolcanic basaltic dyke from Beremend, Southeast Transdanubia, Hungary. Acta Mineralogica-Petrographica, **37**, 181–187.

NÁRAY-SZABÓ, I., PÉTER, É. (1967): Die quantitative Phasenanalyse in der Tonmineralforschung. Acta Geologica Hungarica, **11/4**, 347–356.

NÉDLI, ZS., M. TÓTH, T. (2003): Late Cretaceous alkali basalt volcanism in the Villány Mts (SW Hungary). Földtani Közlöny (Bulletin of the Hungarian Geological Society) **133/1**, 49–67.

PAZONYI, P. (2006): Palaeoecological and stratigraphic study of the Quaternary Vertebrate communities of the Carpathian Basin. Ph. D. Thesis, Loránd Eötvös University, Faculty of Sciences, Budapest. (In Hungarian)

RÁLISCH-FELGENHAUER, E. (1987): Villány Mts., Villány, Templom-hegy, lower quarry. Geological Key Sections of Hungary 43. Magyar Állami Földtani Intézet (Geological Institute of Hungary). (In Hungarian)

RISCHÁK, G., VICZIÁN, I. (1974): Mineralogical factors determining the intensity of basal reflections of clay minerals. MÁFI Évi Jelentés (Annual Report of Hungarian Geological Institute), 1972, 229–256. (In Hungarian)

SINGER, A. 1980: The paleoclimatic interpretation of clay minerals in soils and weathering profiles. Earth Sciences Review, **15/4**, 303–326.

SCHULHOF, Ö. (ed.) (1957): Mineral and medicinal waters of Hungary. Akadémiai Kiadó, Budapest. (In Hungarian)

SCHWEITZER, F. (1993): Relief formation in the central part of the Pannonian Basin in the Late Cainozoic and on the boundary of the Quaternary). D. Sc. Thesis, Budapest. (In Hungarian)

SCHWEITZER, F., SZŐŐR, GY. (1997): Geomorphological and stratigraphic significance of Pliocene red clay in Hungary. Zeitschrift für Geomorphologie, Neue Folge, Supplement-Band, **110**, 95–105.

SZEDERKÉNYI, T. (1980): Petrological and geochemical character of the Bár basalt, Baranya County, South Hungary. Acta Mineralogica-Petrographica, **24/2**, 235–244.

SZEMEREY-SZEMETHY, A. (1976): Quantitative determination of carbonate minerals by X-ray diffraction method). MÁFI Évi Jelentés (Annual Report of Hungarian Geological Institute), 1973, 475–482. (In Hungarian)

TANÁCS, J., VICZIÁN, I. (1995): Mixed-layer illite/smectites and clay sedimentation in the Neogene of the Pannonian Basin, Hungary. Geologica Carpathica, Ser. Clays, **4/1**, 3–22.

VADÁSZ, E. (1968): L'âge géologique de la genèse de la "terra rossa". Földtani Közlöny (Bulletin of the Hungarian Geological Society), **98/2**, 277–279.

VICZIÁN, I. (1965): Basalt aus dem Komitat Baranya. Földtani Közlöny (Bulletin of the Hungarian Geological Society), **95/4**, 448–452. (in Hungarian)

VICZIÁN, I. (1967): Erfahrungen mit der Anwendung der Röntgendiffraktometrie zur quantitativen Bestimmung sedimentärer Mineralien. MÁFI Évi Jelentés (Annual Report of Hungarian Geological Institute), 1965, 567–576. (In Hungarian)

VICZIÁN, I. (1984): Clay mineralogy of Tertiary molasse-type basins adjacent to the Alp-Carpathian system (abstract). **27**th International Geological Congress, Moscow, 1984, Abstracts, vol. **2**, Section 04, Sedimentology, 221.

VICZIÁN, I. (2000): Clay minerals of a German-type Middle Triassic sequence, bore hole Nagykozár 2, Mecsek Mts., S. Hungary. Acta Mineralogica-Petrographica **41**, 9–29.

VICZIÁN, I. (2002a): Clay mineralogy of Quaternary sediments covering mountainous and hilly areas of Hungary. Acta Geologica Hungarica, **45/3**, 265-286.

VICZIÁN, I. (2002b): Mineralogy of Pliocene to Pleistocene pelitic sediments of the Great Hungarian Plain. Acta Mineralogica-Petrographica, **43**, 39–53.

VICZIÁN, I. (2006): Comparison of the main periods of kaolinite formation in Slovakia and Hungary (abstract). 3rd "Mineral Sciences in the Carpathians" International Conference, Miskolc, 2006, Abstracts. Acta Mineralogica-Petrographica, Abstract Ser., **5**, 129.

VINCZE, L., KOZÁK, M., KOVÁCS-PÁLFFY, P., PAPP, I., PÜSPÖKI, Z. (2005): Origin of red clays around Miskolc (North Hungary). Acta Mineralogica-Petrographica, **46**, 15–27.

Received: March 12, 2007; accepted: August 10, 2007

Acta Mineralogica-Petrographica, Szeged 2006–2007, Vol. 47, pp. 47-52

ACTA
Mineralogica
Petrographica

VARIATION OF ROCK-EVAL DATA AS A FUNCTION OF HEATING RATE

MAGDOLNA HETÉNYI, TÜNDE NYILAS

Department of Mineralogy, Geochemistry and Petrology, University of Szeged H-6701 Szeged, P.O.Box 651, Hungary
e-mail: hetenyi@geo.u-szeged.hu

INTRODUCTION

Rock-Eval (RE) pyrolysis has been widely used by petroleum industry and by geosciences for decades. It provides information about the amount, type and and maturity of the organic matter and the petroleum potential of rocks. Although this technique was originally designed for studying the mature organic matter from source rocks, recent work showed that it could be applied also for evaluating the amount and properties of immature organic matter from Recent sediments (Sanei et al. 2005) and soils (Di Giovanni et al. 1998). In addition to the basic information that is given by the bulk RE data, mathematical deconvolution of the pyrograms allows one to follow the evolution of the humification process. It can also be used to quantify the relative contribution of the thermally labile and resistant biomolecules and that of humic substances in organic matter in soils (Disnar et al. 2003, Hetényi et al. 2005) and in wetlands (Hetényi et al. 2006).

Some modification of the standard RE method, used for mature kerogen, is needed when it is applied to immature organic matter present in soil and recent sediments. Limitations of the method include the influence of pollution by drilling fluid and natural impregnation of hydrocarbons, as well as the mineral matrix effect (e.g. Larter 1984, Espitalié et al. 1986, Wilhelms et al., Dembicki 1992, Hetényi 1995). In contrast, the dependence of the bulk data on the analytical conditions has been less investigated (Espitalié et al. 1985). Probably this is because during the last three decades RE was mainly used as a standard method in petroleum exploration and the measurements were performed under standard analytical conditions practically in all laboratories. The publication concerning the analytical conditions highlighted, first of all, the importance of the amount and preparation of sample (Espitalié et al. 1985). The role of the heating rate, however, has been only marginally examined (Bordenave et al. 1993).

In a previous work we have studied a wide range of the experimental RE-conditions to select the most suitable ones for estimating the proportion of the components with different thermal stability in immature organic matter both by mathematical and experimental methods (Hetényi et al. 2005). These results demonstrated that the heating rate influenced not only the Tmax value, as it has already been reported (Bordenave et al. 1993), but also the other RE data.

Here we present RE data measured at two different heating rates in series of experiments performed on (i) immature organic matter isolated from oil shale (ii) peaty gley soil organic matter (iii) in the presence and absence of minerals (calcite or montmorillonite). Furthermore, composition of the organic matter, namely the relative contribution of the labile and resistant biopolymers and geopolymers, was assessed by mathematical deconvolution of RE pyrograms.

EXPERIMENTS

RE pyrolyses were performed on kerogen isolated from Pula oil shale (West Hungary) and on refractory, non-hydrolysable, macromolecular organic matter (ROM) isolated from a slightly acid peaty gley soil from East Hungary. Isolation protocols and geochemical features of whole samples have been previously reported (Hetényi et al, 1995; Hetényi et al, 2006). Bulk RE data were measured and pyrograms were recorded by a Delsi Oil Show Analyzer using standard heating conditions: heating at 180 °C for 4 min, followed by programmed pyrolysis at 25 °C/min (or at 5 °C/min), to 600 °C under He flow and oxidation at 600 °C under an oxygen flow. Relative contributions of major classes of organic constituents (referred to as F1, F2, F3, F4) were calculated by mathematical deconvolution of S2 peaks (Sebag et al. 2005). Biological constituents are composed of a small amount of thermally labile biomacromolecules (F1) such as fresh plant material and rather resistant biopolymers (F2) such as lignin and cellulose. F3 represents the immature geomacromolecules (humic substances in sensu lato) and F4 represents refractory organic fractions such as mature geomacromolecules, naturally stable biological components, weathered fossil OM and black carbon.

RESULTS AND DISCUSSION

Bulk Rock-Eval data

Bulk RE data measured on kerogen isolated from oil shale and on ROM isolated from a peaty gley soil, in the absence and presence of minerals, are summarized in Table 1.

The temperature of the peak of hydrocarbon production varied with the heating rate for both of the studied immature organic matter. Independently of the origin and maturity of OM, higher Tmax values were recorded at rapid heating. Using a heating rate of 25 °C/min, Tmax values were found to be around 430 and 410 °C for kerogen and ROM, respectively. Using a heating rate of 5 °C/min, however, Tmax values were detected at 410 and 386 °C (Table 1). This observation is consistent with the somewhat higher differences (435 and 390 °C) obtained

Table 1. Rock-Eval data measured at different heating rates.

Sample	Heating rate	S1	S2	Tmax	HI	TOC	TOCre	TOCi
	°C/min	mg/grock	mg/grock	°C	mg/gTOC	%	%	%
K	25	1.20	307.20	429	873	35.16	25.60	9.56
K+calc	25	1.02	159.20	430	908	17.53	13.30	4.23
K+mont	25	0.27	170.80	429	1020	16.74	14.20	2.54
K	5	1.50	474.80	398	1105	42.94	39.53	3.41
K+calc	5	0.90	238.40	401	1000	23.83	19.87	3.96
K+mont	5	0.15	235.80	402	989	23.84	19.58	4.26
ROM	25	0.55	75.25	410	147	51.13	6.29	44.84
ROM+calc	25	0.42	37.75	411	146	25.73	3.16	22.57
ROM+mont	25	0.25	33.65	410	169	19.85	2.81	17.04
ROM	5	0.35	84.75	386	542	15.63	7.06	8.57
ROM+calc	5	0.20	40.82	386	634	6.43	3.40	3.03
ROM+mont	5	0.22	37.65	384	155	24.15	3.14	21.01

K: kerogen isolated from Pula oil shale, ROM: organic matter isolated from a marsh soil, calc: calcite, mont: montmorillonite (Wyoming), TOCre: reactive carbon, TOCi: inert carbon

by Bordenave et al. (1993) for rocks containing OM the thermal maturity of which corresponded to the oil window. It is noted that the presence of minerals did not modify the values of this maturity parameter (Table 1).

Contrary to the temperature of the highest hydrocarbon production (Tmax), the influence of heating rate on the amount of hydrocarbonaceous compounds formed during pyrolysis appeared to change with the nature of the source biomass. In agreement with S2 values measured on recent lacustrine sediments (Sanei et al. 2005), the present results suggested that rapid thermal alteration (25 °C/min) is insufficient for complete destruction of liptinite-rich immature well-preserved type I kerogen in oil shale deposited in a small maar-type lake. About two-thirds of pyrolysis products were monitored at 25 °C/min heating rate comparing with the results obtained at 5 °C/min heating rate. The necessity of a longer thermal residence time or slower heating rate for complete destruction of the immature liptinitic macerals has been corroborated by organic petrography performed on a recent lacustrine sediment (Sanei et al. 2005). Their experiments demonstrated the presence of fluorescing liptinites after release of S2-compounds. These findings were due to the fact that RE method was designed for rock samples that had previously undergone natural thermal diagenetic changes. The increase of the heating rate, however, reduced only with 11 % of the amount of hydrocarbons formed from immature plant-derived OM occurring in the studied peaty gley soil (Table 1). Consequently, considering the measurement reproducibility, which is ±10 % for S1 and S2 peaks, the minor difference (11 %) between the S1+S2 values measured at the two different heating rates allows one to use the rapid heating rate to evaluate the hydrocarbon potential of immature plant-derived OM.

The present experiments revealed that the yield of OM cracking (S2 value) was not modified essentially by the presence of calcite and only a little by the presence of montmorillonite. (It is noted that for the interpretation of the RE data, summarized in Table 1, it is important to take into consideration that mixtures of OM and minerals contained only half of the OM

Table 2. Proportion of biopolymers and geopolymers.

Sample	Heating rate	F1	F2	F3	F4	R
	°C/min	%	%	%	%	
K	25	2.2	43.5	36.2	18.1	0.05
K+calc	25	2.0	40.1	38.5	19.4	0.05
K+mont	25	1.6	39.5	40.6	18.3	0.04
K	5	1.5	35.0	42.6	20.9	0.04
K+calc	5	3.1	32.8	40.5	23.6	0.09
K+mont	5	3.0	34.3	42.3	20.4	0.09
ROM	25	16.7	28.8	44.5	10.0	0.58
ROM+calc	25	21.3	30.9	38.5	9.3	0.69
ROM+mont	25	10.6	30.5	49.6	9.3	0.35
ROM	5	21.6	37.7	32.1	8.6	0.57
ROM+calc	5	22.3	37.4	28.4	12.0	0.60
ROM+mont	5	17.8	40.5	32.2	9.6	0.44

F1: labile bio-macromolecules, F2: resistant bio-macromolecules, F3: immature geo-macromolecules, F4: refractory organic fraction, R = F1/F2

compared with kerogen and ROM samples in the absence of minerals).

Our experiments provided evidence that heating rate controlled TOC values and the effect strikingly depended on the nature of the source biomass. The differences between TOC values monitored at the two different heating rates were 18 % for kerogen and 69 % for ROM. Furthermore, while the lower heating rate resulted in higher TOC values for kerogen, it resulted in an essential drop in TOC content measured for ROM. TOC content recorded by Rock-Eval pyrolysis is defined as the sum of pyrolysed organic carbon content and organic residue content. Pyrolysed organic carbon, representing the part of OM which generates hydrocarbons, is calculated by Rock-Eval micro-processor from the sum of S1 and S2 and it is termed as reactive organic carbon (TOC_{re}). Consequently, differences as a function of heating rate observed for TOC_{re} are determined by differences occurring in the amount of pyrolysis products. The proportions of reactive TOC measured at rapid heating rate (73 and 12 %) correspond to the widely accepted transformation ratios of kerogen type I and III. Pyrolysis of immature organic matter has shown that 70-80 % of type I kerogen and only 10-25 % of type III are transformed into hydrocarbons (e. g. Tissot and Welte 1984, Bordenave et al. 1993).

In contrast with the RE data detected during pyrolysis, the sample residence time during the oxidation phase exerted a considerable influence on the measured organic carbon content of the inert kerogen (TOCi in Table 1) which produces no hydrocarbons. The bigger portion of the carbon dioxide formed from the inert carbon appeared to be lost during the long residence time in the oxidation module. That is the sample is processed in the oxidation module while the next one is processed in the pyrolysis module. Furthermore, the presence of minerals has also modified the measured values of inert carbon. The latter effect is also especially conspicuous in the case of ROM.

The results detailed above display the importance of the heating rate applied during RE pyrolysis and suggest to perform these measurements using the standard heating rate (25 °C/min).

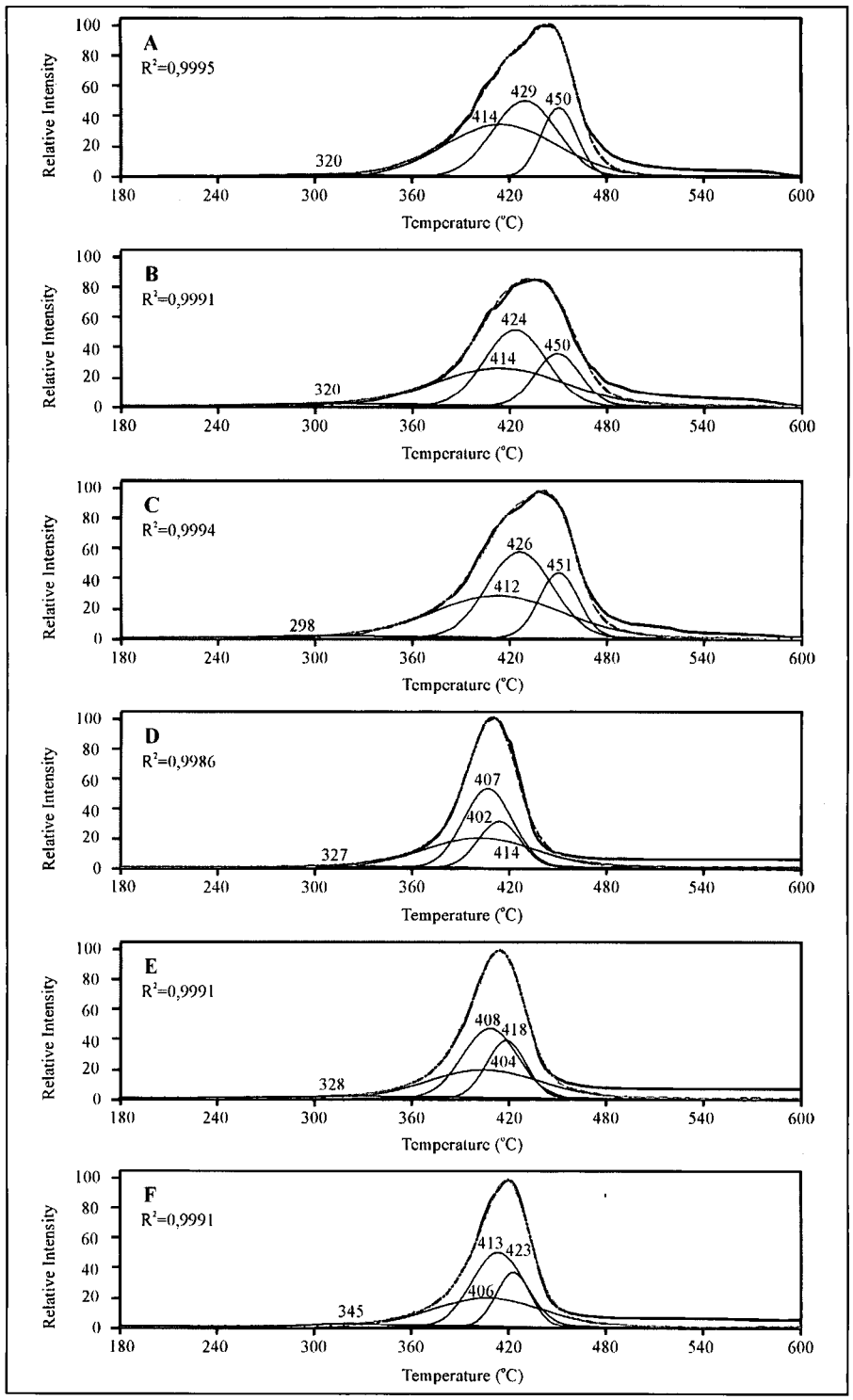

Fig. 1. Mathematical deconvolution of pyrograms monitored on (A) ROM in the absence of minerals and a mixture (1:1) of (B) ROM and calcite, (C) ROM and montmorillonite at 25 °C/min heating rate, as well as on (D) ROM in the absence of minerals and a mixture (1:1) of (E) ROM and calcite, (F) ROM and montmorillonite at 5 °C/min heatig rate. Refractory, non-hydrolysable organic matter (ROM) was isolated from a slightly acid peaty gley soil from East Hungary.

Organic matter composition

The contribution of bio-macro-molecules (the sum of F1 and F2 in Table 2, determined at heating rate of 25 °C/min), exceeding 40 % both in kerogen (45.7 %) and ROM (45.5 %), revealed organic matter corresponding to the diagenesis stage. Nevertheless, strikingly different ratios of the labile and resistant biological constituents

(R-values in Table 2) reveal very immature OM in ROM and OM at the end of the diagenesis stage in the studied kerogen. These findings are in agreement with organic maturity indicated by Tmax values (Table 1), which reflect the early and the late diagenesis for ROM and for kerogen, respectively.

The twice higher proportion of the refractory organic matter constituted the fraction of geomacromolecules (F3+F4 in Table 2) in the ROM (about 4/1) compared with kerogen (about 2/1). The highly refractory ROM fraction contained a relatively high abundance of black carbon (BC) as it was displayed by mathematical deconvolution of its RE pyrogram (Fig. 1) and as it had previously been evidenced both by isolation of BC and by its electron microscopy observation (Hetényi et al. 2006). BC is a collective term for residues of incomplete combustion of organic materials and it exhibits a high resistance to diagenetic degradation (Schmidt et al. 2001, Poirier et al. 2001). Notwithstanding that this carbon form is widely distributed over the entire surface of the earth and play a major role as a sink in the global C cycle via burial in marine sediments (Vandenbroucke and Largeau 2007), there is no standard, generally accepted technique to identify and quantify BC and the results are in poor agreement among the alternative protocols (Schmidt et al. 2001). However, recent publications have shown that high Tmax values (higher than 460 °C) might be caused by the presence of BC. The good correlation determined between the yield of isolation and the abundance of BC calculated by the integration the pyrogram revealed that Rock-Eval pyrolysis could be applied for the estimation of BC contribution (Hetényi et al. 2006). The peaks with Tmax values between 458 °C and 515 °C (Fig. 1) suggested the presence of BC in the studied ROM sample. Mathemathical deconvolution of pyrograms containing peaks with Tmax values lower than 460 °C (Fig. 2) displayed that there was no BC contribution to the type I kerogen.

Although the heating rate did not influence the S2 value essentially (Table 1), it exerted a considerable influence on the organic composition

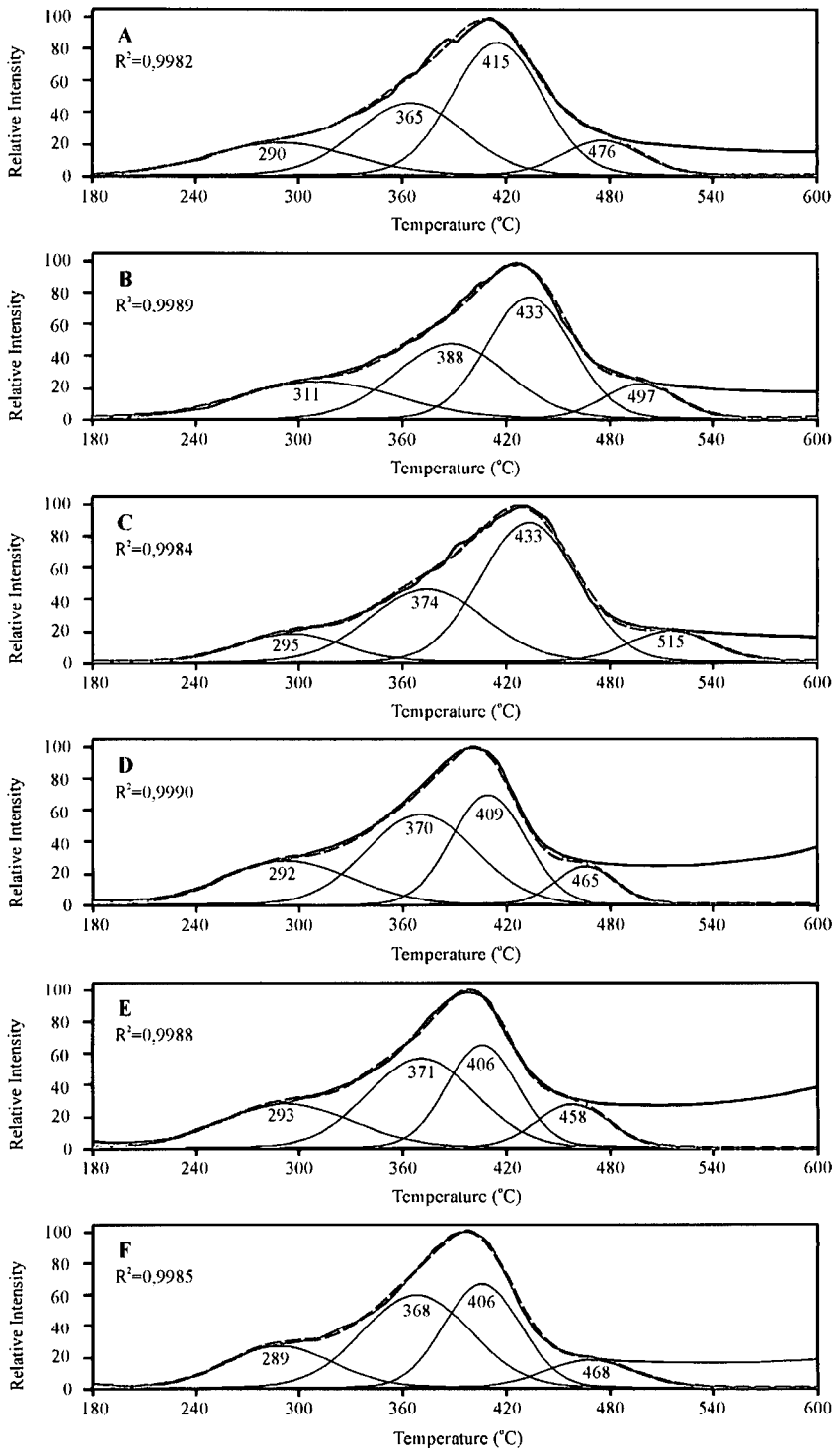

Fig. 2. Mathematical deconvolution of pyrograms monitored on (A) kerogen in the absence of minerals and a mixture (1:1) of (B) kerogen and calcite, (C) kerogen and montmorillonite at 25 °C/min heating rate, as well as on (D) kerogen in the absence of minerals and a mixture (1:1) of (E) kerogen and calcite, (F) kerogen and montmorillonite at 5 °C/min heatig rate. Type I kerogen was isolated from Pula oil shale (West Hungary).

calculated by mathematical deconvolution of S2-peak monitored on ROM (Table 2). A significantly lower proportion of biomacromolecules and a slightly lower ratio of the highly refractory components within geomacromolecules were detected during slow pyrolysis than during rapid pyrolysis. Nevertheless, changes were not observed in the ratio of labile and

refractory biomacromolecules as a function of heating rate in the absence of minerals. The presence of minerals modified the ROM composition calculated from mathematical deconvolution of pyrograms monitored at different heating rates. The results presented here suggested that the effect of minerals was less significant during slow pyrolysis.

Bulk RE data, detailed above, showed that the heating rate significantly controlled the total amount of pyrolysis products formed from a lipid-derived type I kerogen. Furthermore, a series of pyrolyses carried out on sedimentary rock samples (Hetényi et al. 2005) have already demonstrated that mathematical deconvolution of RE pyrograms, which could effectively be used for quantifying the major classes of organic constituents in soils, was not a reliable tool for the estimation of thermally labile and refractory components in type II kerogen. The present results revealed that differences occurring in source biomass, formation pathways and chemical structure of type I and III kerogens could be recognized not only in the shape of the S2 peaks but also in the effect of heating rate comparison (Fig. 2). The latter influenced mainly the proportion of the moderately resistant components and only slightly the proportion of the refractory constituents. The small contribution of the most labile components (F1 in Table 2) appeared to be negligible. Although the above method could not be applied reliably for quantifying the labile and resistant biopolymers and geopolymers in type I kerogen, it provided further evidence about the homogeneity of this Botryococcus-derived kerogen. Botryococcus-origin and homogeneity of the studied kerogen have already been reported: Palynological examinations clearly showed the overwhelming contribution of fossil colonies of Botryococcus algae (Kedves 1983), excellent preservation of which was directly evidenced by Scanning and Transmission Electron Microscopy observations (Derenne et al. 1997). Stepwise oxidation results exhibited the high degree of polymerization and homogeneity of the kerogen (Hetényi and Sirokmán 1978). Our results, namely the narrow S2-peak, monitored at 5 °C/min, and the hardly different Tmax values, obtained by its mathematical deconvolution, (Fig. 2) reflected very homogeneous character of the studied type I kerogen confirming the results of previous studies.

Conclusions

Overall, the above results showed that the heating rate modified RE data measured on lipid-derived and plant-derived OM to different degree. Independently of the nature and maturity of organic matter, standard RE conditions - namely heating rate of 25 °C/min - proved to be more suitable for determination of bulk RE data. The results presented here suggested that thermal residence time exerted an especially significant influence on measuring of the inert organic carbon content, which constitutes the major part of the plant-derived OM and only a minor part of the lipid-derived OM. The heating period influenced the pyrolysis yields, obtained from reactive OM, insignificantly in the case of plant-derived OM and significantly in the case of lipid-derived OM. The relative contributions of the labile and resistant biopolymers and geopolymers calculated by mathematical deconvolution of RE pyrograms, monitored on ROM fraction, varied moderately with heating rate. Rapid heating displayed a more advanced stage of humification process and a more intense mineral matrix effect relative to slow heating. The method, which was developed for evaluating the composition of soil organic matter, has not proved to be an effective tool for evaluating the proportion of organic components of different thermal stability in a lipid-derived, very homogeneous kerogen.

Acknowledgements

The authors thank the Hungarian National Science Foundation (OTKA grant No. T-48325) for funding this work. Helpful comments and constructive suggestions of reviewers (Dr. Cs. Sajgó and G. Abbot) are gratefully appreciated.

References

Bordenave, M.L., Espitalé, J., Leplat, P., Oudin, J.L., Vandenbroucke, M. (1993): Screening techniques for source rock evaluation. In: Bordenave, M.L. (ed.) Applied Petroleum Geochemistry, Éditions Technip, 217–278.

Dembicki, H. Jr (1992): The effects of the mineral matrix on the determination of kinetic parameters using modified Rock-Eval pyrolysis. Organic Geochemistry, **18**, 531–539.

Derenne, S., Largeau, C., Hetényi, M., Brukner-Wein, A., Connan, J., Lugardon, B. (1997): Chemical structure of the organic matter in a Pliocene Maar-type shale: Implicated Botryococcus race strains and fomation pathways. Geochimica and Cosmochimica Acta, **61/9**, 1879–1889.

Di Giovanni, C., Disnar, J.R., Bichet, V., Campy, M., Guillet, B. (1998): Geochemical characterization of soil organic matter and variability of a postglacial detritical organic supply (Chaillexon Lake, France). Earth Surface Processes and Landforms, **23**, 1057–1069.

Disnar, J.R., Guillet, B., Keravis, D. Di Giovanni, C., Sebag, D. (2003): Soil organic matter (SOM) characterization by Rock-Eval pyrolysis: scope and limitations. Organic Geochemistry, **34**, 327-343.

Eespitalé, J., Dereoo, G., Marquis, F. (1985): Rock-Eval pyrolysis and its applications. Revue de L'Institute Francais du Pétrole, 1–72.

Espitalé, J., Dereoo, G., Marquis, F. (1986): La pyrolyse Rock-Eval et ses applications. Revue de L'Institute Francais du Pétrole, **40/5**, 563–578.

Hetényi, M. (1995): Simulated thermal maturation of type I and III kerogens in the presence and absence of calcite and montmorillonite. Organic Geochemistry, **23**, 121–127.

Hetényi, M., Nyilas, T., M.Tóth, T.(2005): Stepwise Rock-Eval pyrolysis as a tool for typing heterogeneous organic matter in soils. Journal of Analytical and Applied Pyrolysis, **74**, 45–54.

Hetényi, M., Nyilas, T., Sajgó, Cs., Brukner-Wein, A. (2006): Heterogeneous organic matter from surface horizon of a temperate-zone marsh. Organic Geochemistry, **37**, 1931–1942.

Hetényi, M., Sirokmán, K. (1978): Structural information of the kerogen of the Hungarian oil shale. Acta Miner. Petrogr. Szeged, **23/2**, 211–222.

Kedves, M. (1983): Etude paléobotanique sur les schistes pétroliféres du tertiaire supérieur de Hongrie. Revue de Micropaléontologie, **26/1**, 48–53.

Larter, S.R. (1984): Application of analytical pyrolysis technique to kerogen characterization and fossil fuel characterization and fossil fuel exploration/exploitation. In Voorhees, K. (ed.): Analytical pyrolysis. Butterworths, London, 212–275.

Poirier, N., Derenne, S., Balesdent, J., Rouzaud, J-N., Mariotti, A., Largeau, C. (2001): Abundance and

composition of the refractory organic fraction of an ancient, tropical soil (Pointe Noire, Congo). Organic Geochemistry, **33**, 383–391.

SEBAG, D., DISNAR, J.R., GUILLET, B., DI GIOVANNI, C., VERRECCHIA, E.P., DURAND, A. (2005): Monitoring organic matter dynamics in soil profiles by „Rock-Eval pyrolysis": bulk characterization and quantification of degradation. European Journal of Soil Science, doi: 10.11111/j.1365-2389.2005.00745.

Sanei, H., Stasiuk, L.D., Goodarzi, F. (2005): Petrological changes occurring in organic matter from Recent lacustrine sediments during thermal alteration by Rock-Eval pyrolysis. Organic Geochemistry, **36/8**, 1190–1203.

SCHMIDT, M.W.I., SKJEMSTAD, J.O., CZIMCZIK, C.I., GLASER, B., PRENTICE, K.M., GELINAS, Y., KULBUSCH, A.J. (2001).: Comperative analysis of black carbon in soils. Global Biochemical Cycles, **15/1**, 163–167.

TISSOT, B.P., WELTE, D.H. (1984): Petroleum Formation and Occurrence. Second revised and enlarged edition. Springer-Verlag, 583–609.

VANDERBROUCKE, M., LARGEAU, C. (2007): Kerogen, origin, evolution and structure. Organic Geochemistry, **38/5**, 720–833.

WILHELMS, A., LARTER, S.R., LEYTHAUSER, D. (1991): Influence of bitumen-2 on Rock-Eval pyrolysis. Organic Geochemistry, **17**, 351–354.

Received: January 31, 2006; accepted: June 31, 2006

*Acta Mineralogica-Petrographica, Szeged 2006–2007, Vol. **47**, pp. 53-59*

ACTA Mineralogica Petrographica

MOBILIZATION CONDITIONS OF LEAD IN FOREST SOILS FROM THE CSERHÁT MTS., NE HUNGARY

PÉTER SIPOS

Institute for Geochemical Research, Hungarian Academy of Sciences H-1112 Budapest, Budaörsi út 45., Hungary
e-mail: sipos@geochem.hu

ABSTRACT

The possible mobilization conditions of lead compared to other heavy metals (Zn and Cr) in four forest soil profiles was studied by sequential extraction to verify the relatively high lability of lead in soils at the woodlands of an undisturbed area (Cserhát Mts., NE Hungary).

The results show that lead can be mobilized in a wide range of environmental conditions. The most significant amount of lead can be bound to the residual fraction (26-57%), but the role of organically bound fraction (16-49%) and amorphous oxide bound fraction (11-28%) is also important in binding Pb. Contrarily, the mobilization of the other studied metals is restricted in these profiles.

Metal/Ti ratios show that lead has been significantly redistributed during the soil formation and it is presented in more labile form as compared to the other studied metals in the profiles. These differences can be resulted by the different source minerals of the studied metals on one hand, or by an external lead source on the other.

Key words: lead, lability, sequential extraction, forest soils, Cserhát Mts.

INTRODUCTION

Lead is widely distributed in the environment, primarily because of anthropogenic contamination. The largest lead emissions to the atmosphere occurred between 1950 and 1990 because of its combustion in Pb-containing petrol, but many other anthropogenic sources contribute to the lead distribution, such as metal smelting, coal burning, or the using of sewage sludge and commercial fertilizers in agriculture (Adriano 1986). In addition, there are natural sources of Pb deposition, as well, such as windborne soil particles, volcanic dust, sea spray, forest foliage and several biogenic processes (Settle and Patterson 1980).

Most recent results on atmospheric heavy metal deposition (Ötvös et al. 2003) show relatively low atmospheric Pb deposition in Hungary as compared to the other European countries (14.8 mg/kg on mosses). Higher concentrations (up to 126.7 mg/kg) were measured only close to industrial areas and roads characterized by intense traffic. Szalai (1998) found an approximate 1-3% increase per year in the Pb content of the topsoil on the Isle of Háros, Budapest. As compared to the results of other studies referring to Middle-Europe (e.g. Friedland et al. 1984, Sturges and Barrie 1989) 2-3 times lower atmospheric lead deposition were measured in Hungary (81 g/ha per year and 77 g/ha per year by Molnár et al. (1993) and Mészáros et al. (1993), respectively) showing its spatial and temporal heterogeneity. The enhanced lead concentrations of anthropogenic origin may result in

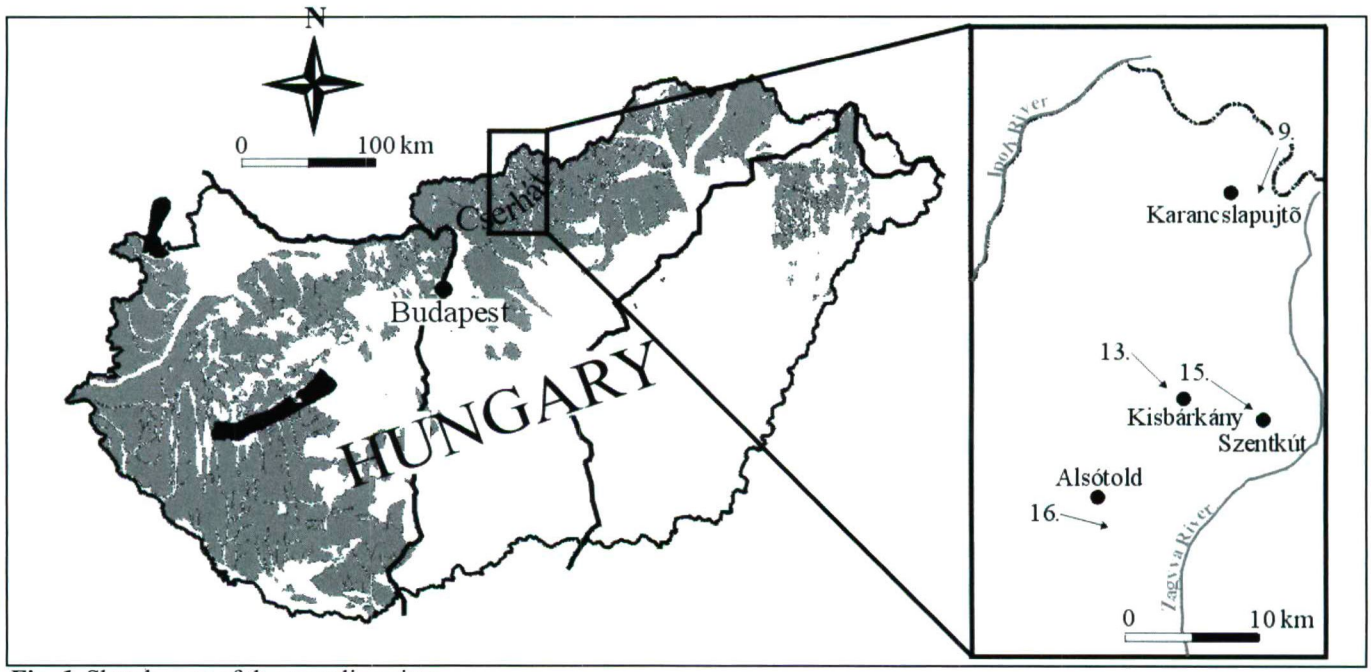

Fig. 1. Sketch map of the sampling sites

changes of lability and bioavailability of this element in soils (Asami et al. 1995).

In forest soils of the Cserhát Mts., Sipos (2003) found a relative high bioavailability of lead as compared to other trace metals, such as Cu, Ni and Zn. In this paper the possible mobilization conditions of lead is studied as compared to a relatively mobile (Zn) and also to an immobile (Cr) heavy metal to verify the relatively high lability of lead in soils at the woodlands of an undisturbed area. Soil profiles developed from different parent materials were sampled to avoid the similarities in mineralogical and chemical compositions of the studied soils.

Materials and methods

Four forest soil profiles were sampled to study the mobilization conditions of Pb as well as Zn and Cr. All of the studied profiles are Luvisols (Driessen et al. 2001) with silt loam texture, and are found in the Cserhát Mts., NE Hungary in short distance from each other (Fig. 1). The detailed characterization of the studied soil profiles can be found in Table 1 and also in the papers by Sipos (2003 and 2004). The variation of Ti/Zr ratios (Milnes and Fritzpatrick 1989) in the studied soil profiles with depth show the homogeneity of soils and parent materials.

Sequential extraction method after Li et al. (1995) was used to characterize the possible mobilization conditions of metals in the studied profiles. Five fractions were separated in five steps as follows: (1) exchangeable with $MgCl_2$ (EX); (2) bound to carbonates or specifically adsorbed, extracted by NaOAc (SAC); (3) bound to Fe-Mn oxides, extracted by NH_2·OH·HCl (OX); (4) bound to organic matter and sulphides, extracted by H_2O_2 and HNO_3 (ORG); and (5) residual, extracted by HNO_3, $HClO_4$ and HF (RES). Concentrations of the studied metals in the solutions were analyzed by ICP-AES method (Jobin Yvon Ultima 2 Sequential ICP).

According to Johnson and Petras (1998) the EX, SAC, OX and ORG fractions can be interpreted as being pedogenic and labile. On the other hand metals in RES fraction are tightly bound in silicate mineral lattices or in crystalline oxide minerals. Metals released through weathering or deriving from anthropogenic sources are assumed to be soluble initially and it can not be added to the crystalline fraction, therefore they enter to the EX and SAC soil pool (Han et al. 2001). Based on these assumptions, we estimated the mobilization of metals by the estimating the depletion of metals from the crystalline fraction (RES). According to the suggestion of McBride et al. (1999), it can be estimated by using a relatively immobile element as an index, such as Ti. The total concentrations (TOT) and the amounts in RES fraction of metals were "normalized" as follows: $(M_{TOT\ or\ RES})N = (M_{A\ or\ E\ or\ B}/M_C)-(Ti_{A\ or\ E\ or\ B}/Ti_C)$, where M is metal concentration (Pb, Zn, Cr) and A, E, B, C are genetic soil horizons. The Ti and Zr contents of samples were determined by a Philips PW1410 X-ray fluorescence spectrometer.

Results and Discussion

Total metal contents and their distribution in the studied soil profiles

The mean total lead content of the studied soil samples is 30.6 ± 7.5 mg/kg, which is in the range observed world-wide in different soils (Siegel 2002). Highest concentrations were found in the soil over andesite (P16) with a relatively small deviation (33.6 ± 2.8 mg/kg), while the soil over siltstone (P13) and calcareous sandstone (P15) are characterized by similar lead concentrations with relatively high deviation

Table 1. Some physico-chemical properties of the studied soil profiles.

Profile Bedrock	Horizon	Depth cm	Munsell color	pH (H_2O)	TOC* %	Carb* %	Texture* Sand	Silt	Clay	Ti mg/kg	Zr	Ti/Zr
P09 calca-reous siltstone	A	0-5	10YR3/4	5.66	6.74	-	41	51	8	4 495 ± 61	302 ± 11	15
	E	5-20	7.5YR5/8	6.39	0.92	-	38	55	7	5 195 ± 32	252 ± 12	21
	B	20-40	10YR5/8	6.85	0.39	-	26	62	12	4 512 ± 30	323 ± 13	19
	BC	40-60	10YR6/8	8.08	<0.10	10	37	54	9	3 962 ± 60	194 ± 6	20
	C	60-75	2.5YR6/4	8.41	<0.10	25	43	50	7	2 792 ± 55	155 ± 4	18
P13 siltstone	A	0-45	10YR4/2	5.49	2.31	-	15	75	10	5 679 ± 47	403 ± 2	14
	E	45-60	2.5YR5/2	5.05	0.25	-	9	77	13	5 485 ± 123	288 ± 3	19
	B	60-150	7.5YR5/2	5.05	0.20	-	8	74	18	4 730 ± 14	252 ± 2	19
	C	150-200	2.5YR6/2	5.41	0.14	-	8	79	13	4 773 ± 8	253 ± 4	19
P15 calca-reous sandstone	A	0-30	10YR3/3	5.27	3.48	-	29	61	10	5 340 ± 44	401 ± 12	13
	E	30-40	7.5YR4/4	5.27	1.06	-	10	77	13	5 532 ± 18	350 ± 3	16
	B	40-100	10YR5/4	5.67	0.78	-	7	76	17	5 198 ± 23	343 ± 10	15
	C	100-120	10YR6/4	7.84	<0.10	40	31	60	9	2 368 ± 38	160 ± 4	15
P16 andesite	A	0-40	10YR3/3	5.84	2.29	-	24	67	9	7 133 ± 186	439 ± 2	16
	E	40-60	7.5YR4/2	6.30	1.05	-	4	87	9	7 301 ± 160	522 ± 11	14
	B	60-130	10YR5/6	6.03	0.35	-	4	82	14	6 093 ± 88	362 ± 10	17
	C	130-150	2.5YR5/4	6.12	<0.10	-	6	82	12	6 340 ± 54	370 ± 13	17

*TOC was analyzed by Rock-Eval method (Delsi Oil Show Analyzer), carbonate (carb) content by XRD analyses (Philips 1710), texture by the pipette method, Ti and Zr concentrations by XRF analyses

(31.7 ± 6 and 30.5 ± 12 mg/kg, respectively), and the lowest lead contents were measured in the soil over calcareous siltstone (P9) with a relatively high deviation (25.1 ± 9.6 mg/kg). The similar lead concentrations of these soils developed on different litholgies shows that the parent rock does not influence the concentration of lead in the studied profiles significantly.

The variation of lead concentration in the studied profiles show in each case the same distribution: the amount of this metal decreases with depth (from 34.3 to 15.2 in P9, from 40.0 to 32.4 in P13, from 41.9 to 18.1 in P15, and from 37.4 to 31.4 mg/kg in P16), in spite of the fact that in the studied soils the downward leaching is the most significant pedogenic process resulting an accumulation in the B horizon. The amount of this metal in the surface horizon can be as high as twice of the value in the C horizons. The downwards decreasing lead content suggests the strong association of Pb to soil organic matter or its potential enrichment from external sources, which corresponds with the observations of Johnson and Petras (1998) and Sanchez-Camazano et al. (1998), as well as Fujikawa et al. (2000). According to Hansmann and Köppel (2000) the often considerably high Pb content of surface soil horizons is attributed to organic matter accumulation on the surface due to plant dry matter recycling rather than anthropogenic sources. However, Pb of anthropogenic origin exhibits the same accumulation pattern on the surface layer.

The mean total zinc (70.1 ± 11.4 mg/kg) and chromium (75.7 ± 14 mg/kg) content of the studied soils are also in the range reported for soils by other studies (Siegel 2002). There are only little differences among the Zn and Cr content of the studied profiles, which is also shown by the small relative deviations. The distribution of these metals with depth is mostly uniform, only a weak depletion in the C horizons of soils developed on calcareous parent material, as well as a weak enrichment on andesite was found showing the effect of parent materials. The uniform distribution type suggests the presence of these metals in minerals highly resistant to weathering.

Mobilization conditions of heavy metals in the studied soil profiles

Sequential extraction studies were performed on three parallel samples from each of the different genetic horizons of the four studied profiles (Table 2. and Fig. 2.). The results show that the most significant amount of metals can be bound to the RES fraction (26-62% of lead, 75-91% of zinc

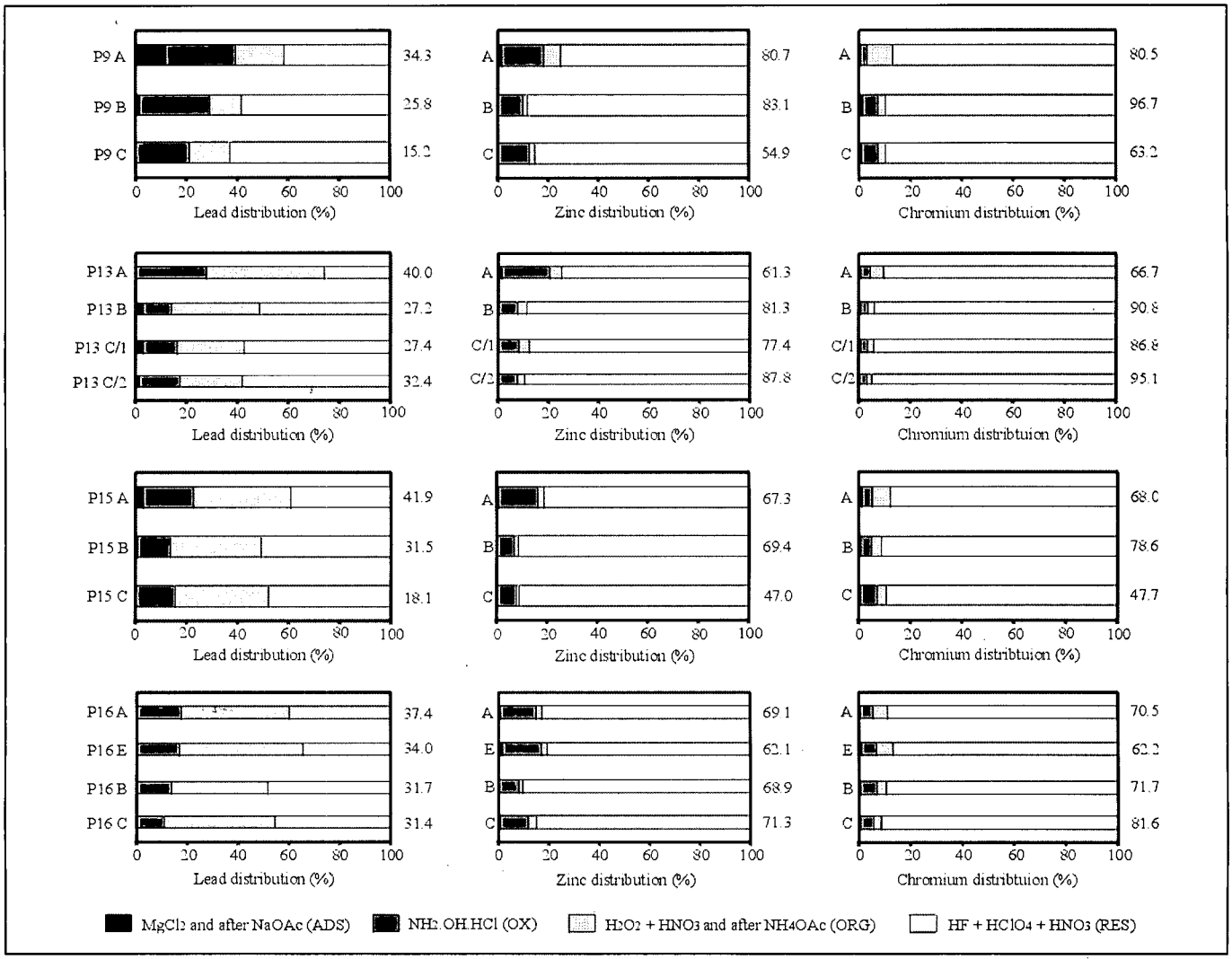

Fig. 2. Distribution of the studied metals among the different extracted fractions (ADS = adsorbed, OX = amorphous oxide bound, ORG = organically bound, RES = residual). The figure also shows the total metal contents of the studied samples in mg/kg.

Table 2. Results of sequential extractions and the titanium content of the studied soil samples.

Element	Step	Profiles/Horizons													
		P9			P13				P15			P16			
		A	B	C	A	B	C/1	C/2	A	B	C	A	E	B	C
Pb	1	<0.13	<0.13	<0.13	<0.13	<0.13	<0.13	<0.13	<0.13	<0.13	<0.13	<0.13	<0.13	<0.13	<0.13
	2	3.9 ± 0.3	0.6 ± 0.2	<0.28	<0.28	1.2 ± 0.2	1.1 ± 0.2	0.6 ± 0.2	1.6 ± 0.2	0.4 ± 0.2	<0.28	<0.28	<0.28	<0.28	<0.28
	3	9.2 ± 0.5	6.5 ± 0.2	3.7 ± 0.2	16.7 ± 0.8	4.2 ± 0.1	4.4 ± 0.1	6.6 ± 0.2	10.1 ± 0.6	5.7 ± 0.4	4.1 ± 0.2	9.4 ± 0.8	9.2 ± 0.1	6.3 ± 0.1	5.4 ± 0.3
	4	6.4 ± 0.3	1.9 ± 0.1	0.6 ± 0.01	7.9 ± 0.2	2.4 ± 0.1	2.8 ± 0.2	2.6 ± 0.6	9.2 ± 0.7	3.1 ± 0.3	0.9 ± 0.05	6.6 ± 0.04	6.1 ± 0.3	3.5 ± 0.3	3.4 ± 0.1
	5	14.8 ± 1.7	16.8 ± 3.0	10.9 ± 0.3	15.4 ± 1.1	19.5 ± 0.1	19.1 ± 1.3	22.6 ± 1.7	21.1 ± 0.6	22.4 ± 2.4	13.0 ± 1.3	21.4 ± 1.2	18.8 ± 1.1	21.9 ± 2.5	22.5 ± 1.1
	Sum	34.3 ± 2.9	25.8 ± 3.5	15.2 ± 0.5	40.0 ± 2.0	27.2 ± 0.7	27.4 ± 1.9	32.4 ± 2.5	41.9 ± 2.1	31.5 ± 3.3	18.1 ± 1.5	37.4 ± 2.0	34.0 ± 1.5	31.7 ± 2.9	31.4 ± 1.5
Zn	1	<0.02	<0.02	<0.02	<0.02	<0.02	<0.02	<0.02	<0.02	<0.02	<0.02	<0.02	<0.02	<0.02	<0.02
	2	1.9 ± 0.7	0.3 ± 0.2	0.1 ± 0.1	0.9 ± 0.5	0.03 ± 0.03	0.3 ± 0.3	0.3 ± 0.2	0.5 ± 0.4	0.9 ± 0.2	<0.02	0.6 ± 0.5	1.1 ± 0.1	0.1 ± 0.1	0.3 ± 0.3
	3	13.4 ± 0.4	8.4 ± 0.3	7.1 ± 0.1	11.6 ± 0.2	6.6 ± 0.05	6.5 ± 0.3	7.0 ± 0.5	10.5 ± 0.3	4.7 ± 0.3	3.7 ± 0.1	9.7 ± 0.4	9.6 ± 0.4	5.7 ± 0.3	8.0 ± 0.4
	4	5.4 ± 0.3	1.7 ± 0.5	1.2 ± 0.1	3.2 ± 0.6	2.9 ± 0.3	3.1 ± 0.2	2.7 ± 0.3	1.7 0.1	1.2 ± 0.6	0.6 ± 0.4	1.8 ± 0.4	1.6 ± 0.4	1.4 ± 0.6	2.4 ± 0.8
	5	60.1 ± 2.3	72.7 ± 5.4	46.5 ± 1.1	45.6 ± 1.3	71.8 ± 3.1	67.5 ± 1.5	77.8 ± 3.2	54.7 0.4	62.6 ± 2.5	42.8 ± 0.2	57.1 ± 0.4	49.8 ± 1.3	61.8 ± 2.5	60.5 ± 0.4
	Sum	80.7 ± 3.8	83.1 ± 6.5	54.9 ± 1.4	61.3 ± 2.6	81.3 ± 3.8	77.4 ± 2.5	87.8 ± 4.4	67.3 1.4	69.4 ± 3.6	47.0 ± 0.7	69.1 ± 1.7	62.1 ± 2.2	68.9 ± 3.5	71.3 ± 1.9
Cr	1	<0.03	<0.03	<0.03	<0.03	<0.03	<0.03	<0.03	<0.03	<0.03	<0.03	<0.03	<0.03	<0.03	<0.03
	2	0.6 ± 0.04	1.7 ± 0.7	0.7 ± 0.1	0.6 ± 0.05	0.6 ± 0.02	0.5 ± 0.03	0.4 ± 0.02	0.9 0.1	0.7 ± 0.2	0.4 ± 0.04	0.6 ± 0.05	0.7 ± 0.1	0.6 ± 0.03	0.7 ± 0.05
	3	2.0 ± 0.1	5.7 ± 0.3	4.0 ± 0.1	2.5 ± 0.1	2.9 ± 0.01	2.7 ± 0.05	2.8 ± 0.1	2.7 0.1	3.3 ± 0.2	3.1 ± 0.01	3.4 ± 0.2	3.8 ± 0.2	4.1 ± 0.1	4.1 ± 0.1
	4	8.0 ± 0.7	2.8 ± 0.04	1.8 ± 0.02	3.4 ± 0.1	2.3 ± 0.1	2.1 ± 0.1	2.0 ± 0.04	4.8 0.3	3.0 ± 0.04	1.6 ± 0.1	3.9 ± 0.1	4.2 ± 0.4	3.0 ± 1.1	2.3 ± 0.1
	5	69.9 ± 1.2	86.5 ± 0.9	56.7 ± 3.7	60.3 ± 2.9	85.0 ± 5.3	81.5 ± 10.6	89.9 ± 2.0	59.6 2.7	71.7 ± 2.8	42.7 ± 2.0	62.7 ± 5.1	53.5 ± 7.7	64.1 ± 9.5	74.5 ± 1.4
	Sum	80.5 ± 2.0	96.7 ± 2.0	63.2 ± 3.9	66.7 ± 3.1	90.8 ± 5.4	86.8 ± 10.7	95.1 ± 2.1	68.0 3.1	78.6 ± 3.2	47.7 ± 2.2	70.5 ± 5.4	62.2 ± 8.5	71.7 ± 0.8	81.6 ± 1.6

Sum = total metal concentrations summarized from the 1-5 extraction steps

and 87-94% of chromium). The role of RES fraction in binding heavy metals increases with depth in each studied profile showing the increasing effect of soil parent material on the distribution of metals. Similar phenomenon was found both in natural (Arunachalan et al. 1996, Palumbo et al. 2000) and contaminated (Li et al. 2000) soils. According to the metal proportions bound to the RES fraction it can be stated that Pb is more labile than Zn or Cr. As compared to other studies (Tyler 1978, Plant and Raiswell 1983, Fujikawa et al. 2000) the lead shows unexpected high lability, this may be due to the different sources of the studied metals. In general, metals of anthropogenic origin are mostly found in labile fractions of soil as compared to metals inherited from the soil parent material (Asami et al. 1995).

The role of ORG fraction in binding metals is the most important in the case of lead (16-49% of total lead can be bound to it), while only a few percent of zinc and chromium can be bound to this fraction. In general, the amounts of Pb in this fraction decrease with depth in the studied soil profiles suggesting the relation between lead and organic matter. However, the highest metal amounts in ORG fraction are not always in the horizons having the highest organic matter content. The metal adsorption capacity of soil organic matter depends not only on its quantity but also on its quality (Fujikawa and Fukui 2001). For example humic acid is highly resistant to weathering, and its proportion in the soil organic matter highly influences the adsorption capacity (Schnitzer 1995).

Significant amount of lead (11-28%) and zinc (7-19%) can be bound to OX fraction, while in the case of chromium its role is secondary, only 1-6% of this metal is bound to this fraction. The co-precipitation and the subsequent adsorption of heavy metals by amorphous iron and manganese oxides is a well known phenomenon in soils (Taylor and McKenzie 1996, Maskall and Thornton 1996 etc.). The role of SAC fraction in binding the studied metals is negligible. Significant lead amount (12%) can be only bound to this fraction in the A horizon of soil P9.

The mobilization conditions of the studied metals shows similarities in the different soil profiles suggesting similar effects forming their distributions in these soils. The high lability of lead is unexpected; in addition this metal can be mobilized in a wide range of environmental conditions. These results suggest significant redistribution of lead during the pedogenic processes as compared to zinc and chromium. The lack of this kind of redistribution in the case of zinc (which is known as a mobile metal in soil conditions) rises the differences in source minerals of the studied metals or the presence of an external lead source, which comes the lead in phases weakly resistant to weathering from.

Table 3. The normalized values of the total and residual lead, zinc and chromium concentrations.

Profile	Horizon	$(Pb_{TOT})N$	$(Pb_{RES})N$	$(Zn_{TOT})N$	$(Zn_{RES})N$	$(Cr_{TOT})N$	$(Cr_{RES})N$
P9	A	-0.2547	0.6433	-0.3179	-0.1383	-0.3764	-0.3361
	B	-0.0844	0.0726	-0.0552	-0.1042	-0.0927	-0.0885
	C	0.00	0.00	0.00	0.00	0.00	0.00
P13	A	-0.5149	0.0371	-0.6099	-0.4972	-0.5248	-0.4942
	B	-0.1351	-0.1574	-0.0725	-0.0693	-0.0498	-0.0416
	C/1	-0.1659	-0.1652	-0.1431	-0.1290	-0.1034	-0.0976
	C/2	0.00	0.00	0.00	0.00	0.00	0.00
P15	A	-0.7560	0.0598	-0.9772	-0.8228	-0.8574	-0.8318
	B	-0.5210	-0.4536	-0.7309	-0.7178	-0.5157	-0.5484
	C	0.00	0.00	0.00	0.00	0.00	0.00
P16	A	-0.1745	0.0689	-0.1820	-0.1548	-0.2836	-0.2613
	E	-0.3155	-0.0660	-0.3287	-0.2803	-0.4342	-0.3899
	B	0.0100	0.0489	0.0600	0.0058	-0.1008	-0.0825
	C	0.00	0.00	0.00	0.00	0.00	0.00

Normalized distribution of the different metal fractions in the studies profiles

The Ti-normalized metal concentration values show the degree of redistribution of metals in soil. These values were calculated for the total metal amounts and for the metal concentrations in RES fraction, as well (Table 3). The normalized distribution of chromium and zinc concentrations, as well as of the residual lead amount show a decreasing mobilization with depth in each studied profile (Fig. 3). In the P16 profile the highest depletion of the studied metals has been found in the E horizon due to the intense leaching from this horizon. This trend corresponds to the increasing effect of soil parent material downwards, and inversely, to the increasing effect of weathering and pedogenic processes upwards. The similarity of the normalized total and residual concentration values indicates that the mobilization of Zn and Cr is restricted in these profiles, and the weathering of phases containing these metals is not in advanced stage. The zinc shows a slight mobilization only in the case of profile P9.

The normalized distribution of Pb_{TOT} shows a different trend as compared to the other metals. The total lead concentration shows relative enrichment in the upper horizons of all the studied soil profiles. This enrichment is the most significant in the case of P9 profile, where this phenomenon is present in the B horizon, as well. However, there is only a slight lead enrichment in the other three profiles. These differences can be due to the erosion of the upper soil horizons, or, in the case of an external lead source its heterogeneity.

Variation of metal/Ti ratios shows that lead has been significantly redistributed during the soil formation and it is presented in more labile form as compared to the other studied metals in the profiles. These differences can be resulted by the different source minerals of the studied metals on one hand, or by an external lead source on the other. In the first case, the detailed chemical characterization of soil minerals should be performed to determine the source phases of the studied metals, e.g. by heavy mineral separation. In general, Pb occurs in soils as discrete minerals, but since it can replace K, Sr, Ba and even Ca and

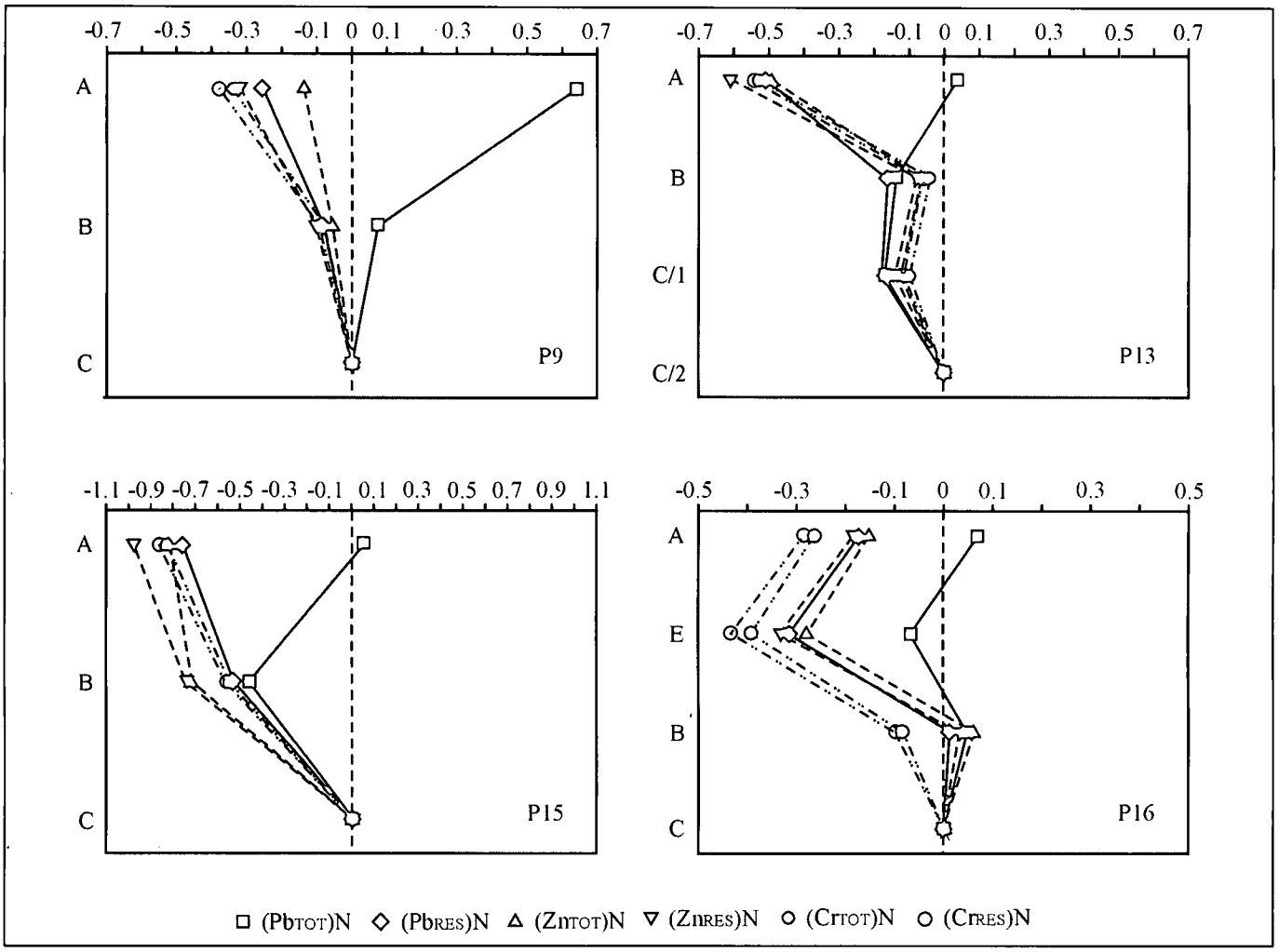

Fig. 3. Normalized distributions of total and residual metal concentrations in the studied soil profiles. P9, P13, P15 and P16 are the numbers of the studied profiles

Na, it can be fixed in the mineral lattice of silicates, which can be also weakly resistant to weathering (such as feldspars) (Nriagu 1978). Taking the geological and pedological characteristics of the study area into account, in the case of an external lead source, the natural origin of mobile lead is not probable. However, the verification of anthropogenic lead and the determination of its ratio to natural lead content of these soils need further studies, which may be based on lead isotope analyses (Erel et al. 1997, Weiss et al. 1999).

Conclusions

The lead presents unique distribution type and redistribution characteristics in the studied soil profiles. The results show that the effect of soil parent material on the concentration and distribution of lead was significantly overwritten by pedogenic processes (or even anthropogenic influences).

The enrichment of lead in the upper horizons of these soils, its unexpected high lability (or extractability) and intense redistribution and mobilization as compared to other heavy metals (primarily to zinc) all suggest the presence of different lead source.

These differences can be resulted by the different source minerals of the studied metals on one hand, or by an external lead source on the other. The determination of the exact reason of the increased lability and bioavailability of this highly toxic heavy metal needs further studies.

Acknowledgements

This study was financially supported by the Hungarian National Research Found (OTKA No. T-043445). The author is grateful to Dr. Chung Choi (University of Bristol) for the ICP analyses as well as for his help at sequential extractions. Use of analytical facilities at the Department of Earth Sciences, University of Bristol was funded by the European Community Access to Research Infrastructure action of the Improving Human Potential Programme, contract HPRI-CT-1999-00008, awarded to Prof. B. J. Wood (EU Geochemical Facility, University of Bristol). Dr. Béla Raucsik and Dr. Géza Szendrei are also thanked for their helpful reviews.

References

Adriano, D.C. (1986): Trace elements in the terrestrial environment, Springer-Verlag, New York, 219–262.

Arunachalam, J., Emons, H., Krasnodebska, B., Mohl, C. (1996): Sequential extraction studies on homogenized forest soil samples. The Science of the Total Environment, **181**, 147–159.

Asami, T., Kubota, M., Orikasa, K. (1995): Distribution of different fractions of cadmium, zinc, lead and copper in unpolluted and polluted soils. Water, Air and Soil Pollution, **83**, 187–194.

DRIESSEN, P., DECKERS, J., SPAARGAREN, O., NACHTERGAELE, F. (2001): Lecture notes on the major soils of the world, FAO, Rome.

EREL, Y., VERON, A., HALICZ, L. (1997): Tracing the transport of anthropogenic lead in the atmosphere and in soils using isotopic ratios. Geochimica et Cosmochimica Acta, **61**, 4495–4501.

FRIEDLAND, A.J., JOHNSON, A.H., SICCAMA, T.G. (1984): Trace metal content of the forest floor in the Green Mountains of Vermont – Spatial and temporal patterns. Water, Air and Soil Pollution, **21**, 161–170.

FUJIKAWA, Y., FUKUI, M., KUDO, A. (2000): Vertical distributions of trace metals in natural soil horizons from Japan. Part 1. Effect of soil types. Water, Air, and Soil Pollution, **124**, 1–21.

FUJIKAWA Y., FUKUI, M. (2001): Vertical distributions of trace metals in natural soil horizons from Japan. Part 2: Effects of organic components in soil. Water, Air, and Soil Pollution, **131**, 305–328.

HAN, F. X., BANIN, A., TRIPLETT, G. B. (2001): Redistribution of heavy metals in arid-zone soils under a wetting-drying cycle soil moisture regime. Soil Science, **166**, 18–28.

HANSMANN, W., KÖPPEL, V. (2000): Lead-isotopes as tracers of pollutants in soils. Chemical Geology, **171**, 123–144.

JOHNSON, C.E., PETRAS, R.J. (1998): Distribution of zinc and lead fractions within a forest Spodosol. Soil Science Society of America Journal, **62**, 782–789.

LI, X., COLES, B.J., RAMSEY, M.H., THORNTON, I. (1995): Sequential extraction of soils for multielement analysis by ICP-AES. Chemical Geology, **124**, 109–123.

LI, X., SHEN, Z., WAI, O., LI, Y. (2000): Chemical partitioning of heavy metal contaminants in sediments of the Pearl River Estuary. Chemical Speciation and Bioavailability, **12**, 17–25.

MASKALL, J., THORNTON, I. (1996): The distribution of trace and major elements in Kenyan soil profiles and implications for wildlife nutrition. In Appleton, J.D., Fuge, R., McCall, G.J.H. (eds.): Environmental geochemistry and health. Geological Society Special Publication No. **113**, 47–62.

MCBRIDE, M.B., RICHARDS, B.K., STEENHUIS, T., SPRIES, G. (1999): Long-term leaching of trace elements in a heavily sludge-amended silty clay loam soil. Soil Science, **164**, 613–623.

MÉSZÁROS, E., MOLNÁR, A., HORVÁTH, ZS. (1993): Atmospheric wet deposition of microelements in Hungary (in Hungarian). Agrokémia és Talajtan, **42**, 221–228.

MILNES, A.R., FRITZPATRICK, R.W. (1989): Titanium and zirconium minerals. In Dixon, J.B., Weed, S.B. (eds.): Minerals in soil environments. Soil Science Society of America Book Series, Madison, 1131–1205.

MOLNÁR, A., MÉSZÁROS, E., BOZSÓ, L., BORBÉLY-KISS, I., KOLTAY, E., SZABÓ, GY. (1993): Elemental composition of atmospheric aerosol particles under different conditions in Hungary. Atmospheric Environment Part A, **27**, 2457–2461.

NRIAGU, J.O. (1978): The biogeochemistry of lead in the environment, Elsevier, Amsterdam.

ÖTVÖS, E., PÁZMÁNDI, T., TUBA, Z. (2003): First national survey of atmospheric heavy metal deposition in Hungary by the analysis of mosses. The Science of the Total Environment, **309**, 151–160.

PALUMBO, B., ANGELONE, M., BELLANCA, A., DAZZI, C., HAUSER, S., NERI, R., WILSON, J. (2000): Influence of inheritance and pedogenesis on heavy metal distribution in soils of Sicily, Italy. Geoderma, **95**, 247–266.

PLANT, J.A., RAISWELL, R. (1983): Principles of environmental geochemistry, In Thornton, I. (ed.): Applied environmental geochemistry. Academic Press, London–New York, 1–39.

SANCHEZ-CAMAZANO, M., SANCHEZ-MARTIN, M.J., LORENZO, L.F. (1998): Significance of soil properties for content and distribution of cadmium and lead in natural calcareous soils. The Science of the Total Environment, **218**, 217–226.

SCHNITZER, M. (1995): Organic-inorganic interactions in soils and their effects on soil quality. In Huang, P. M., Berthelin, J.M., McGill, W.B., Page, A.L. (eds.): Environmental impact of soil component interactions. Lewis Publishers, Boca Raton, Florida, 3–19.

SETTLE, D.M., PATTERSON, C. (1980): Lead in Albacore: guide to lead pollution in Americans. Science, **207**, 1167–1176.

SIEGEL, F.R. (2002): Environmental geochemistry of potentially toxic metals, Springer-Verlag, Berlin Heidelberg.

SIPOS, P. (2003): Distribution of Cu, Ni, Pb and Zn in natural brown forest soil profiles from the Cserhát Mts., NE Hungary. Acta Mineralogical-Petrographica, Szeged, **44**, 43-50.

SIPOS, P. (2004): Geologic and pedogenic effects on heavy metal distributions in forest soils from the Cserhát Mts. and the Karancs area, NE Hungary. Acta Geologica Hungarica, **47**, 411–429.

STURGES, W.T., BARRIE, L.A. (1989): Stable lead isotope ratios in arctic aerosols: evidence for the origin of arctic air pollution. Atmospheric Environment, **23**, 2513–2519.

SZALAI, Z. (1998): Determination of heavy metal deposition through the analysis of soil and vegetation samples (Budapest, Isle of Háros). Földrajzi Értesítő, **47**, 515–522. (in Hungarian)

TAYLOR, R.M., MCKENZIE, R.M. (1966): The association of trace elements with manganese minerals in Australian soils. Australian Journal of Soil Research, **4**, 29–39.

TYLER, G. (1978): Leaching rates of heavy metal ions in forest soils. Water, Air, and Soil Pollution, **9**, 137–148.

WEISS, D., SHOTYK, W., KEMPF, O. (1999): Archives of atmospheric lead pollution. Naturwissenschaften, **86**, 262–275.

Received: August 30, 2007; accepted: November 30, 2007

INSTRUCTIONS FOR AUTHORS

General

Acta Mineralogica-Petrographica (AMP) publishes articles (papers longer than 4 printed pages but shorter than 16 pages, including figures and tables), notes (not longer than 4 pages, including figures and tables), and short communications (book reviews, short scientific notices, current research projects, comments on formerly published papers, and necrologies of 1 printed page) dealing with crystallography, mineralogy, ore deposits, petrology, volcanology, geochemistry and other applied topics related to the environment and archaeometry. Articles longer than the given extent can be published only with the prior agreement of the editorial board. Occasionally, in the form of supplement issues AMP publishes materials of conferences, or other events of scientific interest.

The journal accepts papers that represent new and original scientific results, which have not appeared elsewhere before, and are not in press either.

All articles and notes submitted to AMP are reviewed by two referees (short communications will be reviewed only by one referee) and are normally published in the order of acceptance, however, higher priority may be given to Hungarian researches and results coming from the Alpine-Carpathian-Dinaric region. Of course, the editorial board does accept papers dealing with other regions as well, let they be compiled either by Hungarian or foreign authors.

The manuscripts (prepared in harmony of the instructions below) must be submitted to the Editorial office in triplicate. All pages must carry the author's name, and must be numbered. At this stage (revision), original illustrations and photographs are not required, though, quality copies are needed. It is favourable, if printable manuscripts are sent on CD, as well. In these cases the use of Microsoft Word or any other IBM compatible editing programmes is suggested.

Language

The language of AMP is English.

Preparation of the Manuscript

Title

The title has to be short and informative. No subtitles if possible. If the main title is too long, an additional shortened title is needed for the running head.

Author

The front page has to carry (under the main title) the full name(s) (forename, surname), affiliation(s), current address(es), e-mail address(es) of the author(s).

Abstract and keywords

The abstract is required to be brief (max. 250 words), and has to highlight the aims and the results of the article. The abstracts of notes are alike (but max. 120 words). As far as possible, citations have to be avoided. In the near future the abstracts are going to be distributed in digital form, as well.

The abstract has to be followed by 4 to 10 keywords.

Text and citations

The format of the manuscripts is required to be: double-spacing (same for the abstract), text only on one side of the page, size 12 Times New Roman fonts. Margin width is 2.5 cm, except the left margin, which has to be 3.5 cm wide. Underlines and highlights ought not be used. Please avoid the use of foot and end notes. Accents of Romanian, Slovakian, Czech, Croatian etc. characters must be marked on the manuscript clearly.

When compiling the paper an Introduction – Geological setting – Materials and Methods – Results – Conlclusions structure is suggested.

The form of citations is: the author's surname followed by the date of publication e.g. (Szederkényi 1996). In case of two authors: (Rosso and Bodnar 1995) If there are more than two authors, after the first name the co-authors must be denoted as "et al.", e.g. (Roser et al. 1980). Publications are divided by "," e.g. (Rosso and Bodnar 1995, Szederkényi 1996)

References

The reference list can only consist of published papers, M.Sc., Ph.D. and D.Sc. theses, and papers in press.

Only works cited previously in the text can be put in the reference list.

Examples:

ADRIANO, D.C. (1986): Trace elements in the terrestrial environment, Springer-Verlag, New York, 219–262.

BAKKER, R. J. (2002): http://www.unileoben.ac.at/~buero62/minpet/Ronald/Programs/Computer.html. accessed: June 15, 2003.

CSEH NÉMETH, J. (1975): A recski mélyszinti színesfémérc előfordulás és annak teleptani, ércföldtani képe (Deep-seated base metal ore occurrence of Recsk: geological pattern of ore accumulation). Földtani Közlöny, **105**, 692–708. (in Hungarian)

LE MAITRE, R. W. (ed.) (1989): A Classification of Igneous Rocks and Glossary of Terms. Blackwell, Oxford, 192.

PÁL-MOLNÁR, E. (1998): Geology and petrology of the Ditró Syenite Massif with special respect to formation of hornblendites and diorites. PhD. thesis, University of Szeged, Szeged, Hungary.

ROSSO, K. M., BODNAR, R. J. (1995): Microthermometric and Raman spectroscopic detection limits of CO_2 in fluid inclusions and the Raman spectroscopic characterization of CO_2. Geochimica et Cosmochimica Acta, **59**, 3961–3975.

SZEDERKÉNYI, T. (1996): Metamorphic formations and their correlation in the Hungarian part of Tisia Megaunit (Tisia Megaunit Terrane). Acta Mineralogica-Petrographica, **37**, 143–160.

ZIEGLER, A. M., SCOTESE, C. R., BARETT, S. F. (1983): Mesosoic and Cenozoic paleogeographic maps. In Borsche, P., Sundermann, J. (eds.): Tidal Friction and the Earth's Rotation, II. Springer Verlag, New York, 240–252.

The full titles of journals ought to be given. In case more works of the same author are published in the same year, then these has to be differentiated by using a, b, etc. after the date.

Figures and Tables

Finally, each figure, map, photograph, drawing, table has to be attached in three copies, they must be numbered and carry the name of the author on their reverse. All the illustrations ought to be printed on separate sheets, captions as well if possible. Foldout tables and maps are not accepted. In case an illustration is not presented in digital form then one of the copies has to be submitted as glossy photographic print suitable for direct reproduction. Photographs must be clear and sharp. The other two copies of the illustrations can be quality reproductions. Coloured figure, map or photograph can only be published at the expense of the author(s).

The width of figures and tables can be 56, 87, 118, or 180 mm. The maximum height is 240 mm (with caption).

All figures, maps, photographs and tables are placed in the text, hence, it is favourable if in case of whole page illustrations enough space is left on the bottom for inserting captions. In the final form the size of the fonts on the illustrations must be at least 1,5 mm, their outline must be 0,1 mm wide. Digital documents should be submitted in JPG-format. The resolution of line-drawings must be 400 dpi, while that of photographs must be 600 dpi. The use of Corel Draw for preparing figures is highly appreciated, and in this case please submit the .CDR file, as well. In terms of tables follow the style seen in this volume.

Proofs and Offprints

After revision the author(s) receive only the page-proof. The accepted and revised manuscripts need to be returned to the Editors on CD or as an e-mail attachment. Proofreading must be limited to the correction of typographical errors. If an illustration cannot be presented in digital form, it must be submitted as a high quality camera-ready print.

The author(s) will receive 25 free offprints. On payment of the full price, further offprints can be ordered when the corrected proofs are sent back.

Manuscripts for publication in the AMP should be submitted to:

Dr. Elemér Pál-Molnár
e-mail: palm@geo.u-szeged.hu
Phone: 00-36-62-544-683, Fax: 00-36-62-426-479
Department of Mineralogy, Geochemistry and Petrology
University of Szeged
P. O. Box 651
H-6701 Szeged, Hungary

Published in 450 copies/issue (300 in Hungary, 150 abroad).
Distributed by the Department of Mineralogy, Geochemistry and Petrology, University of Szeged, Szeged, Hungary.
Price of subscription to volume 47, 2006-2007 (including Postage): HUF 10000 in Hungary, EUR 45 in all other countries.

established in 1922

ACTA MINERALOGICA-PETROGRAPHICA

VOLUME 47 2006-2007
HU ISSN 0365-8066

CONTENTS:

ARTICLES

Printed in Hungary by Páskum Nyomda, H-7103 Szekszárd, P.O. Box 627